# UNIVERSITY OF SPLIT

## FACULTY OF CIVIL ENGINEERING, ARCHITECTURE AND GEODESY

**Marino Jurišić, mag.ing.aedif.**


# IMPACT OF BALANCED CANTILEVER CONSTRUCTION ON CAST-IN-PLACE POST-TENSIONED CONCRETE BRIDGES

**Doctoral Dissertation**


**Split, 2024.**

Marino Jurišić, mag.ing.aedif.

Number: 058

**This doctoral dissertation has been submitted for evaluation to the University of Split, Faculty of Civil Engineering, Architecture and Geodesy, for the purpose of obtaining the doctoral academic degree in Technical Sciences, field of Civil Engineering**

**Supervisor (mentor):** Alen Harapin, PhD, prof.

**Additional Supervisor (co-mentor)**: Dragan Ćubela, PhD, assoc. prof.

**Committee for the assessment of doctoral dissertation:**

Nikola Grgić, PhD, assoc. prof.

Mladen Glibić, PhD, prof.

Đani Rahimić, PhD, assoc. prof.

**Committee for the doctoral dissertation defense:**

Nikola Grgić, PhD, assoc. prof._____

Mladen Glibić, PhD, prof. _____

Đani Rahimić, PhD, assoc. prof. _____

The dissertation has been defended on xx$^{th}$ of Month, 2024.

Secretary:

Saša Delić, dipl. iur.

**The dissertation contains:**

80 pages of text

82 figures

2 tables

53 references

**Moto radnje, posvete, zahvale i sl.**

UDC 624.35.012.46:624.04]:519.87](043.3)

Marino Jurišić, mag.ing.aedif.

# Impact of balanced cantilever construction on cast-in-place post-tensioned concrete bridges

**Abstract:**

In this dissertation the impact of balanced cantilever bridge construction method on the deformations and stresses of prestressed concrete bridges built on site is considered. The special scientific contribution of the dissertation are the measurements that were carried out on site and on real structures during construction, specifically on the Vranduk 1 and Vranduk 2 bridges, located on the Vc corridor. Measurements were made on the base segments above the piers, and all phases of the balanced cantilever construction were monitored, from the first segment to the final connection of the bridges.

Deformations and stresses in different cross section points measured during construction were compared with the results obtained by numerical analysis on a complex spatial model. Good matching between measured and numerical results, as well as observed deviations, were commented and explained.

The presented results offer practical guidelines for designers, contractors and project managers involved in balanced cantilever bridge construction, as well as valuable knowledge for optimizing construction methods and increasing the safety and efficiency of bridge projects.

**Keywords:** balanced cantilever method, prestressed concrete, concrete bridges, strain, stress, monitoring, numerical model, creep, shrinkage

UDK 624.35.012.46:624.04]:519.87](043.3)

Marino Jurišić, mag.ing.aedif.

# Utjecaj slobodnog konzolnog načina gradnje betonskih grednih mostova na njihovo ponašanje i sigurnost

**Sažetak:**

U ovom radu je obrađen problem utjecaja jednog načina gradnje mostova, u ovom slučaju slobodne konzolne gradnje, na deformacije i naprezanja prednapetih betonskih mostova građenih na licu mjesta. Posebni doprinos disertacije su mjerenja koja su provedena na licu mjesta i na stvarnim građevinama tijekom gradnje, konkretno na mostovima Vranduk 1 i Vranduk 2, na koridoru Vc. Mjerenja su provedena na baznom segmentu nad stupom, te su praćene sve faze izrade konzolnih segmenata, od prvog segmenta do konačnog spajanja mostova.

Deformacije i naprezanja u pojedinim dijelovima mosta mjerena tokom izgradnje su uspoređena s rezultatima dobivenim numeričkom analizom na složenom prostornom modelu. Dobro slaganje mjerenih i numeričkih rezultata, a također i uočena odstupanja komentirana su i objašnjena.

Predstavljeni rezultati nude praktične smjernice za projektante, izvođače i voditelje projekata uključenih u izgradnju ovakvog tipa mostova od prednapetog betona, te inženjerima nudi vrijedna znanja za optimizaciju metoda izgradnje i povećanje sigurnosti i učinkovitosti projekata mostova.

**Ključne riječi:** slobodno konzolna metoda gradnje, prednapeti beton, betonski mostovi, relativne deformacije, naprezanja, monitoring, numerički model, puzanje, skupljanje

# LIST OF APPENDED PAPERS AND MY CONTRIBUTION

The doctoral dissertation is based on four (4) papers (see Appendix), referred by Roman numbers in the text of the dissertation.

| No. | Paper and my contributions | JCR Rank* | SJR Rank* |
|---|---|---|---|
| [I] | **Jurišić M.** and Cvitković M.: *STUDENČICA BRIDGE TESTING*, e-gfOs, no. 12, pp. 1-9, 2016, http://dx.doi.org/10.13167/2016.12.1 Participation in planning and conducting the testing of the bridge | Q4 | - |
| [II] | Harapin A., **Jurišić M.**, Bebek N. and Sunara M.: *Long-Term Effects in Structures: Background and Recent Developments*, Appl. Sci. 2024, 14, 2352. https://doi.org/10.3390/app14062352 Participation in design of the numerical models for Long-term effects in concrete | Q2 | Q2 |
| [III] | **Jurišić M.**, Bebek N., Ćubela D. and Harapin A.: *Balanced cantilever construction method in post-tensioned concrete bridges*, submitted for publication in Structural Engineering International Participation in study of various ways and technologies of cantilever construction | Q4 | Q2 |
| [IV] | **Jurišić M.**, Bebek N., Ćubela D. and Harapin A.: *Strain Analysis on Cast-In-Place Balanced Cantilever Prestressed Concrete Bridges During Construction*, Structural Engineering International, Published online: 02 Feb 2024, https://doi.org/10.1080/10168664.2023.2296979 Participation in planning and conducting the testing of the bridges | Q4 | Q2 |

(*) Quartiles are determined for the year of submission or the paper publication, according to the more favorable classification for the candidate

# CONTENTS

# 1. INTRODUCTION

With the development of civilization, the demands for number and quality of roads are increasing. Such roads have more demanding route elements, which include larger curve radii and limited longitudinal gradient. This phenomenon is more accentuated when it comes to roads of a higher rank (for example, highways). Due to the demanding elements of the route, the need for a large number of structures, including bridges, arises.

The balanced cantilever construction method represents a sophisticated and dynamic approach to the creation of superstructures, offering a nuanced interplay of engineering principles and construction techniques. As this method has evolved over time, it has transitioned from its initial application in steel bridge construction to becoming a staple in the realm of prestressed concrete bridges, where the variable superstructure height adds an additional layer of complexity and adaptability to the construction process.

The balanced cantilever construction method is very common and very practical in inaccessible and high terrains. The main advantages of the method are that it avoids high and expensive conventional scaffolding and allows relatively large spans which reduce the number of piers. Balanced cantilever construction can be carried out by in-situ concreting or the assembly of prefabricated superstructure segments. The construction technology is such that the foundation and column are made first. After the construction of the column, a base segment (pier head) is made at the top of the column, which is wide enough to start construction. Movable scaffolding is mounted on the base segment, which consists of: main load-bearing frames, floor rails, secondary supports (steel profiles or grids), steel ropes or rods that support the secondary supports, floors and formwork. The front end of the frames rests approx. 0.4-0.5 m from the edge of the concrete, while the rear end of the frames is anchored approx. 4-5 m behind the front support in the concrete of the span construction. After the construction of an individual segment, the movable scaffolding is moved to a new edge of the concrete, where it is secured for the construction of the next segment. This procedure is most often done on both sides so that the column is not burdened with an additional bending moment ("Balanced cantilever method").

Figure 1 shows the construction method of bridges using the cantilever method. The left picture shows the principle of construction, and the right picture shows a real bridge (Figure 1). In the case of prefabricated elements, the shorter length of the segments reduces the total weight of the segment and thus reduces the cost of installation machinery.

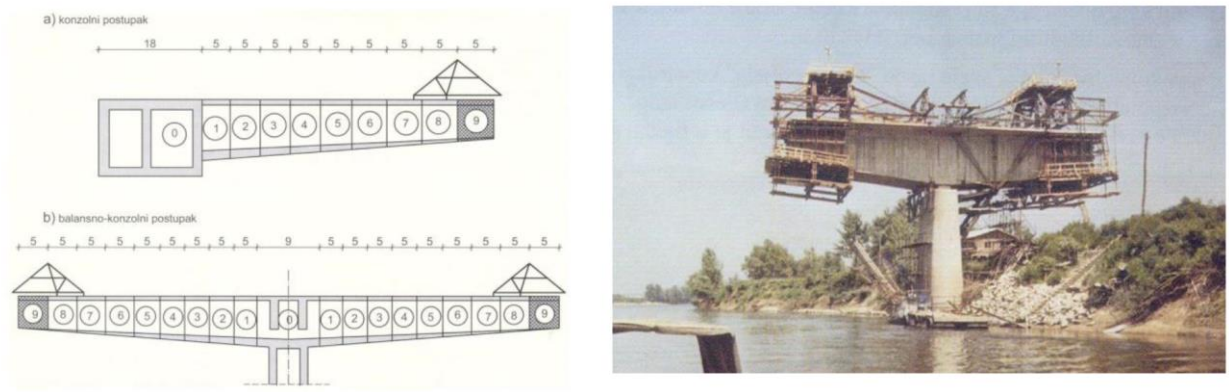


*Figure 1.* Classic design of bridges with free cantilever construction

In the realm of prestressed concrete bridges, the balanced cantilever construction method capitalizes on the inherent strength and durability of concrete. The incorporation of prestressing steel cables into the upper slab of the superstructure cross-section is a key innovation. These cables are strategically placed to counteract the forces exerted during the construction phase, ensuring that the bridge can support substantial loads even before its completion. This proactive approach not only enhances the load-bearing capacity but also contributes to the longevity of the structure, aligning with the growing emphasis on sustainable and resilient infrastructure. The utilization of prestressed concrete in conjunction with the balanced cantilever method empowers engineers and construction teams to achieve expansive spans, overcoming geographical challenges and providing efficient solutions for diverse topographies. The segments of the superstructure, whether constructed on-site through meticulous concreting processes or integrated seamlessly with prefabricated segments, showcase the method's adaptability to different project requirements.

Moreover, the balanced cantilever construction method introduces a progressive construction sequence. Each newly completed segment, post-hardening, not only contributes to the structural integrity of the bridge but also serves as a stable foundation for the ongoing construction. This iterative process allows for a continuous and systematic progression, minimizing disruptions and optimizing construction efficiency.

The balanced cantilever construction method has become a cornerstone in contemporary bridge engineering, embodying a fusion of traditional principles with cutting-edge technologies. Its adaptability, sustainability, and capacity for achieving impressive spans make it a favoured choice for engineers tackling the challenges of modern infrastructure projects. As the method continues to evolve, it stands as a testament to the ingenuity and innovation within the realm of civil engineering and construction [1].

## 1.1. History of cantilever construction

Cantilever construction method has been used in ancient times to build bridges worldwide. The first bridges to be constructed with this method were made with wood. Caesar writes about Gallic works on wooden bridges built by placing timber in orthogonal horizontal rows filled with boulders that acted like counterweight and supported protruding timber beams. Similar structures can still be found in Tibet, China and India (Figure 2) [2].

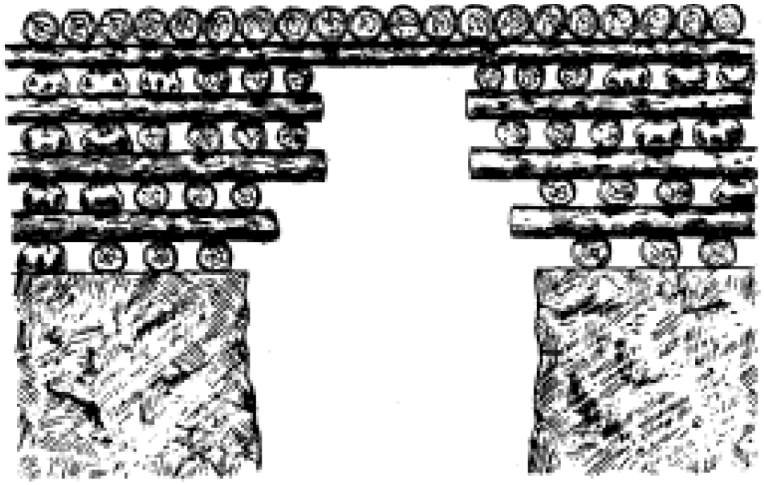

*Figure 2.* Principle of a Gallic wooden bridge
(Setra Design guide [2])

American engineer Thomas Pope designed a 550 m span wooden bridge with a shallow arch resting on two masonry abutments from where it was supposed to be built by the cantilever method with prefabricated segments (Figure 3) [1].

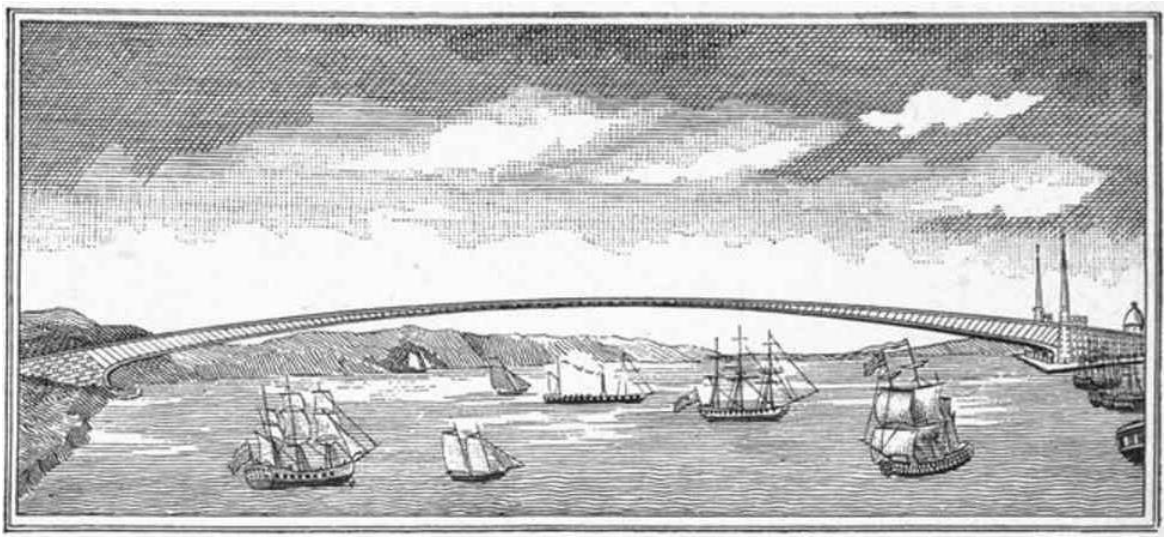

*Figure 3.* Thomas Pope – proposed timber bridge
(Public domain, https://www.clipart-history.com/picture.php?/7461)

Engineers from 19th century understood that continuous beams have a better moment distribution due to the negative support moment compared to simple beams, and can be used to achieve greater spans [3]. Heinrich Gerber was one of those who patented a hinge in a span of a continuous girder, and is considered to be the first to build such a structure [4]. The hinge creates a statically determinate system which is not subjected to parasitic effects due to loads like temperature, differential settling and creep and shrinkage (Figure 4). Besides that, the calculation of stresses and forces in the structure is simpler [3].

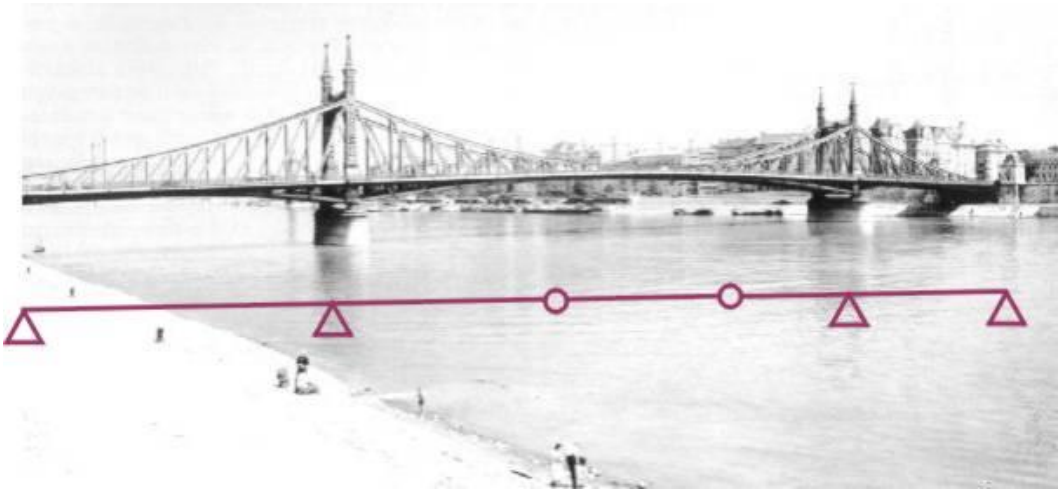

*Figure 4.* Gerber hinge principle
(Tamas Balogh, Pal Turan, https://epito.bme.hu/news/20140613/Danube-ship-trip-with-Brazilian-students?language=en)

Throughout 19th and 20th century the cantilever construction method is mainly used for building arch and truss metal bridges with suspended central span. The Hassfurt Bridge, which was completed in 1867, is considered the first modern cantilever bridge with a main span of 38 m (Figure 5).

*Figure 5.* Hassfurt Bridge
(An Engineer Imagines, Peter Rice, Ellipsis, London, 1993, pp 32, https://fallowmedia.com/2018/nov/bridge-in-hassfurt/)

Other important bridges are: The High Bridge in Kentucky completed in 1877, the Niagara Railroad Bridge completed in 1883, the Poughkeepsie Bridge completed in 1889, and the most famous cantilever bridge in Scotland, Forth Bridge, that was completed in 1890 and held the record for the longest span in the world (518.16 m) for 29 years (Figure 6) [5].

*Figure 6.* Forth bridge, Scotland
(Encyclopædia Britannica, © J4james/Dreamstime.com,
https://www.britannica.com/topic/Forth-Bridge)

One of the designers of Forth bridge, Benjamin Baker, demonstrated the static principle of a bridge with the added central span hanging on the cantilever superstructure (Figure 7). The man sitting in the middle represents the central span. To represent compression forces in bottom chord wooden sticks are used, while the hands represent tensile forces in the upper chord. Weights on the end represent the counterweight abutments holding the added central span.

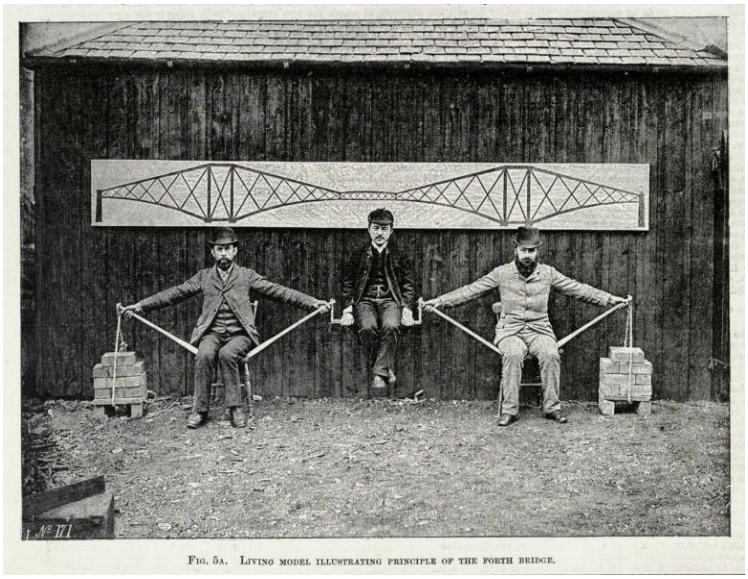


*Figure 7.* Demonstration of the Forth bridge statical principle
(Public domain,
https://en.wikipedia.org/wiki/Forth_Bridge#/media/File:Cantilever_bridge_human_model.jpg)

After the development of reinforced concrete, the cantilever method is used for concrete bridges. In 1928, Freyssinet was already working on the construction of the segments of the arches of the Plougastel Bridge with a span of 185 m (Figure 8). These segments had a significant overturning moment (47 000 kNm) due to the heavy weight of the mobile scaffolding during construction. In order to balance this moment, Freyssinet devised a system in which it connects the opposite parts of the two arches with steel cables and thus creates temporary pre-tensioning.

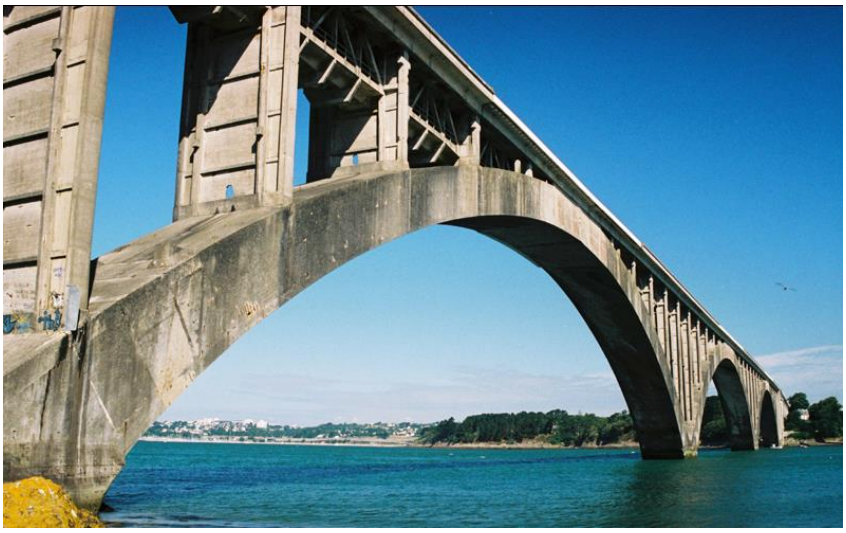

*Figure 8.* Plougastel Bridge

(Public domain, https://en.wikipedia.org/wiki/Plougastel_Bridge#/media/File:Pont-albert-louppe.jpg)

In the form in which it exists today, this method was first applied in 1930 on the Herval Bridge over the Rio Peixe River in Brazil, where reinforcing bars were continued with serrated elements (Figure 9).

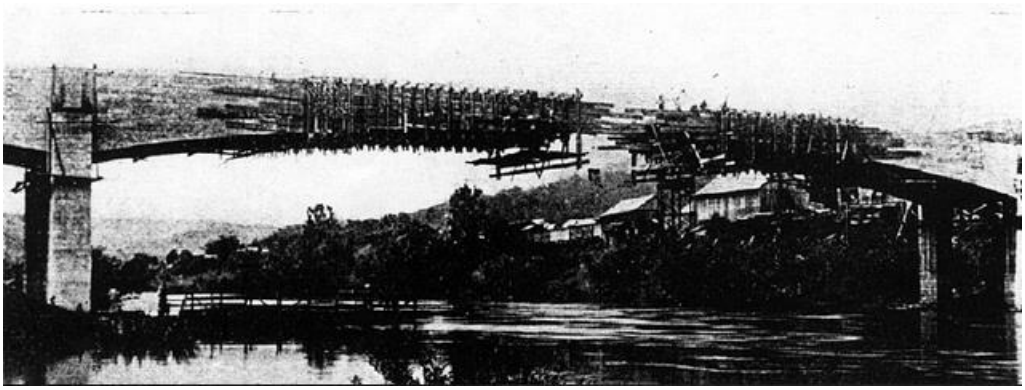

*Figure 9.* Herval Bridge

(Public domain, https://picryl.com/media/ponte-herval-1931-3456fd)

Caquot designed the 100 m span Donzere Bridge in France, but this technique has not been widely adopted on reinforced concrete bridges due to the large amount of reinforcement required to secure the cantilevers and the crack widths in the upper zone of the span structure (Figure 10).

*Figure 10.* Donzere Bridge

(Structurae, Nicolas Janberg, https://structurae.net/en/structures/donzere-mondragon-canal-bridge)

After the development of prestressing, which is suitable for cantilever construction, the method receives wide application. Freyssinet used it in 1945-1950. for the construction of the Luzancy Bridge, five bridges over the Marne River and the Caracas Viaduct. The bridges over the Marne had a cantilevered section next to the abutment, while the middle section of the arch was set in place by mast cranes. The Caracas Viaduct is a cantilevered arch bridge where the segments are concreted on a formwork that is suspended from the main columns (Figure 11).

*Figure 11.* Caracas Viaduct

(Veronidae, CC BY-SA 3.0,

https://www.wikidata.org/wiki/Q109781167#/media/File:Autopista_Caracas_-_La_Guaira_dicembre_2000_029.jpg)

In Germany Finsterwalder introduces cantilever construction in 1950 on the Balduinstein and Neckarrens bridges. The contractor company Boussiron used the method for the construction of the la Voulte railway bridge over the Rhône in 1952 (Figure 12).

*Figure 12.* La Voulte railway bridge
(FredSeiller, CC BY-SA 4.0,
https://fr.wikipedia.org/wiki/Viaduc_de_la_Voulte#/media/Fichier:Viaduc_ferroviaire_(La_Voulte-sur-Rh%C3%B4ne).jpg)

From this moment on, the development of cantilever construction accelerated. In the period from 1952-1953. in Germany, the company Dyckerhoff and Widman works on structures with prestressed bars. The first bridge in France where the segments are concreted on site is Chazey (Figure 13). It was made in 1955 using prestressing cables. At the same time cable prestressing starts in Germany, Austria and several other countries. Except for arches and span structures with inclined columns, all structures had a joint in the middle of the span.

*Figure 13.* Chazey bridge

(Public domain, https://www.chazey-sur-ain.fr/accueil/actualite/147-inspection-detaillee-du-pont-de-chazey-sur-ain)

A new step was taken in 1962 when the joint was removed and the continuity of the span construction was introduced on the Lacroix-Falgarde and Vallon du Moulin a Poudre bridges (Figure 14).

*Figure 14.* Vallon du Moulin a Poudre Bridge

(Gombert, Didier du bout du Monde, https://didierduboutdumonde.blogspot.com/2017/04/le-quartier-de-kerinou-brest.html)

Another step forward was made with the introduction of prefabricated elements. One of the first bridges with prefabricated elements was Choisy-le-Roi built in 1962 in France where the joints were glued and the segments integrated by prestressing.

*Figure 15.* Choisy-le-Roi Bridge

(Structurae, Jacques Mossot, https://structurae.net/en/media/4427-seine-river-bridge-at-choisy-le-roi)

Similar techniques are soon used all over the world and imposing structures such as the Chillon Viaduct and the Rio Niteroi Bridge in Brazil (total length of 8 km) were built. The cantilever construction method was also developed for cable-stayed bridges, for example the Brotonne bridge with a main span of 320 m, which at one time held the record for the longest span made of prestressed concrete [1]. The longest balanced cantilever cast-in-place span is currently the Shibanpo Bridge (2006) over the Yangtze River in China with a span of 330 m (). It is followed by the Stolma Bridge (1998) in Norway with a span of 301 m.

*Figure 16.* Shibanpo Bridge

(Glabb, CC BY-SA 3.0,

https://upload.wikimedia.org/wikipedia/commons/5/5e/Shibanpo_Bridge-1.jpg)

## 1.2. Post-tensioned concrete balanced cantilever bridges

As previously stated, the most usual method of balanced cantilever post-tensioned concrete bridge construction is to first build a column on top of which the initial part of the span construction is built often referred to as the base segment or the pier head. Then, mobile scaffolding called the cantilever forming travellers, which will support the formwork of individual bridge segments, are installed. The main load-bearing part of the moving traveller is a rhombus, which is attached to the upper edge of the span structure with anchors through a steel rail. After the formwork is placed, the segment is reinforced and concreted.

As soon as the concrete reaches sufficient strength, the cables of the cantilever construction in the upper part of the segment are pre-tensioned in order to activate the segment. Then the formwork is released and the traveller is pushed forward over the rails to get into the position for the next segment. This process is repeated until the bridge cantilever is completed. It is important to emphasize that this process with balanced cantilevered bridges takes place simultaneously on the left and right sides of the cantilever, so that the cantilever remains in balance (Figure 17).

In addition to this, there are a number of other ways of construction that are, in principle, a variation of the one described. There are minor differences in the method of formwork placement, which conceptually does not change the method of designing and execution.

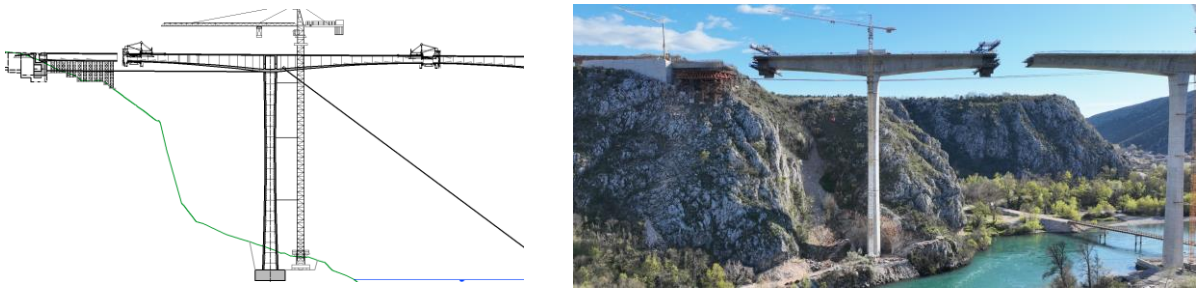

(a) (b)

*Figure 17.* (a) Scheme of a balanced cantilever construction process on a prestressed concrete bridge; (b) Balanced cantilever construction method on a prestressed concrete bridge during construction

The advantages of this type of construction are numerous. First, span structures are made without any contact with the ground, which allows construction over flooded rivers or very deep and steep ravines. This method can also be used to build different geometries. Span structure can be of constant or variable height (linear, parabolic, cubic).

The method is flexible with regard to the geometry of the road on the bridge because, unlike the incremental launching method, any horizontal and vertical geometry can be made without major difficulties. Furthermore, construction in segments of 3-5 m is very feasible in terms of the required amount of formwork for span construction, even if the spans are small and of different lengths (Figure 18).

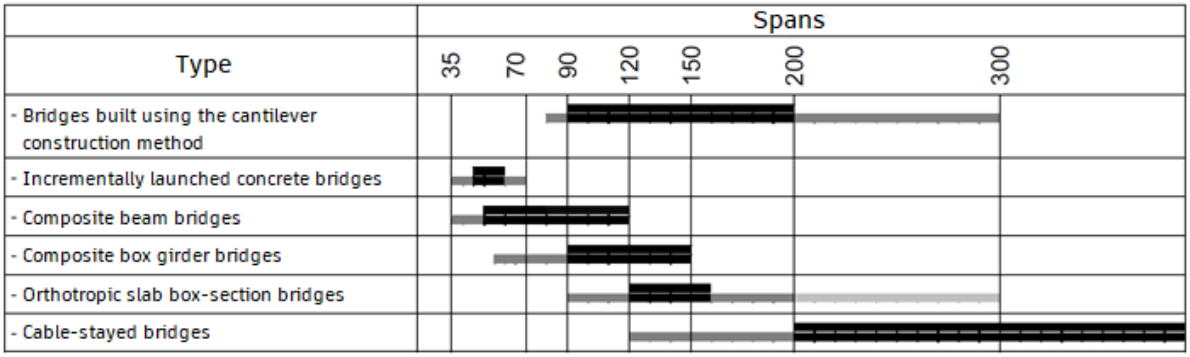


*Figure 18.* Feasibility of different bridge types by span length (m) – (black – feasible, dark grey – possible and possibly feasible, light grey – possible but not feasible)
(Setra Design guide [2])

Cantilever prestressed concrete bridges with a box cross section superstructure can be built in spans of 60-300 m. However, there are other cost-effective construction methods in this range. Cantilever prestressed concrete bridges with spans under 80 m compete with concrete-steel composite bridges in all essential aspects. If the geometry of the road is favourable, then they are competing with prestressed incrementally launched bridges that have a span of 35-70 m. For spans between 70-120 m, cantilever bridges can have a constant or variable span structure height. In these spans, they are competing with concrete-steel girder bridges. For aesthetic reasons, cable stayed bridges are also used in these spans. For spans of 100-200 m, cantilever bridges usually have a variable height of the span structure and compete with box section composite bridges and cable-stayed bridges. The design with light steel webs can also prove to be economical [2].

The disadvantage of this method is that for equal spans these bridges are much heavier than composite bridges. In the case of prefabricated elements, the shorter length of the segments reduces the total weight of the segment and thus reduces the cost of installation. However, the bigger weight request larger foundations and supports, and the problem arises when the bridge is built on weak ground or a seismically active area.

Another major drawback is the large number of tasks that must be completed in the field for the construction of the span structure and access roads. Although the number of these tasks is reduced if the segments are prefabricated, it is still higher than the incremental launching process. When the structure crosses the road, safety can be jeopardized which can lead to road closures. From an aesthetic point of view, bridges made with the cantilever construction method often have a high span cross section, which can be a problem on certain construction sites. As a result of segmental construction and segmental concreting, there may be a difference in the colour of the structure in adjacent segments.

## 1.3. Motivation

The strongest motivation for carrying out research on the behaviour of structures built using balanced cantilever method is to prevent possible disasters due to insufficient knowledge of force transfer and load-bearing capacity. Only two examples will be cited that left a deep mark on the bridge-building community.

One of the earlier notable examples of collapse was a steel bridge in Quebec that collapsed twice during construction. The first collapse took place in 1907 with 75 victims. The collapse occurred due to a wrong calculation, i.e. wrong calculation of the dead weight of the bridge, which was greater than the bridge under construction could handle [6]. The bridge continued to be built in 1916, but during the raising of the central part, there was a problem with the cranes which caused the central part to fall and claimed the lives of 13 workers (Figure 19) [7]. The bridge was finally completed in 1919 and still holds the record for the longest span of a cantilever bridge, at 549 m.

*Figure 19.* Quebec bridge, collapse of the central segment
(Public domain,
https://en.wikipedia.org/wiki/Quebec_Bridge#/media/File:Quebec_Bridge_Collapse.jpg)

Another example is the Koror-Babeldaob balanced cantilever prestressed concrete bridge in Palau built in 1977 (Figure 20). It had a main span of 240.8 m and at the time held the record for the longest span of its type. The bridge had a joint in the middle of the span [8]. Shortly after construction, the bridge developed large vertical deflections. By 1996, the middle of the span had dropped by 1.2 m, which upset the local population who asked the authorities to intervene.

Two studies were made (Louis Berger International and Japan International Cooperation Agency) and both concluded that the bridge is safe and that the large displacements are the result of concrete creep and a lower elasticity modulus. A third study was made in 1993 by ABAM, Seattle, which concluded that the bridge would drop an additional 0.84 m in the next 85 years and a rehabilitation with 40 external pre-stressed cables was proposed.

(a) (b)

*Figure 20.* (a) Koror-Babeldaob bridge after construction; (b) Koror-Babeldaob bridge after collapse

(Public domain, https://upload.wikimedia.org/wikipedia/commons/2/20/Former_Koror-Babeldaob_Bridge1.jpg);

(Ed Zeilnhofer, CC BY 3.0, https://en.wikipedia.org/wiki/Koror%E2%80%93Babeldaob_Bridge#/media/File:Original_Koror-Babeldaob_Bridge_collapse.png)

Renovation was done between 1995 and 1996, during which the joint in the middle of the bridge was removed and external prestressed cables with deviators were installed. Three months after reconstruction on September 26, 1996. the bridge collapsed suddenly and catastrophically, in calm sunny weather and practically unladen. A subsequent study determined that the cause of the collapse was a change in the bridge's static system and a crack in the top slab, where tensile stress occurred. The calculation of the bridge was made using a linear model, not taking into account the redistribution of forces due to the effects of creep and shrinkage (Figure 21) [9-10].

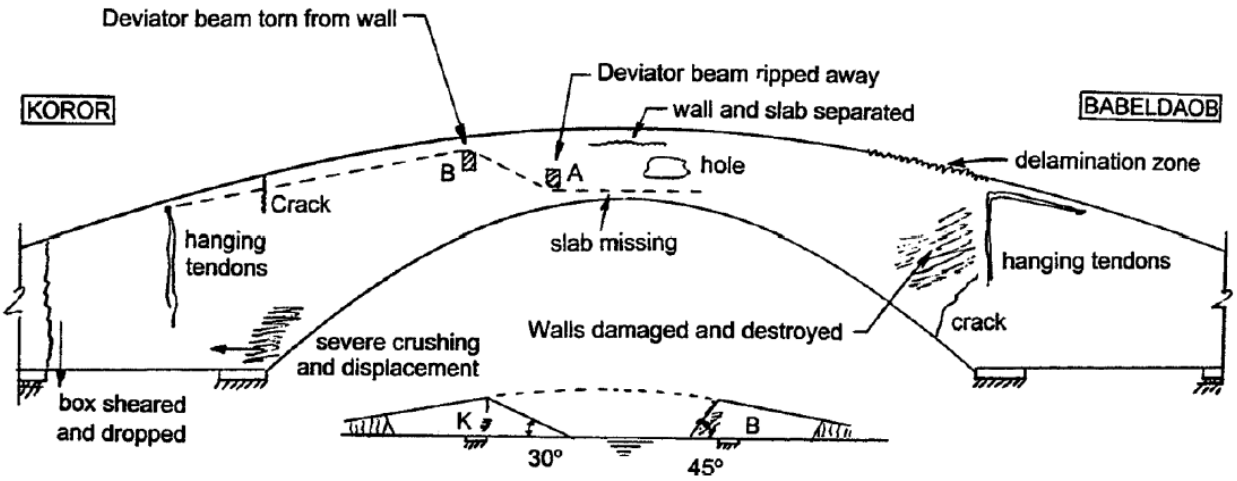


*Figure 21.* Koror-Babeldaob bridge damage overview
(Matthias Pilz, The Koror-Babeldaob Bridge in the Republic of Palau, History and Time Dependent Stress and Deflection Analysis)

As previously described, the balanced cantilever method is, on the one hand, very simple, but at the same time extremely complex regarding the state of stress and deformation, geometry (deflection) and safety of the bridge during its construction and use. Namely, each segment of the bridge has a different age of the concrete, and thus its essential mechanical characteristics over time: strength, modulus of elasticity/stiffness, deformations, displacements, shrinkage, creep and aging of the concrete. They depend on the type of concrete and its composition, but also on the length of the segment production cycle. On the other hand, the losses of force in the post-tensioned cables during and after the construction of the bridge depend on the mechanical characteristics of concrete. During construction, the static system of the bridge changes from a cantilever before joining, to a frame after joining. At the same time, without additional loads and actions, over time there is a redistribution of stress (internal forces) due to changes in the prestressing force and rheological properties of concrete. Usually, there is a relief of previously more strongly stressed sections/elements and an additional stress of previously less stressed sections/elements. In the bridge, there is a constant redistribution of deformations, stresses and deflections, even for constant loads. That is why knowing the actual behavior of such bridges during construction and use is still an extremely complex task.

## 1.4. Previous research on post-tensioned concrete balanced cantilever bridges

Due to the sudden increase in the application of cantilever construction, from the 1970s onwards, there is an increased need for research into force distribution during construction and exploitation of post-tensioned concrete bridges built with this method. Research intensified especially in the 1990s with the development of experimental testing techniques and computer nonlinear numerical methods.

One topic of research was the dynamic characteristics and response of structures, covering natural oscillation frequencies, response to wind loads, seismic response, ambient vibration and forced vibration tests, all using numerical and/or experimental methods.

Skrinar and Strukelj (1996) carried out measurements to determine the natural oscillation frequencies of Carinthia balanced cantilever bridge of variable superstructure height during construction in Maribor, Slovenia, and the frequencies were measured for each segment (Figure 22) [11]. Strommen et al. (2001) investigate the influence of dynamic crosswind loading on vertical oscillations during the construction phase of balanced cantilevered bridges. Research is conducted in a wind tunnel, and based on these experiments, a procedure for predicting the dynamic response of the structure was created [12].

*Figure 22.* Carinthia Bridge in Maribor
(https://www.ponting.si/en/projects/carinthia-bridge-13.html)

Schmidt and Solari (2003) also investigate the influence of wind on balanced cantilever bridges and provide a procedure for determining the influence of wind on the superstructure and piers. The conclusion is that some wind effects in different bridge configurations should not be ignored in order to obtain realistic impact on the structure [13]. Morassi and Tonon (2008) perform a series of forced vibration tests to determine the dynamic characteristics of the three span Palu post-tensioned bridge in north-eastern Italy in a seismically active area [14].

Gentile and Bernardini conduct ambient vibration experiments on the Capriate cantilever bridge using radar measurement. The values of natural frequencies and modal shapes that were obtained through accelerometers with a radar sensor matched with the values obtained by conventional accelerometers (Figure 23) [15]. Bayraktar et al. (2009) conducted research on the vibration characteristics of the Komurhan bridge (Figure 24) [16].

*Figure 23.* Capriate Bridge

(Andrew and Annemarie, CC BY-SA 2.0,

https://upload.wikimedia.org/wikipedia/commons/6/60/Trezzo_sull%E2%80%99Adda_-_ponte_stradale.jpg)

*Figure 24.* Komurhan Bridge

(Sakowski,

https://www.highestbridges.com/wiki/index.php?title=File:KomurhanBeamView.jpg)

Liu et al. determined the dynamic response of a 235 m long three span bridge through a series of ambient vibration tests that were conducted over 12 months [17]. Stathopoulos investigates the dynamic behaviour of the balanced cantilever Metsovo bridge in Greece (Figure 25) [18]. Altunisik et al. (2011) measure the dynamic response of the balance cantilever Gulburn viaduct using ambient vibration tests [19]. In his work, Turan (2012) investigates the dynamic characteristics of balanced cantilever bridges using numerical and experimental methods [20].

*Figure 25.* Metsovo Bridge

(CC BY 4.0, https://www.researchgate.net/publication/341906106_Bayesian_Model-Updating_Using_Features_of_Modal_Data_Application_to_the_Metsovo_Bridge/figures?lo=1)

Kudu et al. (2014) determine the dynamic characteristics of the Berta balanced cantilever post-tensioned bridge using the finite element method and modal analysis (Figure 26) [21]. Sumerkan (2019) gives a simplified expression for frequencies in post-tensioned balanced cantilever bridges [22]. Bayraktar et al. (2020) investigate the influence of vertical displacements in the ground near faults on the seismic behaviour of balanced cantilever bridges. The numerical analysis showed that the vertical movements of the ground significantly affect the seismic behaviour of the bridge [23].

*Figure 26.* Berta Bridge
(https://www.highestbridges.com/wiki/index.php?title=File:BertaByswbauerepfl_.jpg)

Another topic of research was reliability, behaviour and rehabilitation of structures, mostly determined by experimental tests and onsite analyses. In some cases, long term structural monitoring and numerical analysis were used.

Casas (1997) conducted research to determine the reliability partial safety factor on balanced cantilever concrete bridges. The research is conducted on bridges with a span of 80 to 140 m, and an example was made on a bridge with a span of 120 m [24]. Manjure (2001) works on the rehabilitation of balanced cantilever bridges with suspended central part of the span in India, where problems occur during the exploitation phase due to poor concreting and reinforcement detailing [25].

Vonganan conducts structure behaviour research on the Mekong Bridge in Thailand (Figure 27) [26]. Pinmanas et al conduct a study on the Phra-Nangklao post-tensioned balanced cantilever bridge in Thailand (Figure 28) [27]. Ates et al. (2013) investigate the structural behaviour of balanced cantilever bridges taking into account the interaction between the structure and the soil [28]. Chen et al. (2013) conducted dynamic tests and long-term monitoring of the 12-span Newmarket (Auckland, New Zealand) viaduct using wireless sensors shortly after the works were completed [29].

*Figure 27.* Mekong Bridge

(CC BY-SA 3.0,

https://en.wikipedia.org/wiki/List_of_crossings_of_the_Mekong_River#/media/File:Thai-Lao-Freundschaftsbruecke.jpg)

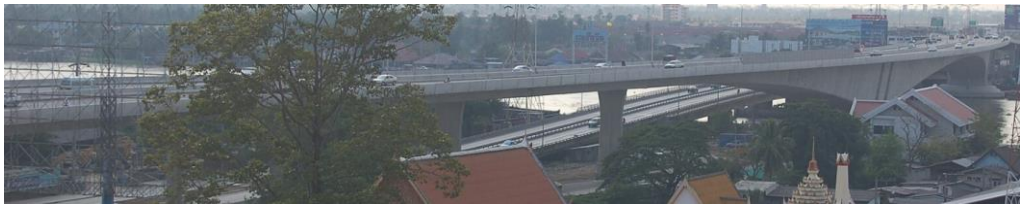

*Figure 28.* Phra-Nangklao Bridge

(CC BY-SA 3.0,

https://en.wikipedia.org/wiki/Phra_Nang_Klao_Bridge#/media/File:New_Pranangklao_Bridge.jpg)

Pimentel and Figueiras (2017) present a new methodology for assessing the condition of post-tensioned balanced cantilever bridges including experimental and numerical investigations [30]. Caner (2021) analyses the reconstruction of the partially collapsed balanced cantilever post-tensioned bridge Begendik (Figure 29) [31].

*Figure 29.* Begendik Bridge
(https://www.highestbridges.com/wiki/index.php?title=File:Begendik13.jpg)

One other interesting topic of research was the design of post-tensioned concrete bridges built using the balanced cantilever construction method, which focused on superstructure optimisations, bending moment variations, simulation models as well as material and geometric nonlinearities.

Kwak and Son (2004) work on determining the span ratios of balance cantilever bridges through time analyses, in which the main guideline is that vertical displacement does not occur at the edge of the cantilever due to the action of weight and post-tensioned cables for cantilever construction [32]. They are also working on determining the variation of the bending moment over time taking into account construction phases and concrete creep. On the basis of these researches, they provide an expression to obtain the bending moment and its variation by elastic analysis without taking into account the construction phases and creep [33]. Hewson (2007) conducts a study on the balanced cantilever method of bridge construction [34].

Marzouk et al. (2008) develop a special simulation model for balanced cantilever bridges built both with prefabricated and onsite concreted segments [35]. Ates (2011) works on the numerical modelling of balanced cantilever bridges taking into account the time-dependent characteristics of the material. Analyses have shown that time-dependent material characteristics and geometric nonlinearity should be taken into account in order to obtain the correct behaviour of concrete bridges [36]. Bravo et al. (2021) conduct research to assess the seismic displacement of balanced cantilever bridges in the construction phase and in the exploitation phase [37].

Time-dependant effects such as creep and shrinkage during and after construction is another important topic of research focusing on the influence on force and stress distribution, as well as additional deformations.

Pimanmas (2007) investigates the influence of long-term creep and prestressing on the redistribution of bending moments in balanced cantilever bridges, using Pathum Thani as an example (Figure 30). The analysis shows that creep in these cases can increase the value of the negative moment and that rough estimates of creep can lead to wrong results. The exact phases of construction should be taken into account [38]. In the same year, Hedjazi and colleagues investigated the influence of concrete creep on deflections and stresses in post-tensioned balance cantilever bridges. Three-dimensional models are made out of areas with included material nonlinearity and concrete creep [39].

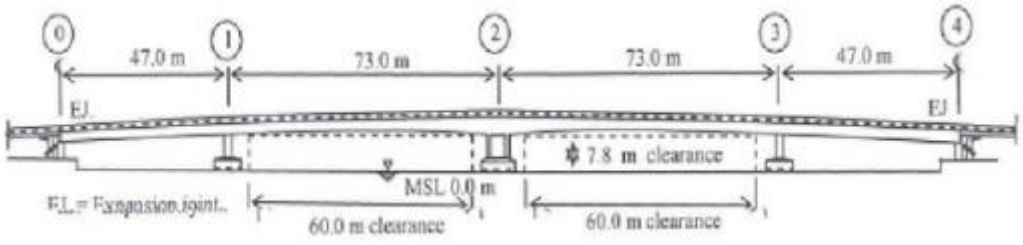


*Figure 30.* Pathum Thani Bridge elevation

(CC BY-NC, https://www.researchgate.net/publication/26469481_The_effect_of_long-term_creep_and_prestressing_on_moment_redistribution_of_balanced_cantilever_cast-inplace_segmental_bridge/figures?lo=1)

Altunisik et al. (2010) conduct an analysis of the construction phases of the Komurhan bridge taking into account the time-dependent material characteristics [40]. Malm and Sunquist perform a time-sensitive analysis of Navile and Sa Pruna segmental balanced cantilever bridges (Figure 31). They concluded that larger than expected deflections and higher stresses in the ribs were obtained due to the prestressing of the bottom slab cables. In addition, they show a significant influence of creep in cantilever construction as well as non-uniform drying shrinkage on the completed bridge [41]. Akbar and Carlie (2021) investigate the effects of creep and shrinkage on the long-term deformations of balanced cantilever bridges [42].

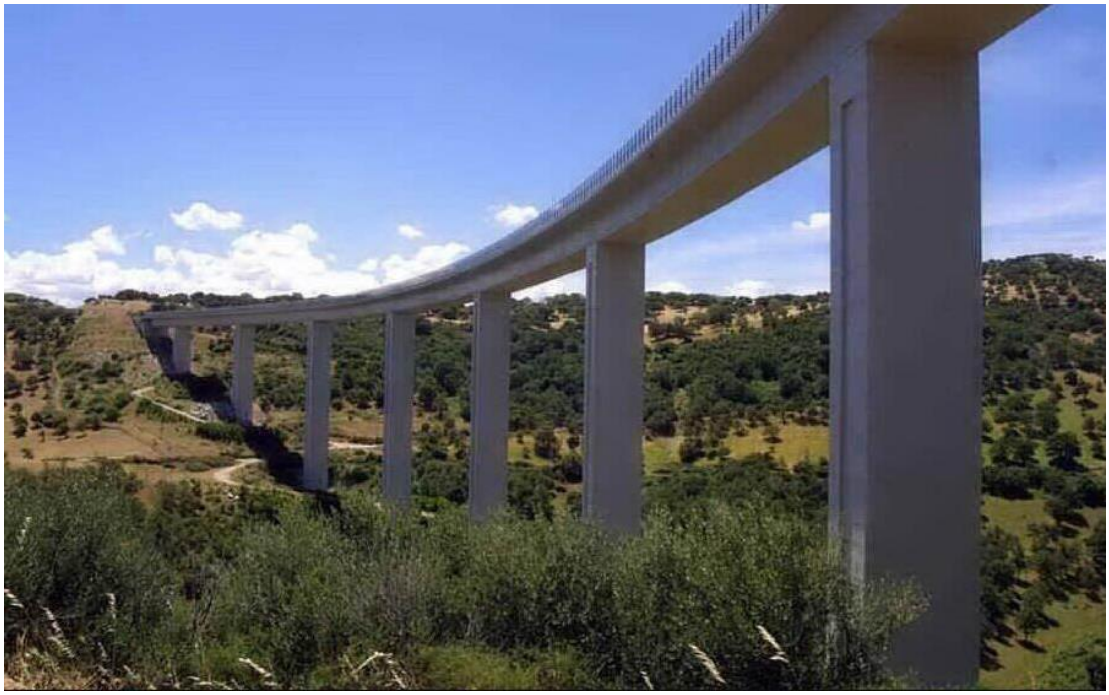

*Figure 31.* Navile Bridge
(https://www.highestbridges.com/wiki/images/d/d2/Navile4.jpg)

Construction aspects of real bridges are a major research focus, using mostly experimental onsite tests and analyses to cover critical errors, precamber and deflection issues before and after stitch segments, concrete installation and various construction processes.

McDonald et al. (2003) investigate the collapse of the Koror-Babeldaob Bridge in Palau. An analysis of the field inspection was performed and calculations of the bridge before and after reconstruction were made. The result of the analysis shows that the most likely cause of the collapse is damage during the removal of the original concrete road surface [43]. Radić et al. deal with precamber and deflections of balanced cantilever bridges, and provide an expression for the approximate calculation of the required precamber [44].

Jung et al. (2007) work on a simulation that uses field measurements to calibrate the numerical deflection results of balanced cantilevered bridges. The quality of the calibration depends on the experience of the engineer on site, and it is important for the correct joining of the bridge [45]. In the same year, Kronenberg studies the continuous installation of concrete in balanced cantilever bridges. As an example, he cites the Hacka bridge in the Czech Republic, which was completed after only two years of construction (Figure 32) [46].

*Figure 32.* Hacka Bridge
(https://www.kudyznudy.cz/aktivity/bungee-jumping-z-mostu-pres-udoli-hacky)

Kamaitis investigates the connections between segments in prefabricated balanced cantilever bridges. The research covers 5 major bridges, classification and statistics of joint problems [47]. Starossek (2009) presents the project of phase I construction of the Shin-Chon balanced cantilever post-tensioned bridge in Korea [48]. Furunes (2021) analyses aspects of the construction of the 260m-span Trysfjord Bridge in Norway using the balanced cantilever process and implementing programming into design (Figure 33) [49].

*Figure 33.* Trysfjord Bridge
(Vidar Moløkken/Multilux AS, https://www.multiconsultgroup.com/projects/tres-fjord-bridge/)

## 1.5. Dissertation goal and contents

With a few exceptions, the majority of previously mentioned articles show research done on completed post-tensioned concrete bridges, and a very small number of research was carried out on bridges under construction, following all the stages that the bridge goes through during construction. The research yields useful insight into post-tensioned balanced cantilever concrete bridges. Wind experiments produced a procedure for dynamic response predictions, and showed that wind loads can prove critical and must not be ignored in some cases. Numerical analysis of vertical displacements in the ground near faults showed that the vertical movements significantly affect the seismic behaviour of the bridge. Research done on reliability, rehabilitation and behaviour identify common problems like poor concreting and reinforcement detailing, as well as providing insight to the real structural capacity of the bridges.

On the topic of design, important span ratios and superstructure optimisation is shown, and an expression to obtain bending moment variations by elastic analysis without creep and construction phases is produced. The importance of time-dependant effects of creep and shrinkage during construction phases and exploitation is emphasized. The research shows that time-dependant effects, as well as material and geometric nonlinearities should be taken into account to properly describe the flow of forces and stresses, deflections, as well as general structural behaviour. Importance of precamber of structure and correct calculation in order to properly join the bridge is highlighted, and an expression to calculate the precamber is given. Different bridges were monitored during construction and various problems and solutions are presented.

The balanced cantilever construction process is complex in terms of stress, strain, deformation, geometry (deflection) and safety changes during its construction and use. Each segment of the bridge has differently aged concrete and thus different rheological characteristics: strength, modulus of elasticity, deformations, shrinkage and creep parameters, etc. These characteristics depend on the type of concrete, segment construction duration and the timing of prestressing, formwork release and form traveller position change.

In addition, a number of previously listed studies show that the behaviour of bridges built using the balanced cantilever method is a continuous topic of research by the academic and professional community. The accelerated construction of road and railway bridges, with greater spans and more demanding geometry, places greater demands on engineers, designers and contractors in terms of saving materials, reducing the cost and speed of construction, while maintaining the same level of mechanical resistance, stability and reliability. Knowing the exact flow of forces in them becomes the primary task of the designer.

As can be seen from recent research, predicting the behaviour of post-tensioned concrete bridges to all the loads that act on them, left the domain of the classic engineer and the usual linear models from commercial computer programs for structural calculations long ago.

Research generally moves in two directions. The first direction is the examination of constructed bridges with the aim of determining their behaviour, which is usually carried out in situ, on real objects. Such research, although not rare, is unfortunately usually carried out on already built structures, where the influence of the construction method and the changes in the flow of forces that arise with it can only be concluded from the final state of stress and deformation. Another direction is the creation of specific numerical models that are calibrated with data measured in situ, thus creating reliable models that can realistically describe the behaviour of the structure.

The dissertation aims to conduct a comprehensive analysis of the effects of the balanced cantilever construction method on cast-in-place post-tensioned concrete bridges. The primary focus of the analysis is on monitoring the strain and stress in both the concrete and prestressing steel of two bridges with different spans but similar features. This involves a detailed examination of how the application of the balanced cantilever construction method influences the structural behaviour of the bridges during the construction phase and subsequent to completion.

To achieve this, the dissertation proposes the implementation of an extensive monitoring system. This system will track and record the variations in strain and stress at key points throughout the construction process and during the service life of the bridges. The data collected will then be compared with numerical models of the bridges, allowing for a rigorous assessment of the accuracy and reliability of these models.

The inclusion of two bridges with different spans introduces a comparative element to the study. By examining bridges with varying spans but similar characteristics, the research aims to identify any trends, patterns, or differences in the impact of the construction method on structural performance. This comparative analysis adds depth to the findings and enhances the generalizability of the conclusions.

Ultimately, the research seeks to provide valuable insights into the behaviour of cast-in-place post-tensioned concrete bridges constructed using the balanced cantilever method. The combination of field monitoring and numerical modelling is anticipated to yield a holistic understanding of the construction method's implications, enabling the derivation of practical conclusions that can contribute to the improvement of future bridge construction practices.

## 1.6. Methodology

The methodology of this scientific research is predominantly grounded in experimental research, leveraging state-of-the-art equipment to measure strain and deflection in the context of bridge construction. The use of contemporary tools, such as measuring devices and strain gauges based on changes in electric resistance, ensures precision and reliability in data collection. Additionally, equipment for gathering and processing data is employed to streamline the experimental process and enhance the accuracy of the results.

The experimental research is conducted based on meticulously devised plans and research programs, aligning with the latest advancements in experimental methodologies. This approach is crucial for ensuring the relevance and applicability of the findings to the current state of bridge construction practices. By adhering to modern developments in experimental research, the study aims to provide insights that are not only scientifically rigorous but also directly applicable to real-world scenarios.

The emphasis on properly planned and successfully executed experimental research is highlighted, as it is posited to yield more accurate results than relying solely on numerical models. Experimental research allows for the direct observation of the physical behaviour of the structures under consideration, providing a tangible and empirical basis for analysis. This approach is particularly important when studying the impact of the balanced cantilever construction method on bridges, as it involves on-site measurements and observations during the construction process.

The mention of modern and quality equipment for structure testing underscores the commitment to precision and reliability in the experimental phase. The conducted experimental research is positioned as a control to the numerical models. This means that the empirical data gathered from the experiments will be compared with the predictions and simulations generated by numerical models. Any disparities or differences in results attributable to the balanced cantilever construction method will be identified and analysed. This comparative aspect enriches the research by offering a comprehensive understanding of how well numerical models align with real-world observations.

In summary, the research methodology prioritizes experimental research using cutting-edge equipment to measure strain and deflection, aligning with contemporary experimental research practices. The combination of rigorous planning, quality equipment, and a comparative approach with numerical models aims to provide a robust analysis of the impact of the balanced cantilever construction method on concrete bridges.

## 1.7. Expected scientific contribution

The research conducted in the dissertation integrates both experimental and numerical approaches to gather comprehensive insights into the behaviour of cast-in-place post-tensioned concrete bridges constructed using the balanced cantilever method.

The dissertation places significant emphasis on experimental research, particularly by collecting strain data from two distinct cast-in-place post-tensioned concrete bridges constructed with the balanced cantilever method. The utilization of real-world data is crucial for understanding the actual performance of these structures during and after construction. The strain data obtained experimentally provides a tangible and direct observation of the physical behaviour of the bridges. This information serves as a valuable basis for drawing conclusions about the structural response to the balanced cantilever construction method.

Complementing the experimental approach, numerical research is employed to create, confirm, and calibrate models. The numerical models are essential for simulating the behaviour of the bridges under various conditions. The dissertation aims to not only validate existing numerical models but also to allow new ones to be created, checked and calibrated based on the experimental strain data.

These numerical models are instrumental in predicting and understanding the impact of the balanced cantilever construction method on the structural integrity of the bridges. Additionally, the numerical research is anticipated to yield broader insights into the behaviour of the structures beyond the specific context of the construction method.

The synthesis of experimental and numerical research is designed to provide meaningful and applicable conclusions. These conclusions contribute to a better understanding of the structural behaviour of post-tensioned concrete bridges during and after construction, specifically when employing the balanced cantilever method. The findings not only validate the reliability of numerical models but also offer practical guidelines for the design and construction of future balanced cantilever bridges. By leveraging both types of research, the dissertation aims to bridge the gap between theoretical models and real-world performance, enhancing the overall knowledge in the field and informing best practices for future infrastructure projects.

The dissertation adopts a holistic approach by combining experimental and numerical research to gain nuanced insights into the structural behaviour of cast-in-place post-tensioned concrete bridges. The integration of these methodologies aims to provide not only a thorough understanding of the impact of the balanced cantilever construction method but also practical guidelines for the design and construction of resilient and efficient bridges in the future.

# 2. EXPERIMENTAL RESEARCH OVERVIEW

## 2.1. Overview of tested bridges

The research was conducted on Vranduk 1 and Vranduk 2 bridges, which are located in Bosnia and Herzegovina on motorway corridor Vc, section Zenica Municipality Northern Administrative Border (Nemila) to Zenica North (Donja Gračanica), subsection Vranduk – Ponirak. The route of the subsection is bound to the Bosna river valley as much as the technical elements and terrain conditions allow it, since the river valley is almost entirely occupied by the existing road Doboj – Zenica and railroad Vrhpolje/Šamac – Sarajevo with several local roads. Bosna river makes an S turn in the area and both bridges cross the river. Each motorway direction has its own construction so there are left and right Vranduk 1 and Vranduk 2 bridges. The measuring instruments are placed on Vranduk 1 right bridge and Vranduk 2 left bridge on superstructure base segments above S1 piers.

Vranduk 1 right bridge starts at station km 1+280.00 to km 1+670.00 (Figure 34). Starting at station 1 + 280.00 in the length of 76.292 m to station 1 + 356.292 is a constant left curve of 755.75 m radius, which continues in the transition curve 92.5 m long at 1 + 448.792. After that there is a transient curve 86 m long to 1 + 546.049 which passes to the constant right curve of 694 m radius in the length of 123.951 m to the end of the bridge to the station 1 + 670.00. The warping is carried out on a 50 m length, 25 m left and right from the crossing slope 2.5% to the left to the cross slope 2.5% to the right. Vertical alignment in the beginning is almost 0% and gradually falls to 1.89%. Width of the roadway is 12.00 m, and the width of protective barriers is 0.46 m. Total bridge width is 0.46 + 1.00 + 2.50 + 3.75 + 3.75 + 0.25 + 0.75 + 0.46 = 12.92 m.

*Figure 34.* Vranduk 1 left and right bridge

The bridge has a prestressed concrete superstructure with spans 80.00 + 120.00 + 120.00 + 70.00 = 390.00 m (Figure 35). Span construction has a box cross section with variable height in main spans and constant height on the rest of the bridge (parts of span built on scaffolding near the abutments). Height of section changes parabolically from 6.80 m on the main piers to 3.20 m in the middle of the span, while the height on the rest of the bridge towards abutments is a constant 3.20 m.

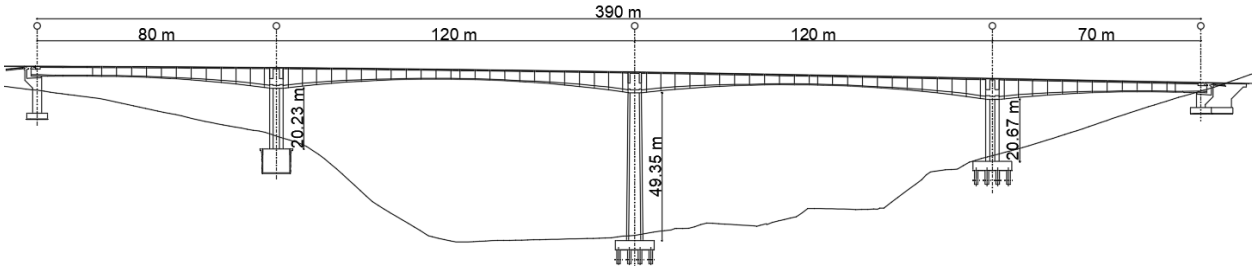


*Figure 35.* Vranduk 1 right bridge longitudinal section

The top slab and box cantilevers have the same shape along the entire bridge, with a thickness of 0.55 m in joint with the web, 0.25 m at the ends of cantilevers and 0.30 in the centre of the box. The box webs are 0.50 m thick with thicknesses of 0.65 m above the piers. Thickening of the webs is done at a slope, 11.25 m from the edge of the piers. The bottom slab is 0.30 m thick (Figure 36). Edges of bottom slab are thickened in the length of 0.60 m to 0.42 m. The bottom slab is thicker on the supports, so above the abutments the thickness increases in the length of 5.00 m up to 0.50 m, while at the connection with the main piers it has a thickness of 1.00 m, which changes at a length of 36.25 m from the edge of the pier. Above the piers in the span construction there are two transverse diaphragms of 0.70 and 0.60 m thick, which are mapped out by the outer contours of the pillar, with openings at the bottom 2.00 m high and 1.20 m wide. Above the abutment bearing diaphragm thickness is 3.00 m, height 1.70 m and width 1.20 m. The middle piers are monolithically connected to the span structure, while the abutments have 2 bearings.

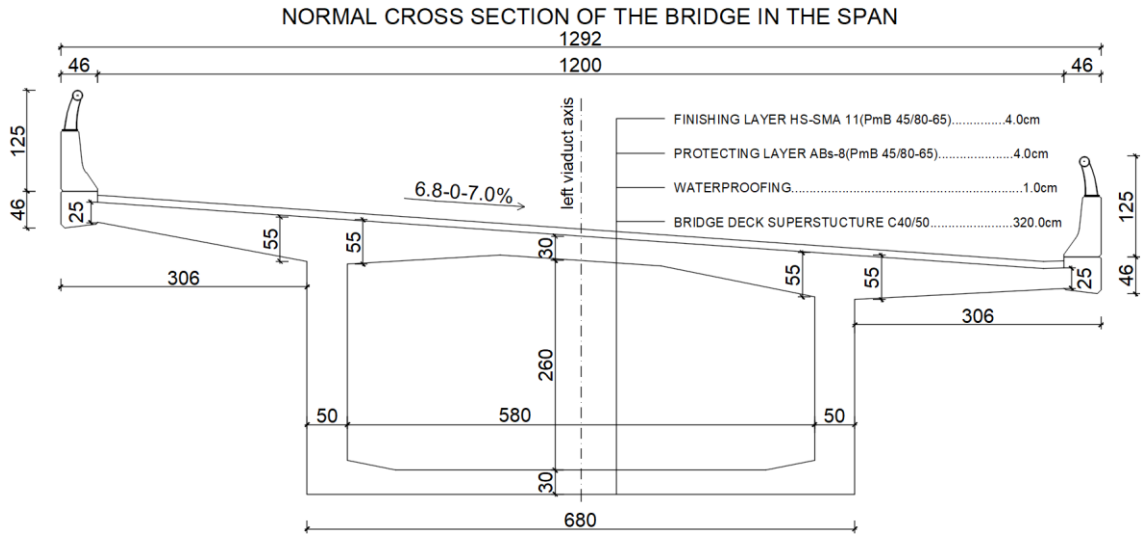


*Figure 36.* Vranduk 1 bridge characteristic cross section

Pier S2D has a box cross-section 6.80 x 4.50 m in contact with the span construction that follow a 100:1 widening slope to ground contact. The middle pier (S2D) has a wall thickness of 0.70 m, while piers S1D and S3D consist of two parallel walls. Walls on S1D are 1.20 m thick and walls on S3D are 1.40 m thick. The pier S1D is based on a round well foundation with a diameter of 9.00 m and a well depth of 8.00 m. The S2D pier is placed on 16 piles 1.20 m in diameter ,9 m long that are connected to a 13.00 x 13.00 x 3.00 m base slab. The S3D pier is placed on 16 piles 1.20 m in diameter ,19 m long that are connected to a 13.00 x 13.00 x 3.00 m base slab.

The U1D and U2D abutments are located on the embankment and are placed on shallow foundations. U1D abutment has a side wing wall that is founded on 8.00 x 3.50 x 2.00 m foundation. The main wall foundation is 13.92 x 7.00 x 2.00 m. The wall thickness is 3.00 m and there are two bearings on which the structure will be supported. On the left side there is no side wing wall. The U2D abutment foundation has a base dimension of 13.92 x 7.00 x 2.00 m with a 4.40 m high main wall 3.00 m thick on which 2 bearings will be placed. There is a right wing wall, founded on a 7.23 x 3.50 x 2.00 m foundation. There is no right side wing wall. The abutments have approach slabs 4.00 m in length at an incline of 10%.

The bridge has been designed according to EN rules for a design life of 100 years. The superstructure and piers are made with C40/50 concrete, and the rest of the structure (piles, pile slabs, well, abutments) are made with C30/37. Reinforcing steel is B 500B and prestressing steel is Y1860 [50].

Vranduk 2 left bridge starts at station km 1+816.00 to km 2+156.00 (Figure 37). The bridge starts with a straight part, from station 1+816.00 to 1+840.75 and is 24.75 m long. After that comes a transition curve (chlothoid) 197.00 m long to 2+019.75 which becomes a constant left curve to the end of the bridge with a radius of 987.50 m, 136.24 m long to 2+156.00. Cross slope of the bridge on abutment U1L is 2.5% and is gradually increased to 4.0% on the end of transition curve and it stays constant to the end of the bridge. Width of the roadway is 12.00 m, and the width of protective barriers is 0.46 m. Total bridge width is 0.46 + 1.00 + 2.50 + 3.75 + 3.75 + 0.25 + 0.75 + 0.46 = 12.92 m.

*Figure 37.* Vranduk 2 bridge under construction

The bridge has a prestressed concrete superstructure with spans 95.00 + 150.00 + 95.00 = 340.00 m (Figure 38). Span construction has a box cross section with variable height in main spans and constant height on the rest of the bridge (parts of span built on scaffolding near the abutments). Height of section changes parabolically from 8.40 m on the main piers to 4.00 m in the middle of the span, while the height on the rest of the bridge towards abutments is a constant 4.00 m.

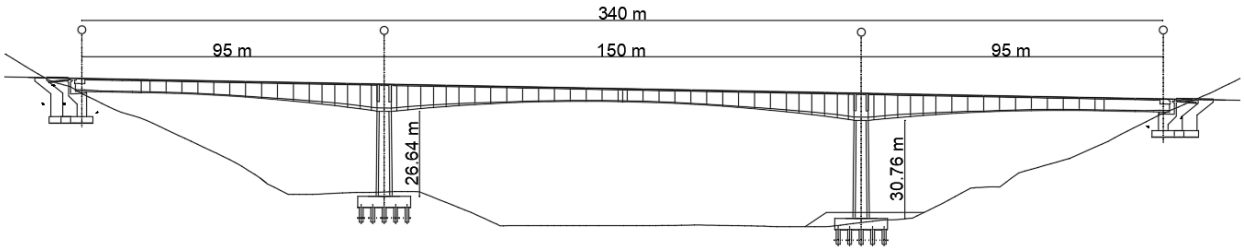


*Figure 38.* Vranduk 2 left bridge longitudinal section

Top slabs and box cantilevers have the same shape along the bridge, with thickness 0.55 m on joint with the webs, 0.25 m on the ends of cantilevers and 0.30 m in the middle of the box. Webs are 0.50 m thick and are thickened to 0.65 m above the piers. Web thickening is done 13.25 m from the edge of the pier. Top slab is 0.30 m thick with thickenings in length of 1.75-1.90 m to the web where it is 0.55 m (Figure 39). Bottom slab is thickened at the supports, above the abutment in 5.00 m length slab is thickened to 0.50 m, while on piers it is 1.00 m, changing in the length of 31.25 m. Two diaphragms stand above piers 0.70 m thick and follow outer contours of the pier. Diaphragms have 2.00 x 1.00 openings. Above the abutment bearings diaphragm is 3.00 m thick with an opening 1.85 x 1.00. Centre piers are monolithically connected to the span structure, and each abutment has 2 bearings.

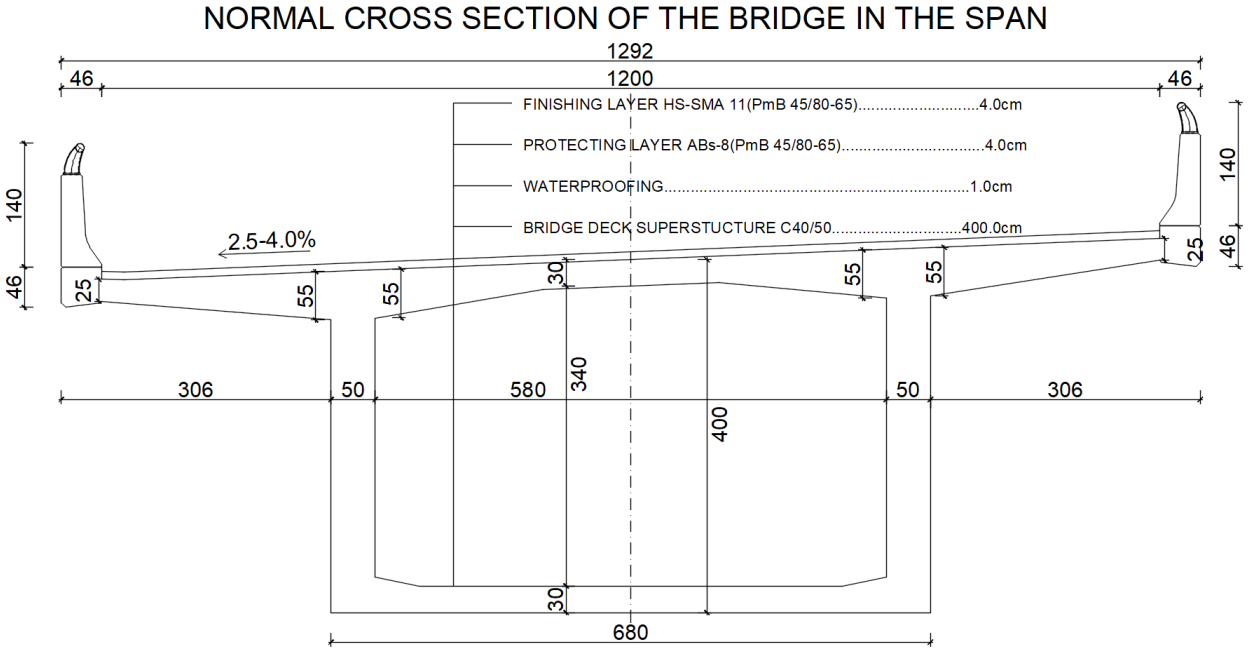


*Figure 39.* Vranduk 2 bridge characteristic cross section

Piers have 6.80 x 4.50 m box cross section on intersection with the span construction and the dimensions are widened in inclination 100:1 to the ground level. All piers have walls 0.70 m thick. Piers are built on 20 piles that are 1.20 m in diameter and have lengths of 12 m for S1L and 12 m for S2L. They are connected to 16.60 x 13.00 x 3.50 m pile slabs.

Abutments U1L and U2L are situated next to an embankment and have shallow foundations. Abutment U1L has a 13.92 x 7.00 x 2.00 m foundation with a main wall 7.28 m high and 3.00 m thick. Bearings will be placed on top of the wall. Abutment wings have a 3.00 and 6.74 m long foundation with same dimensions as abutment wall foundation. Side wing walls are partly founded. Abutment U2L has a 13.92 x 7.00 x 2.00 m foundation with a wall 5.24 m high and 3.00 m thick. Bearings will be placed on top of the wall. Abutment wings have a 3.00 m long foundation with same dimensions as abutment wall foundation. Side wing walls are partly founded. The abutments have approach slabs 4.00 m in length at an incline of 10%.

The bridge has been designed according to EN rules for a design life of 100 years. The superstructure is made with C40/50 concrete, and the rest of the structure (piers, piles, pile slabs, well, abutments) are made with C30/37. Reinforcing steel is B 500B and prestressing steel is Y1860 [51].

## 2.2. Monitoring plan and measuring equipment installation

The monitoring on both bridges was done on base segments of first piers. Only two strain monitoring devices were available, each with a total of 8 measuring points. Because of this the bridges are monitored in only one section on the base segment that allows us to follow the construction process though all phases and measure strain changes in concrete and prestressing steel. The monitoring began on March 25th 2021 and ended on September 17th 2021. The goal was to have a continuous strain data acquisition throughout the construction phase of cantilevers on S1 piers, as well as after the cantilevers were connected and span tendons prestressed. Following Hooke's law stress of the materials can be assumed using strain and Young's modulus of elasticity.

Measuring equipment of German company HBM was used for data acquisition systems and strain gauges, in this case electrical strain gauges that consist of carriers, covering foils, measuring grids and connections. The gauge is fixed to the structure with strong adhesives to ensure equal deformations. Weak electrical current is passed through the measuring grid which gives the reference resistance. Deforming the grid by stretching or compressing changes its resistance.

If the gauge sensitivity factor is known (relation between strain and resistance differences) the strain can be calculated through resistance difference. All used gauges measure strain in one direction (linear gauges) and have a nominal resistance of 120 Ω. For concrete, gauges with 50 mm measuring grid were used because of heterogeneous nature of material. For prestressing steel, gauges with 3 mm measuring grid were used because the material is homogenous and a gauge this size can fit on a prestressing steel wire. QuantumX 840A was used as a data acquisition system. The device has 8 input channels (via 15-pin connectors) and supports half and full Wheatstone bridge configurations for multiple measuring purposes. In this case a quarter Wheatstone bridge configuration was used with special adapters. Precise 120 Ω metal-film resistors were connected in the 15-pin connectors to form a Wheatstone full bridge configuration with the strain gauge. The adapter was located near the strain gauge (15-20 cm) to reduce measuring deviations due to additional resistance in cables that lead from strain gauge to the adapter (Figure 40).

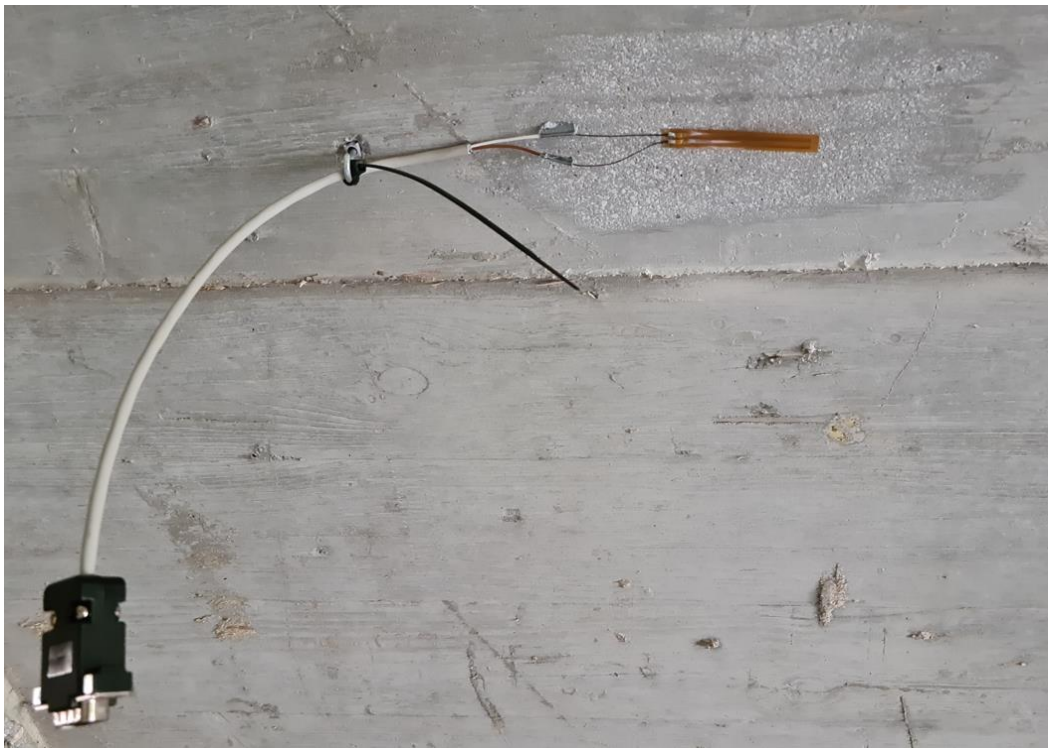

*Figure 40.* Strain gauge with the adapter

All of the strain gauges have been prepared in advance. Depending on the measuring point, 8 extension cables with lengths 17.00 to 24.00 m were made with a male 15-pin connector on one end, and a female 15-pin connector on the other. The strain gauges were soldered on one end of the adapters, and were connected to QuantumX 840A data acquisition system which has an accuracy of 0.05% and can measure up to 40 000 samples per second through extension cables (Figure 41). The universal amplifier QuantumX was connected to a computer through a LAN cable and utilised the CatmanEasy software for data acquisition, storage and analysis. Both the computer and universal amplifier were connected to an uninterruptable power supply which protected from short term power disruptions. The UPS was connected to 220 V power network.

*Figure 41.* QuantumX 840A data acquisition system

Strain gauges for both bridges were applied on concrete and prestressing steel in the same cross section of the superstructure. The section is moved 0.50 m from the edge of diaphragms towards the span to lessen its effect on strain. A total of 16 strain gauges were installed.

On Vranduk 2 bridge eight strain gauges were measured in a section 0.50 m away from the diaphragm toward the span (Figure 42). Four strain gauges were installed on concrete, specifically in the inner corners of the superstructure box cross section. The gauges were offset 0.50 m from the webs of the cross section. Four strain gauges were installed on prestressing steel wires, two on prestressing tendons for construction stage of segment 1, and two on prestressing tendons for construction stage of segment 7 (Figure 43). The gauges did not compensate for temperature change strain.

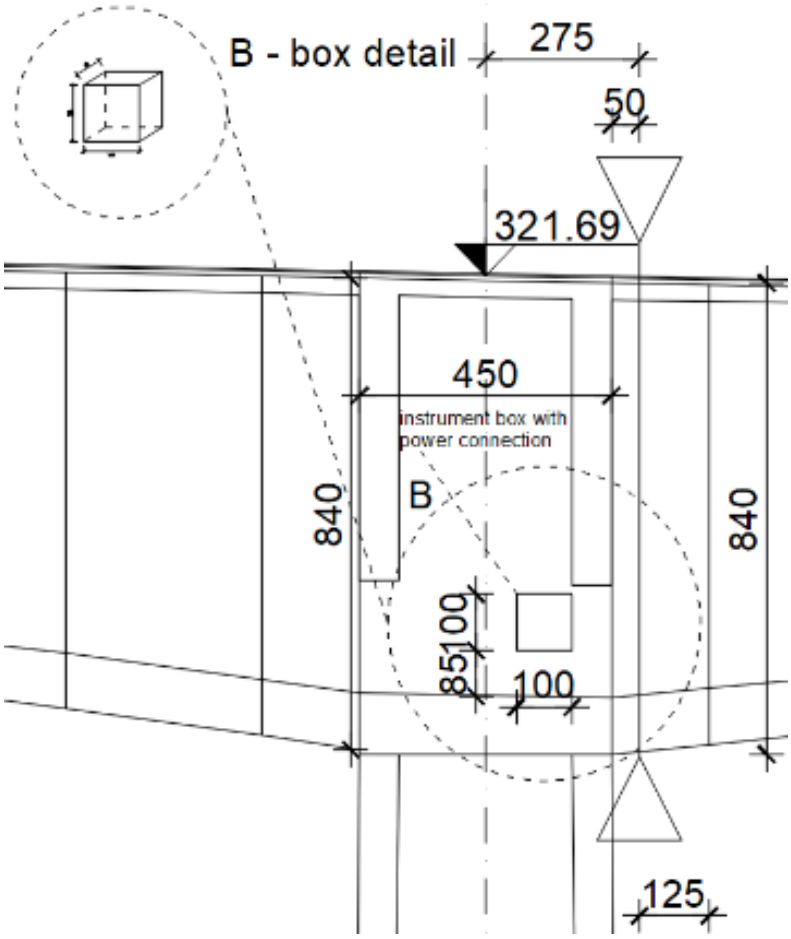


*Figure 42.* Vranduk 2 longitudinal strain gauge section position

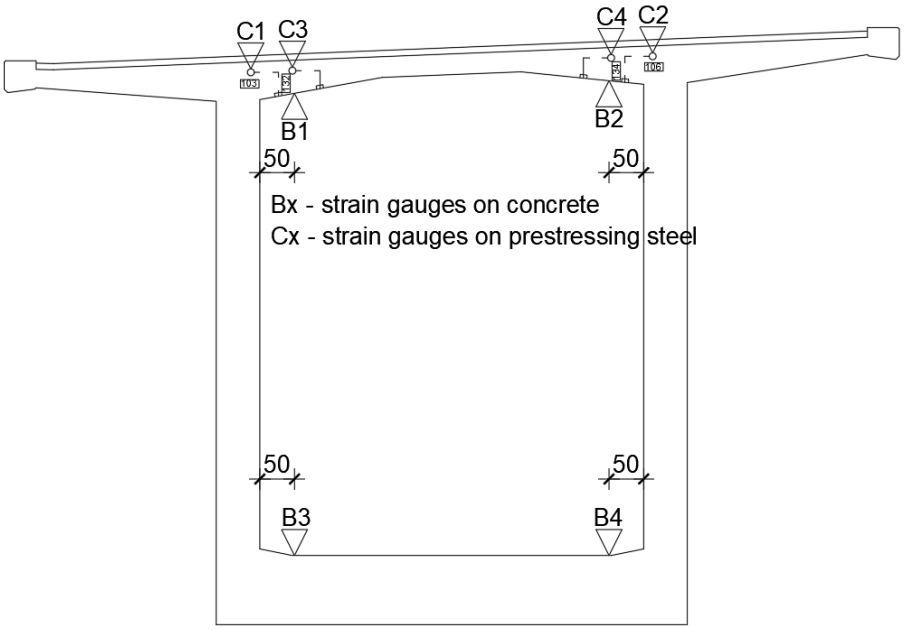


*Figure 43.* Vranduk 2 strain gauge position in the cross section

On Vranduk 1 bridge eight strain gauges were measured in a section moved 0.50 m outside the diaphragm towards the span (Figure 44). Four strain gauges were installed on concrete in the corners of the cross section and two gauges on prestressing steel used for construction stage of the first segment (Figure 45). The gauges were offset 0.50 m from the webs of the cross section.

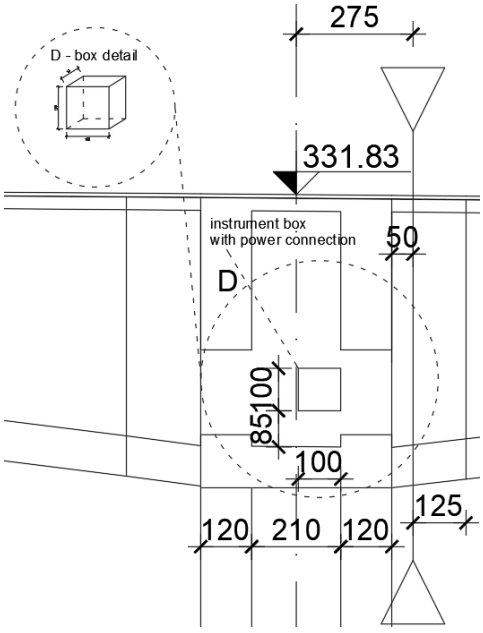


*Figure 44.* Vranduk 1 longitudinal strain gauge section position

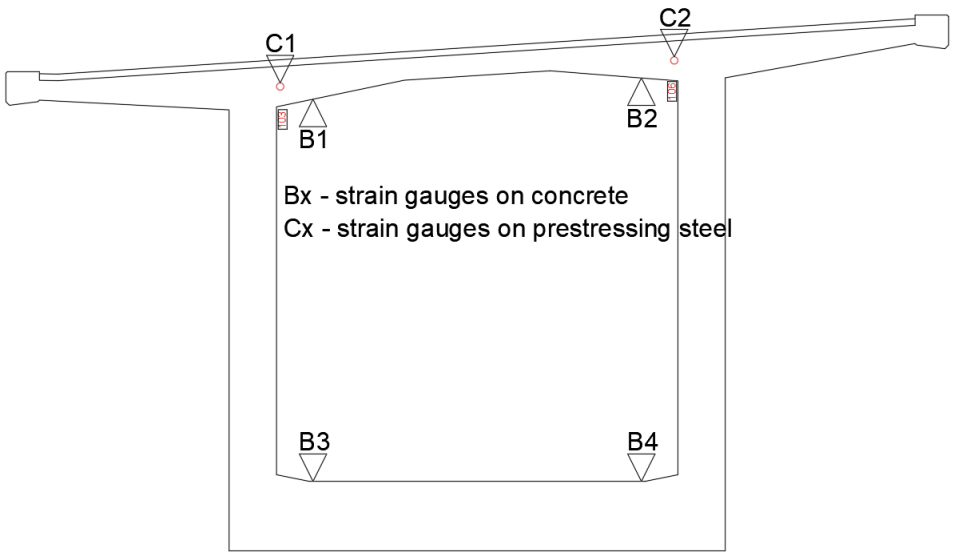


*Figure 45.* Vranduk 1 strain gauge position in the cross section

Two gauges were used for temperature compensation, one on unloaded concrete sample positioned near the upper slab (Figure 46) and one on unloaded prestressing wire sample placed next to prestressing cable (Figure 47).

*Figure 46.* Strain gauge on a concrete sample used for temperature compensation

*Figure 47.* Strain gauge on a prestressing steel sample used for temperature compensation

The procedure for installing strain gauges on concrete was identical for both bridges. Firstly, the concrete surface in the area where the gauge is fixed was grinded with a fine grinder to get a good surface for adhesive. This is especially important on the bottom slab because of the coarse concrete surface. On the top slab concrete is already very smooth because of the formwork. After grinding, a steel hook was anchored near the grinded area to hold the adapter and gauge before fixing, as well as to prevent accidental damage or disconnect during monitoring (Figure 48).

*Figure 48.* Surface prepared for gauge installation

The adapter was fixed to the hook with plastic zip ties. Next step was to clean the area with alcohol to remove leftover dust. Two component adhesive was mixed and applied to the concrete surface, and the strain gauge was put in the adhesive. Excessive adhesive was pushed out manually with the help of a plastic film to avoid sticking, and the adhesive was left to harden (Figure 49).

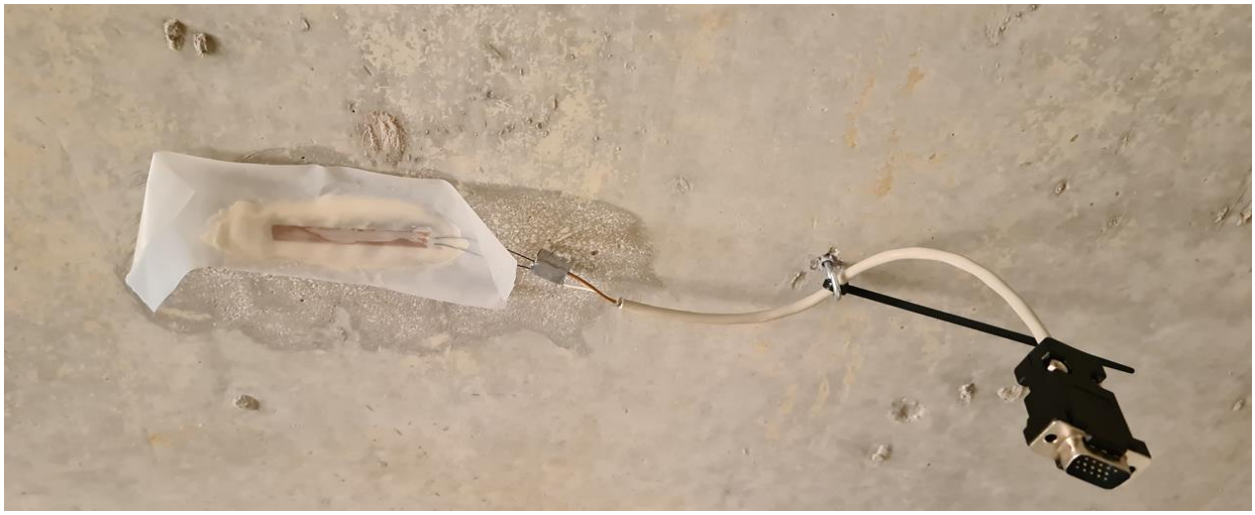

*Figure 49.* Installed gauge with the adapter after glue hardening

After hardening, a protective aluminium foil with kneading compound was put over the strain gauge and lead wires to protect from weather and smaller impacts. The edge of the aluminium foil was covered with silicone to completely isolate the strain gauge (Figure 50). Resistance of the gauge was checked through the adapter to ensure the installation was correct and the gauge works.

*Figure 50.* Strain gauge after protection

For strain gauges installed on prestressing steel alcohol was used to clean the area of the wire where the gauge will be applied. The strain gauges and adapters were fixed to the surrounding steel reinforcement bars with plastic zip ties. Cyanoacrylate super glue was applied to the gauge and the gauge was positioned on the wire and held in place with a thin plastic film. After hardening, a protective aluminium foil with kneading compound was put over the strain gauge and lead wires to protect from water (Figure 51). Resistance was checked to confirm no damage occurred during installation.

*Figure 51.* Strain gauge installation on prestressing cables (with temperature compensation)

After strain gauge installation the adapters were connected to the data acquisition system inside the pier head through extension cables which pass through openings in the diaphragm for gauges on concrete, and through plastic tubes left next to prestressing ducts for gauges on prestressing steel (Figure 52).

*Figure 52.* Box containing data acquisition equipment

# 3. NUMERICAL MODELLING AND RESULT COMPARISON

## 3.1. Numerical models of the bridges

Hybrid 3D FEM numerical models of Vranduk 1 and Vranduk 2 bridges have been made to obtain and compare results with measured stress/strain values. All models are done in computer software SOFiSTiK with respect to realistic bridge dimensions and construction stages. Two models are made for each bridge (four models in total), one model considering creep and shrinkage calculations between construction stages and the other one without creep and shrinkage. The goal was to determine the effect of creep and shrinkage on stress/strain values for these balanced cantilever bridges. A hybrid model consisting of structural lines and structural areas is adopted for both bridges to get a better overview of results. Most of the bridge is modelled with structural lines that are given proper cross-sections, while the pier head and S1 piers where the strains are measured are modelled with area elements to obtain accurate results (Figure 53 and Figure 54).

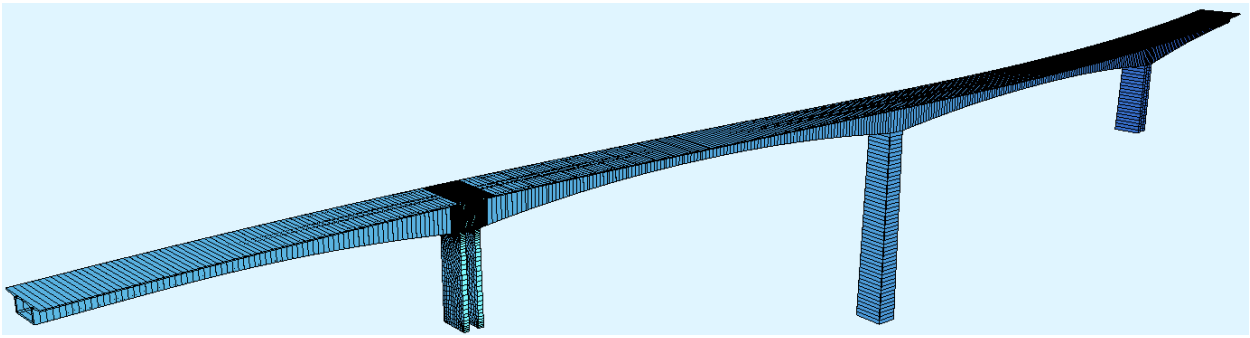

*Figure 53.* Vranduk 1 bridge model

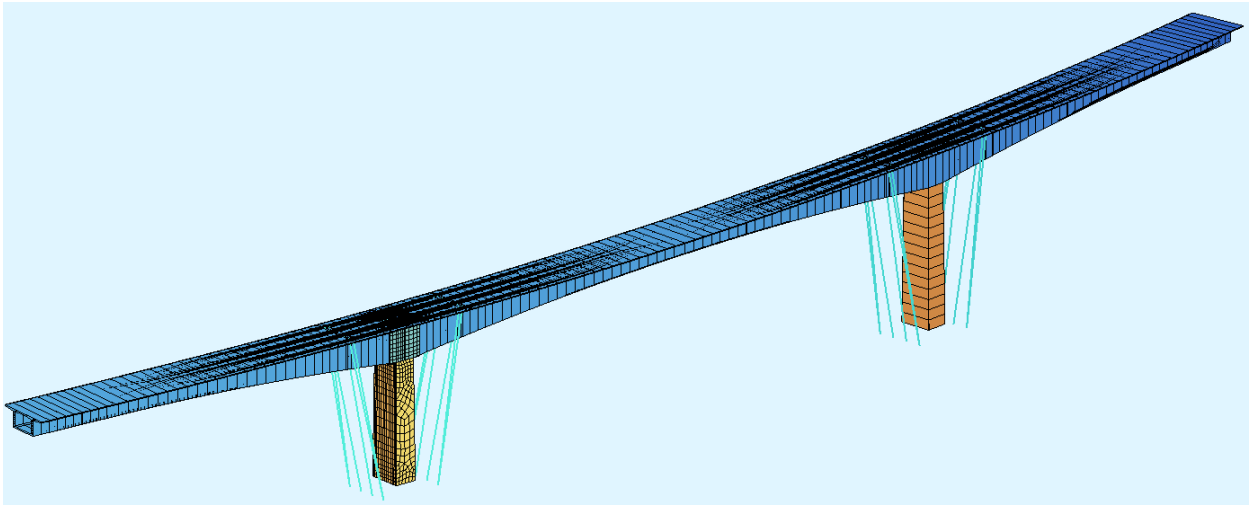

*Figure 54.* Vranduk 2 bridge model

The general layout of the bridges is taken from design drawings [50, 51]. Maximum longitudinal slope of 1.89% on both Vranduk 1 and Vranduk 2 bridge is omitted since it has a negligible effect on the structure. Horizontal curves are not insignificant and are taken into account when modelling the bridges for two reasons. On balanced cantilever bridges creep and shrinkage plays an important part in segment precamber calculations during construction and big bends will affect cable positioning and creep and shrinkage. The other reason is that the pier and its superstructure is a cantilever during construction. For concrete bridges self-weight is a dominant load and the eccentricity of such a load due to road bends and its effect on piers and foundations cannot be ignored. After inspecting the design drawings program SOFiPLUS is used to input the correct axis geometry. Placements (planes linked to a certain chainage on the axis) are input on the axes so segments of the bridge with different cross sections and prestressing cables can the defined. Horizontal curves are also linked to chainage on the axis (Figure 55).

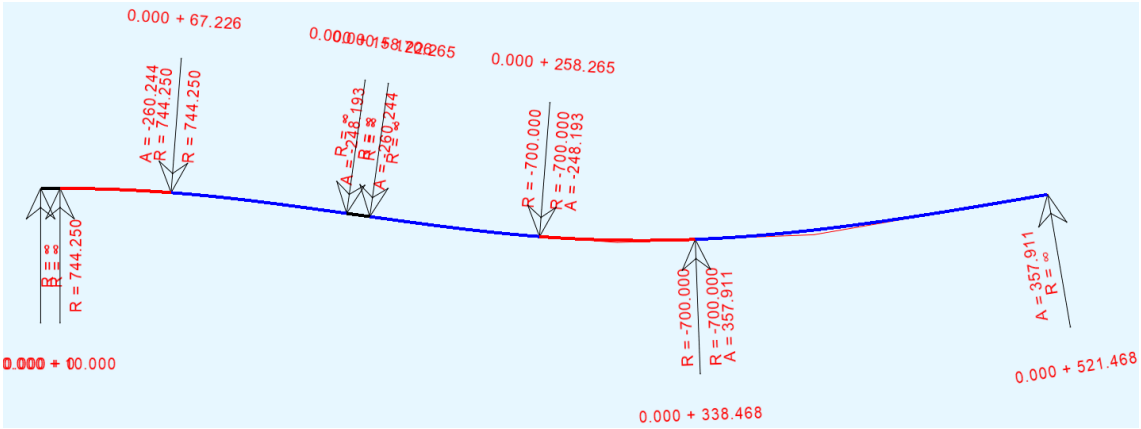


*Figure 55.* Vranduk 1 bridge horizontal axis allignement

After the layout has been set, pier and superstructure cross sections have been simplified and input. Pier cross sections remained the same since they were already simple. Superstructure sections have been modified so the box top slab is horizontal and has no cross slope since it has little effect on the structure and would require more time for input. The parapet has been simplified so that the top slab extends to the end of the parapet and the missing self-weight is added to additional weight in loads (Figure 56).

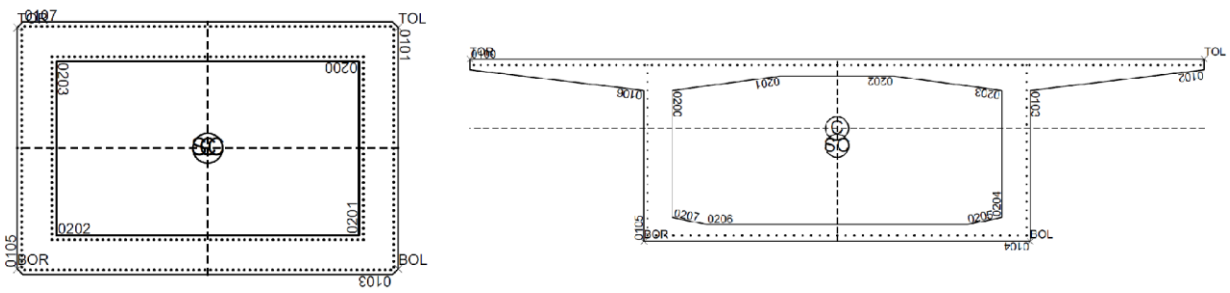


*Figure 56.* Example of generated cross sections: pier (left) and superstructure (right)

The superstructure is highest on piers and lowest in the middle of the spans. Upper box slab follows the longitudinal slope and is horizontal in the model, while the lower slab follows a parabolic trajectory. That means that every segment of the bridge cantilever has different start and end cross sections. In total 13 superstructure cross sections are input for Vranduk 1 bridge, and 17 for Vranduk 2 bridge (Table 1 and Table 2). Vranduk 1 superstructure and piers are input with C40/50 concrete and B500B reinforcement, while on Vranduk 2 the superstructure is input with C40/50 concrete and piers are input with C30/37 concrete. Reinforcement is B500B. Prestressing cables for both bridges are input with Y1860 prestressing steel.

*Table 1.* Vranduk 1 superstructure cross sections

| Section number | Distance from pier edge (m) | Section height (m) | Web thickness (m) | Lower slab thickness (m) |
|---|---|---|---|---|
| 1 | 0 | 6.80 | 0.650 | 0.950 |
| 2 | 1.75 | 6.58 | 0.627 | 0.950 |
| 3 | 6.5 | 6.02 | 0.563 | 0.950 |
| 4 | 11.25 | 5.50 | 0.500 | 0.846 |
| 5 | 16.25 | 5.02 | 0.500 | 0.737 |
| 6 | 21.25 | 4.59 | 0.500 | 0.628 |
| 7 | 26.25 | 4.22 | 0.500 | 0.518 |
| 8 | 31.25 | 3.91 | 0.500 | 0.409 |
| 9 | 36.25 | 3.66 | 0.500 | 0.300 |
| 10 | 41.25 | 3.46 | 0.500 | 0.300 |
| 11 | 46.25 | 3.31 | 0.500 | 0.300 |
| 12 | 51.25 | 3.23 | 0.500 | 0.300 |
| 13 | 56.25 | 3.20 | 0.500 | 0.300 |

*Table 2.* Vranduk 2 superstructure cross sections

| Section number | Distance from pier edge (m) | Section height(m) | Web thickness (m) | Lower slab thickness (m) |
|---|---|---|---|---|
| 1 | 0 | 8.40 | 0.650 | 1.000 |
| 2 | 1.75 | 8.19 | 0.630 | 1.000 |
| 3 | 5.25 | 7.78 | 0.591 | 1.000 |
| 4 | 9.25 | 7.33 | 0.545 | 0.910 |
| 5 | 13.25 | 6.92 | 0.500 | 0.819 |
| 6 | 17.25 | 6.53 | 0.500 | 0.729 |
| 7 | 21.25 | 6.17 | 0.500 | 0.639 |
| 8 | 26.25 | 5.76 | 0.500 | 0.526 |
| 9 | 31.25 | 5.39 | 0.500 | 0.413 |
| 10 | 36.25 | 5.06 | 0.500 | 0.300 |
| 11 | 41.25 | 4.78 | 0.500 | 0.300 |
| 12 | 46.25 | 4.54 | 0.500 | 0.300 |
| 13 | 51.25 | 4.35 | 0.500 | 0.300 |
| 14 | 56.25 | 4.20 | 0.500 | 0.300 |
| 15 | 61.25 | 4.09 | 0.500 | 0.300 |
| 16 | 66.25 | 4.02 | 0.500 | 0.300 |
| 17 | 71.25 | 4.00 | 0.500 | 0.300 |

After the cross sections were input, segments of the superstructure and piers have been formed as construction lines with start and end cross sections. When forming the finite element mesh the software interpolates cross sections between segment ends. Piers and abutments are connected to the superstructure with constraints. Bridge models are mostly line elements and in those sections connections are made with point constraints. On piers S1 for both bridges the pier and pier head is modelled with area elements and those sections are connected to the rest of the superstructure with point to line constraints (Figure 57 and Figure 58).

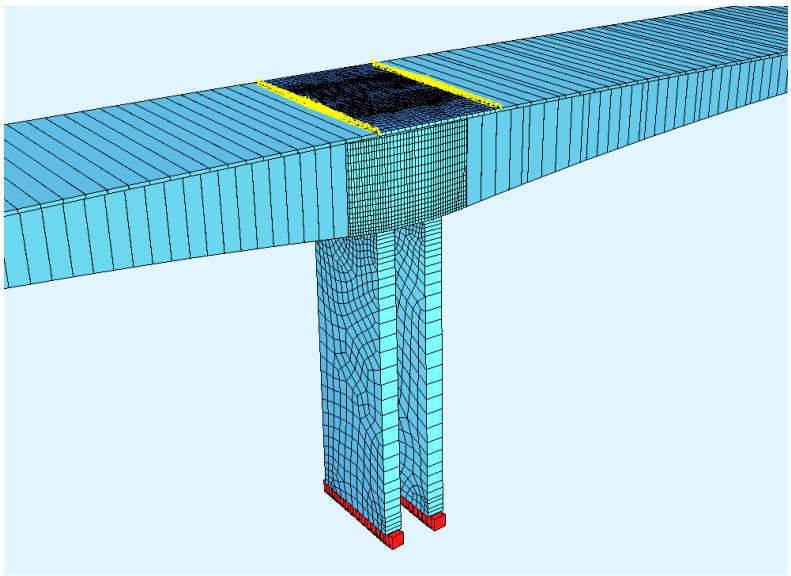

*Figure 57.* Vranduk 1 S1 pier

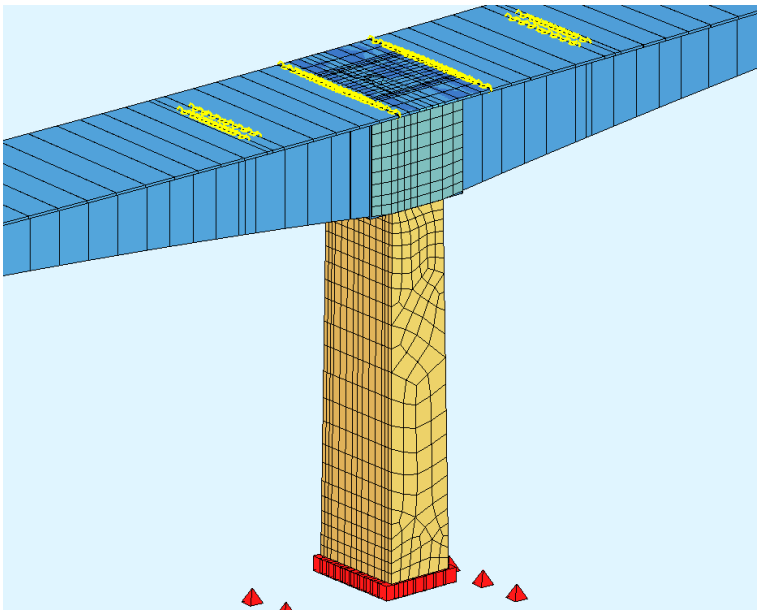

*Figure 58.* Vranduk 2 S1 pier

Structural areas are modelled with realistic geometry and slab thickness with the finite element mesh automatically generated and mostly regular. The abutments and foundations were not modelled since they have little effect on the structure, point and line supports are used to represent foundations. The piers have fixed supports and the abutments have roller supports that allow longitudinal movement and rotation.

All prestressing cables have been modelled individually for both bridges as post tensioned cables embedded in the concrete that are grouted immediately after prestressing, where in reality the grouting was done a day or two after prestressing. Each cable has 19 strands with 1.5 $cm^2$ area (each cable is 28.5 $cm^2$). All cables have a low relaxation value of 2.5 % after 1000 hours stressed at 0.7 * $f_{pk}$.

Vranduk 1 bridge has a total of 168 prestressing cables, 120 cables for balanced cantilevering construction stages in top slab of the superstructure cross section and 48 cables for exploitation phase in bottom slab in spans (Figure 59). Above each pier head there are 40 construction stage cables (20 per web) that are anchored on each finished segment of the structure. 6 cables are anchored on first and second segments, 4 cables on segments 3 to 7, and 2 cables on segments 8 to 11. In main spans there are 16 cables in lower slab (8 per web). These cables are anchored on segments 5 to 8 with 4 cables per segment. There are 8 cables in end spans (4 per web) with 4 cables anchored on two segments [50].

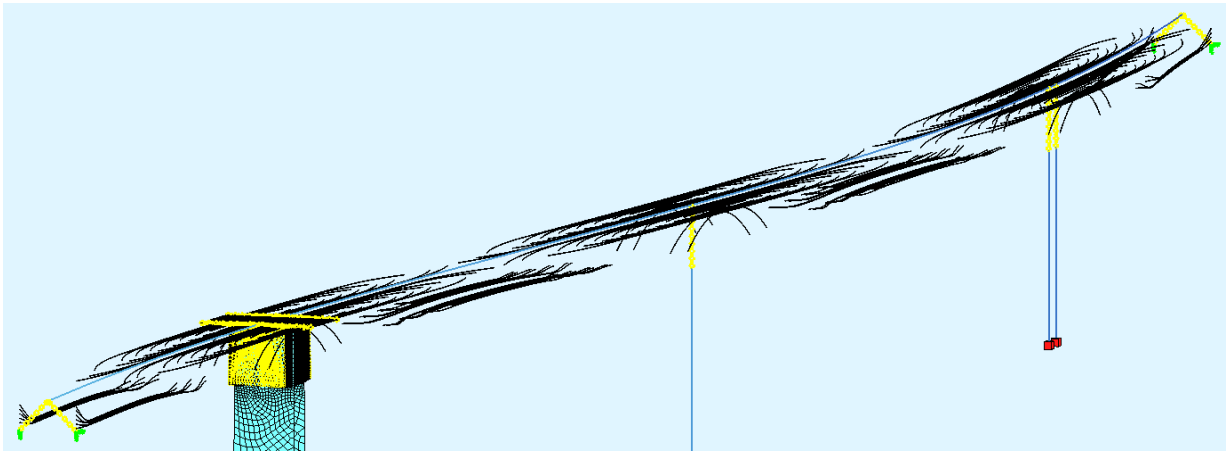

*Figure 59.* Vranduk 1 prestressing cables

Vranduk 2 bridge has a total of 174 prestressing cables, 124 cables for balanced cantilevering construction stages in top slab of the superstructure cross section and 50 cables for exploitation phase in bottom slab in spans (Figure 60). Above each pier head there are 62 construction stage cables (31 per web) that are anchored on each finished segment of the structure. 6 cables are anchored on segments 1 to 3, 4 cables on segments 4 to 13, and 2 cables on segments 14 to 15. In main span there are 20 cables in lower slab (10 per web). These cables are anchored on segments 8 to 12 with 4 cables per segment. There are 14 cables in end spans (7 per web) with 4 cables anchored on three segments and 2 cables anchored on one segment. In main span there are 2 cables in upper slab used for the closing segment in case of sudden temperature change or other accidental loads [51].

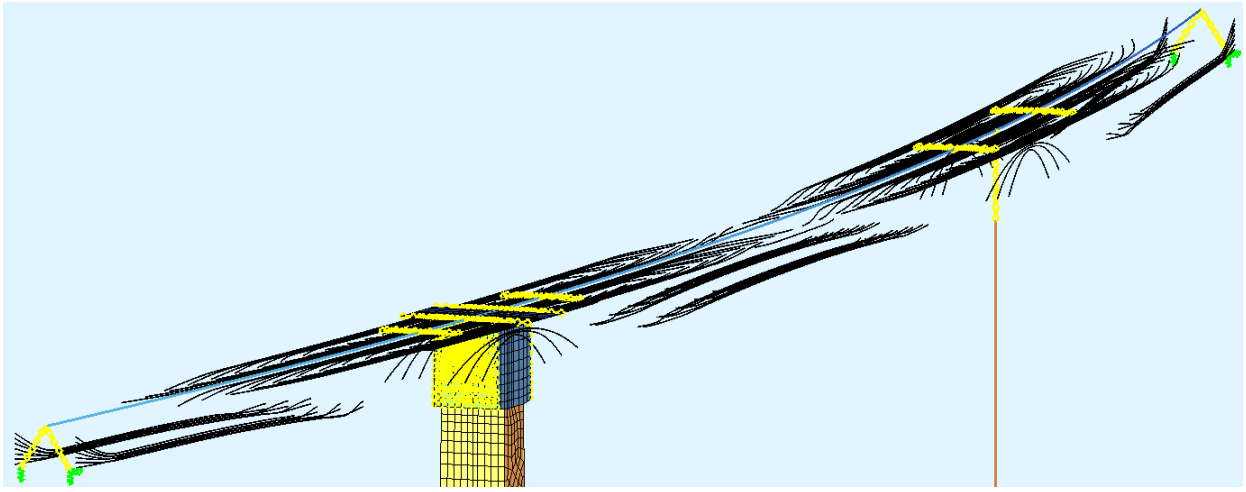

*Figure 60.* Vranduk 2 prestressing cables

Following loads that affect the bridge structures during and immediately after construction are taken into account: dead load of the structure segments, additional dead load per design drawings (parapets, concrete barriers, asphalt, waterproofing, drainage, installations), prestressing, creep and shrinkage and form traveller construction loads.

Construction stages are the most important part of a balanced cantilever bridge calculation since they determine the behaviour of the bridge before and after closing segments. Before the work can begin on the superstructure the pier and the pier head is constructed. After that real construction stages for superstructure segments are input in the program with the following general repeating order:

| | | |
|---|---|---|
| XX10 | S1-SEG1 | -segment dead load and stiffness activated |
| XX11 | S1-SEG1 prestressing | -prestressing of a previously activated segment |
| XX14 | S1-SEG2 form traveller | -form traveller is moved for the next segment |
| XX15 | C+S | -creep and shrinkage step |
| XX17 | S1-SEG2 fresh concrete | -concrete weight of next segment, no stiffness |
| XX20 | S1-SEG2 | -next segment dead load and stiffness activated |

Loads such as form traveller and fresh concrete are artificially moved by activating and deactivating the load for each segment as the construction stages progresses. Bridge Vranduk 1 has a total of 322 construction phases and Vranduk 2 has a total of 312 construction phases (Figure 61 and Figure 62).

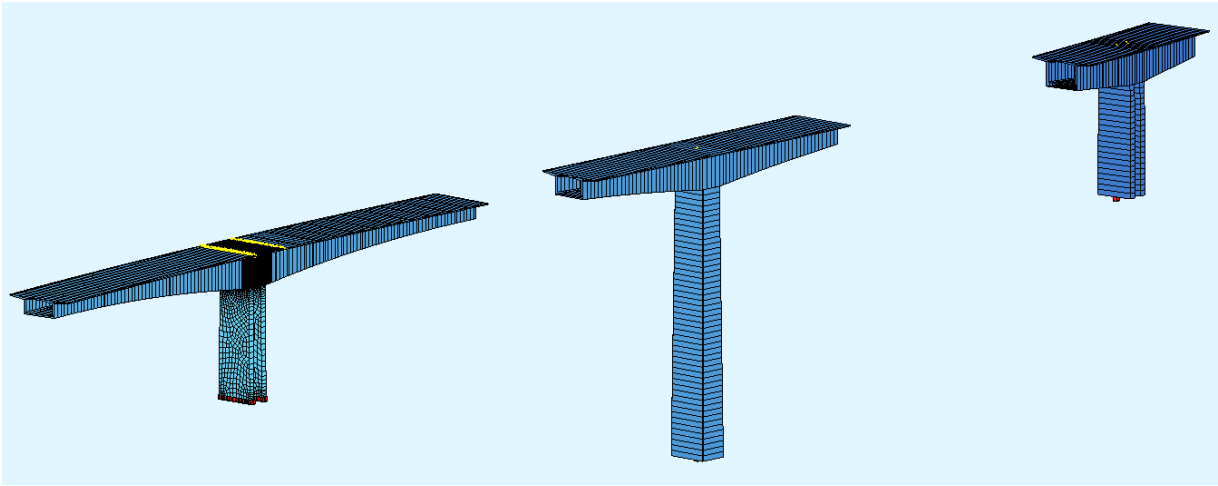

*Figure 61.* Vranduk 1 construction stage

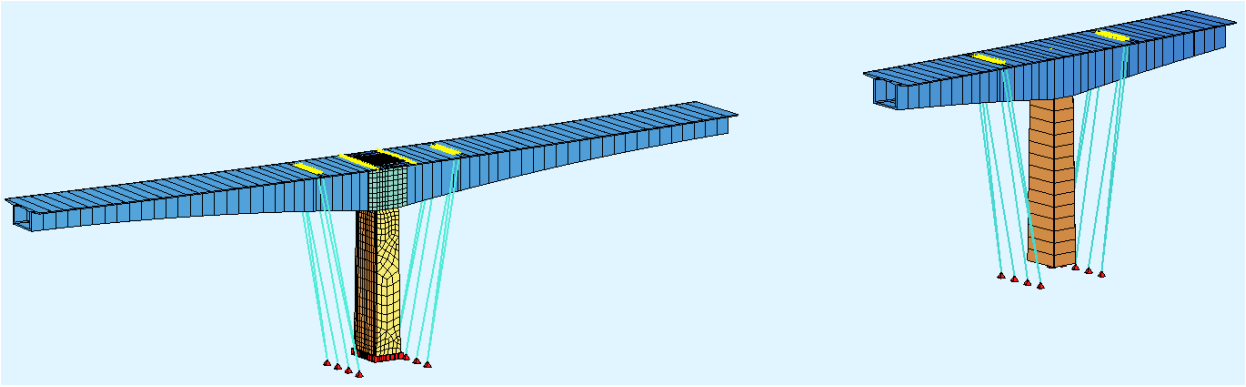

*Figure 62.* Vranduk 2 construction stage

Construction stages are calculated using a full geometrical nonlinear analysis with nonlinear material properties, using SLS material curve which gives realistic results (Figure 63). Creep and shrinkage is calculated according to EN 1992-1-1:2004+AC:2010 [52]. For each time step the correct duration has been provided as well as values for humidity (70 %) and temperature (20 °). For longer periods more time steps are defined. Creep values are calculated individually for each load part so backward creeping is taken into account. Furthermore, each new segment is positioned tangentially on existing structure so the segment positions and deflections are calculated correctly. The time of first loading is input separately for every activated part of the structure because of different construction durations. Losses in prestressing cable forces due to relaxation of prestressing steel as well as creep and shrinkage of concrete are calculated and taken into account. Stiffness development of concrete is taken into account by calculating the temperature adjusted concrete age T1 according to CEB-FIP model code 1990 [53].

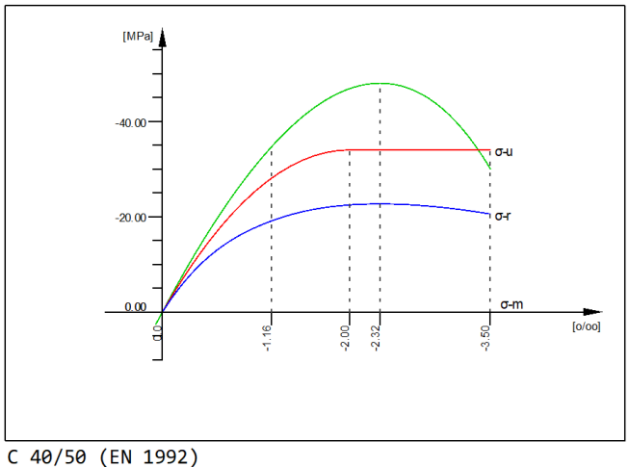


*Figure 63.* Stress-strain concrete diagram used for the numerical model (green curve)

## 3.2. Result comparison

Vranduk 1 bridge was monitored for a total of 77 days, while Vranduk 2 bridge was monitored for 107 days. During monitoring of both bridges samples were taken at a rate of 1 sample every 50 seconds. This meant 1728 samples in one day per measuring point. In a course of a single day there were deviations in the strain curve due to temperature change and different construction stage loads (Figure 64).

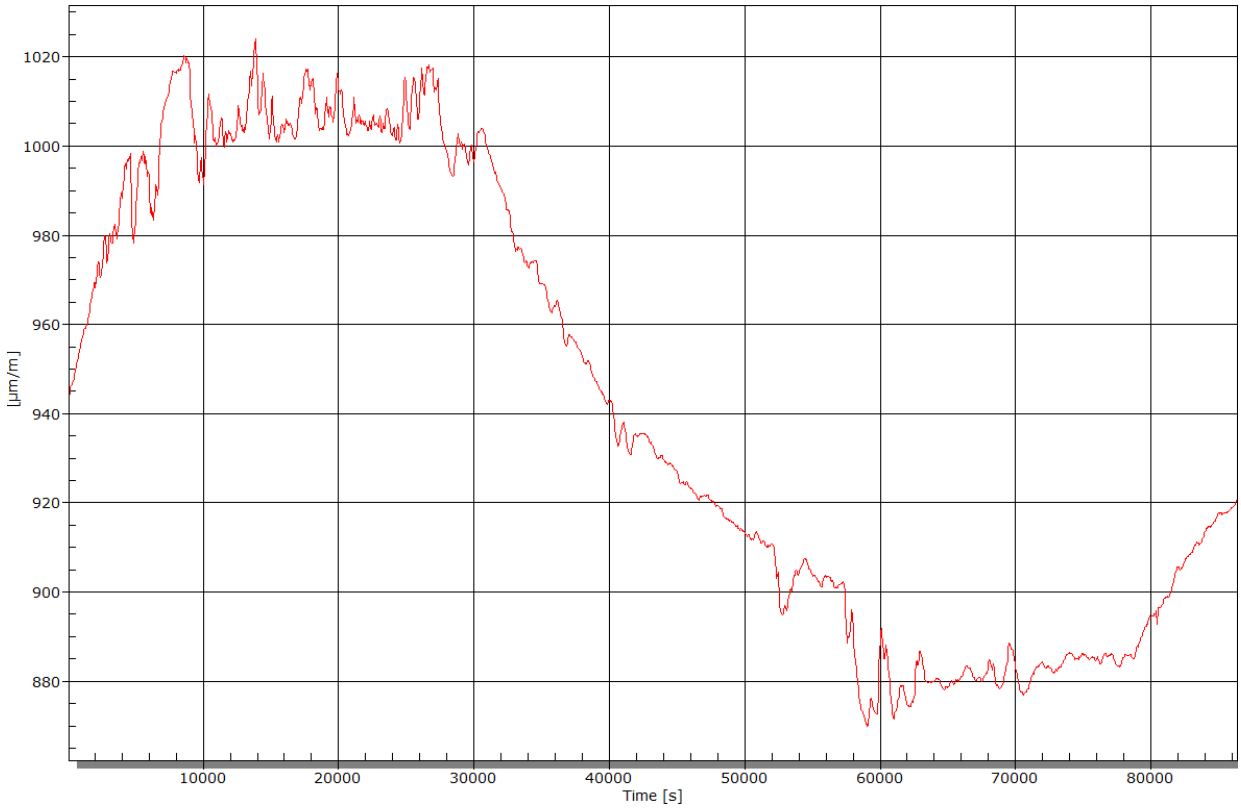


*Figure 64.* Example of a single day strain-time diagram change

In an effort to present clear results, the diagram for each measuring point during the monitoring period was created by using a single reference sample of the point in a day, taken at the same time every day. Original strain samples are approximately converted into stress using Hooke's law. Since the superstructure concrete in both bridges is C40/50, elastic modulus of 35220 MPa (according to EN1992-1-1:2004) was multiplied with strain data to attain stress values. Prestressing steel Y1860 is used with elastic modulus of 195000 MPa. Unfortunately, prestressing steel sensors were damaged during cable grouting and no useful conclusions could be extracted from the data at this time due to small sample sizes. Strain and stress results obtained from the numerical models with and without creep and shrinkage are shown along with measured data.

The strain results comparing measured strain with numerical results with and without creep and shrinkage are shown below (Figure 65 – Figure 72). Furthermore, graphs showing the compressive stress through points B1 to B4 on both bridges relative to characteristic concrete strength $f_{ck}$ are shown (Figure 73 – Figure 80). In addition to strain and stress, vertical deflections during bridge construction were monitored and the measured results are compared to numerical precamber calculations (Figure 81 and Figure 82).

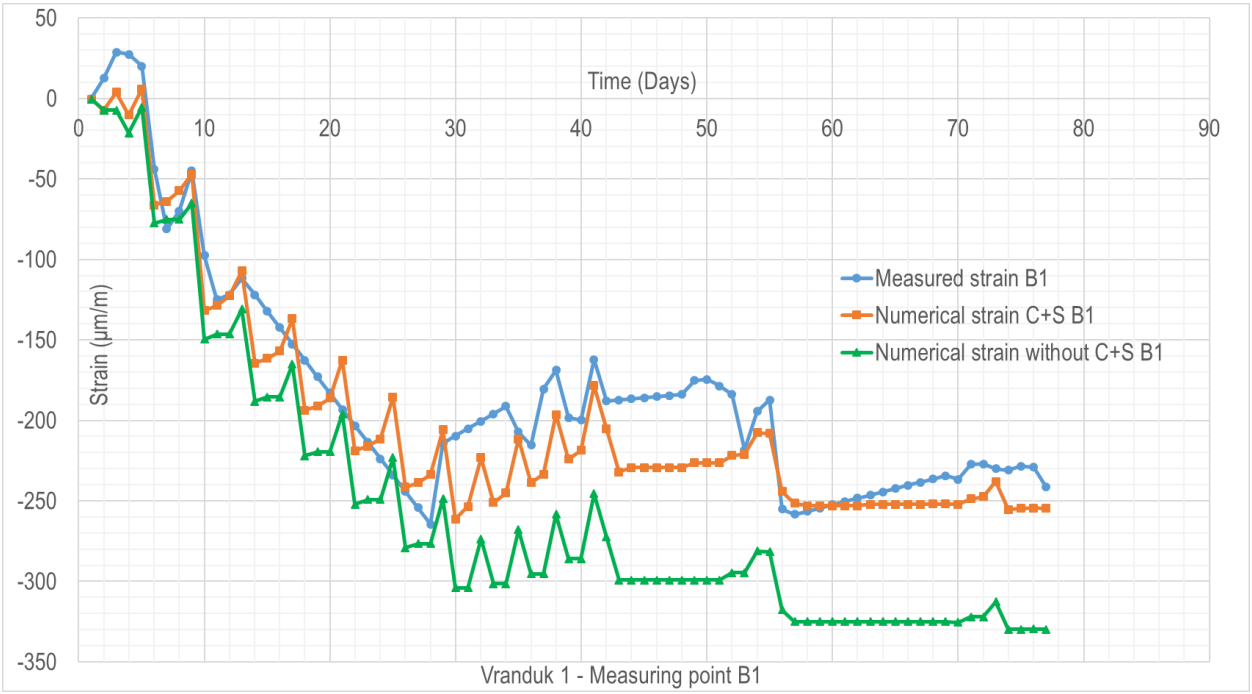


*Figure 65.* Vranduk 1 – measured and numerical strain with and without creep and shrinkage (C+S) – point B1

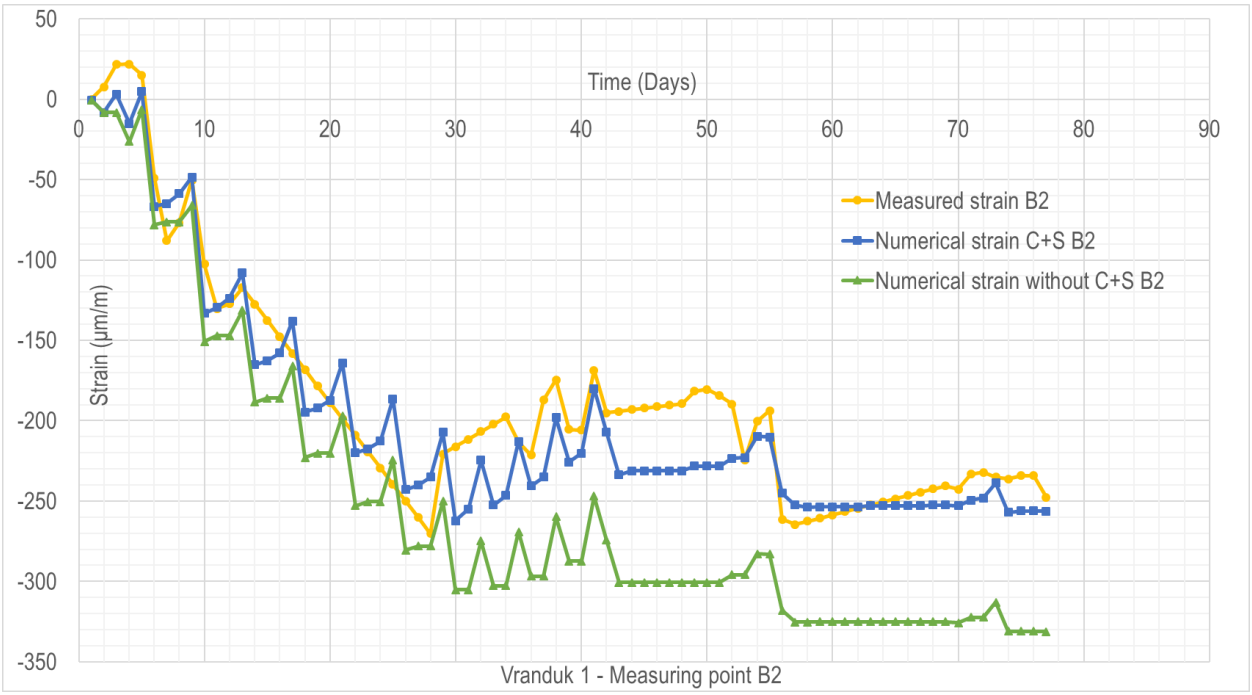


*Figure 66.* Vranduk 1 – measured and numerical strain with and without creep and shrinkage (C+S) – point B2

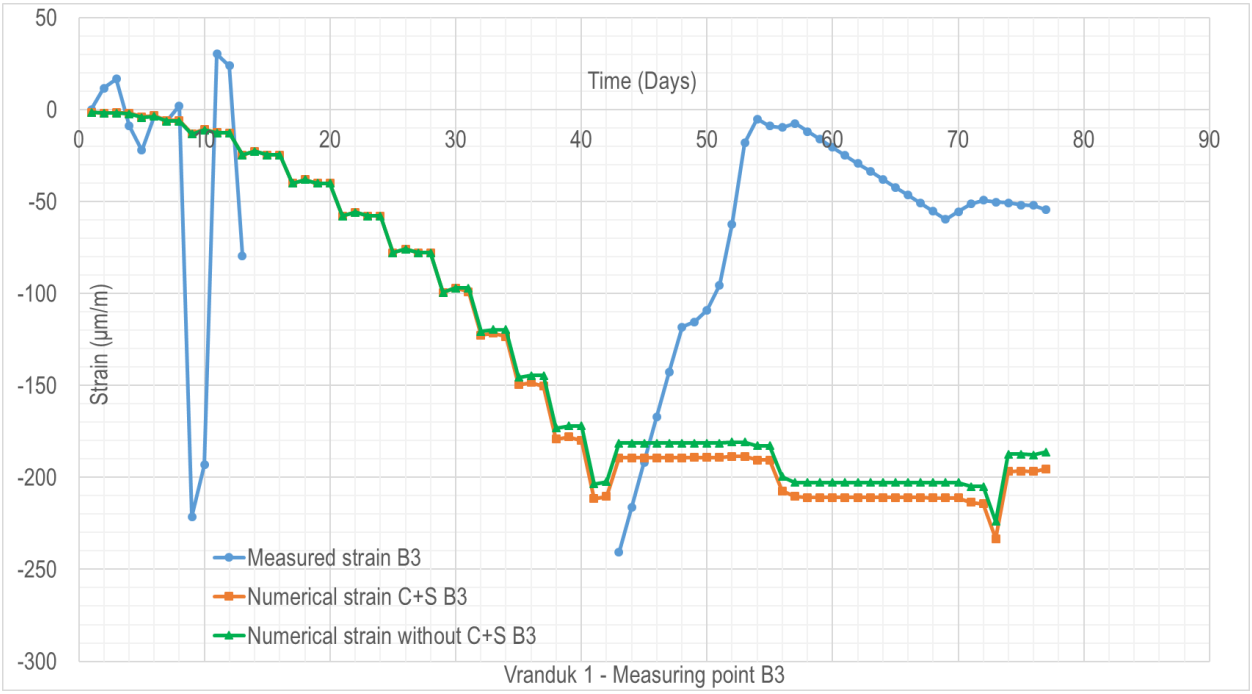


*Figure 67.* Vranduk 1 – measured and numerical strain with and without creep and shrinkage (C+S) – point B3

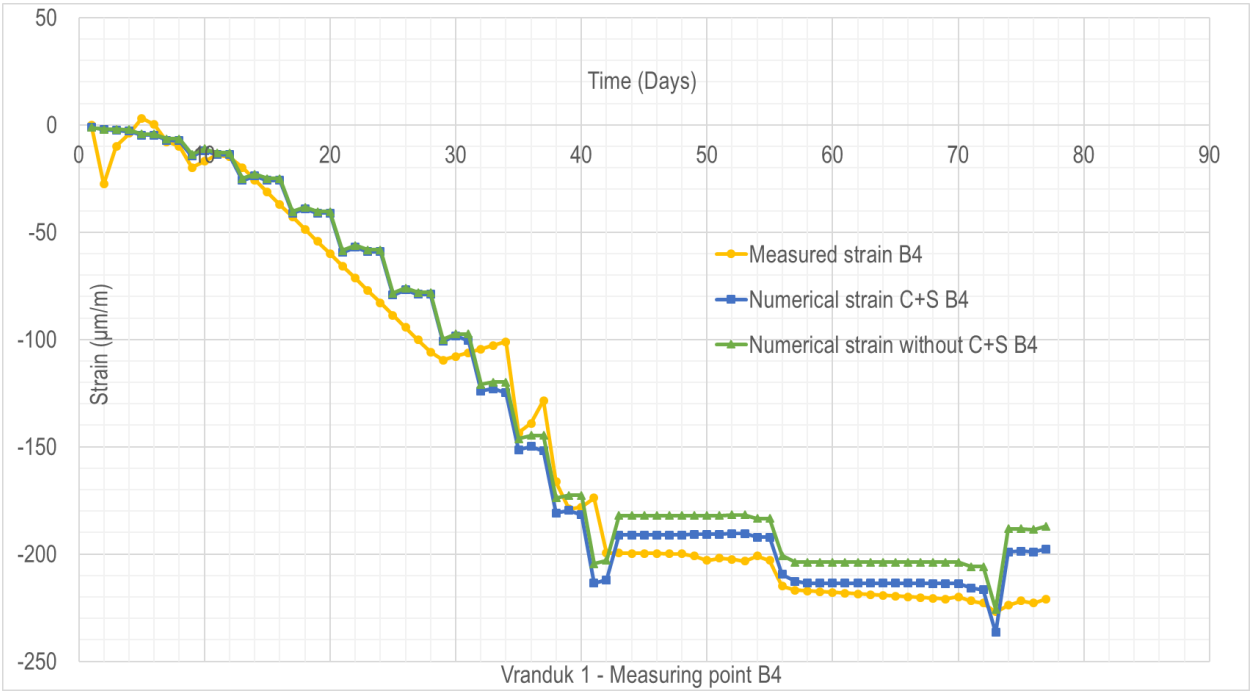


*Figure 68.* Vranduk 1 – measured and numerical strain with and without creep and shrinkage (C+S) – point B4

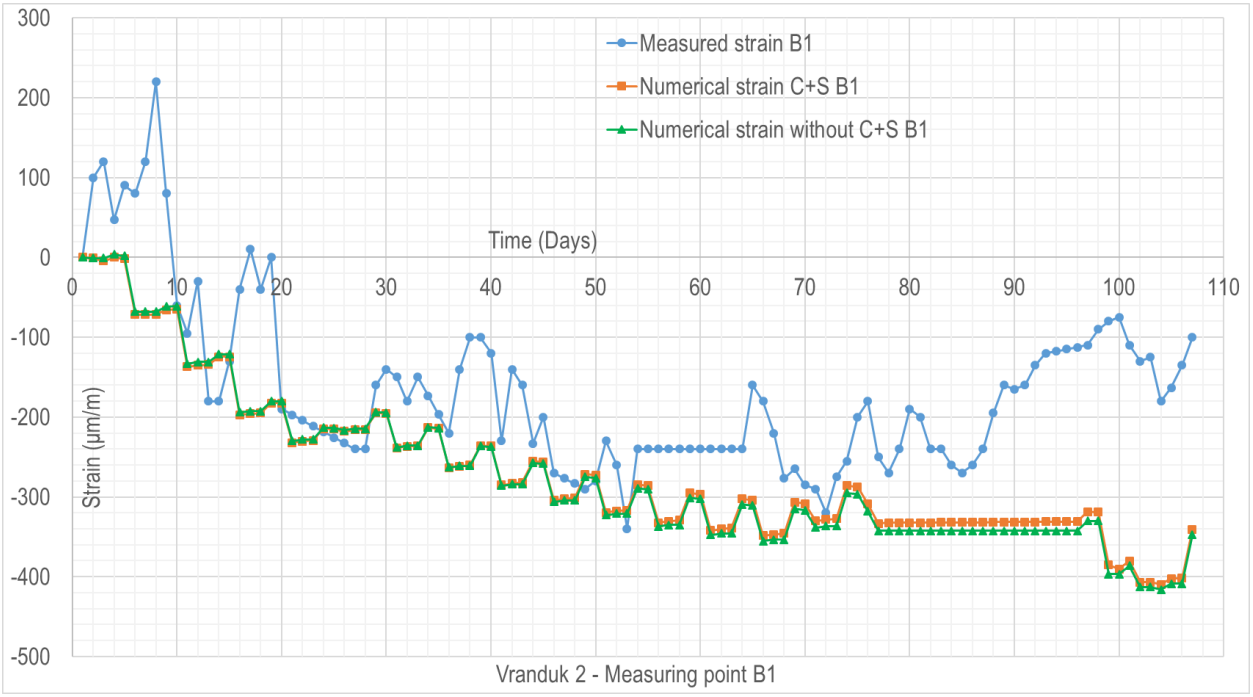


*Figure 69.* Vranduk 2 – measured and numerical strain with and without creep and shrinkage (C+S) – point B1

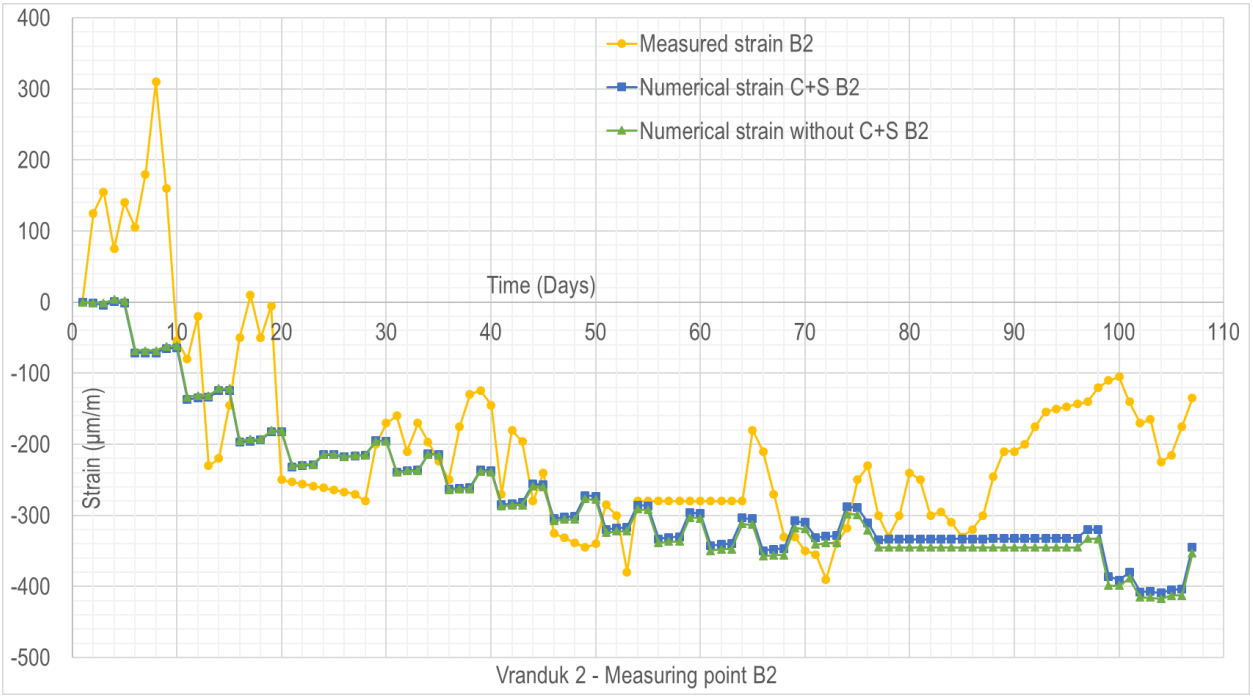


*Figure 70.* Vranduk 2 – measured and numerical strain with and without creep and shrinkage (C+S) – point B2

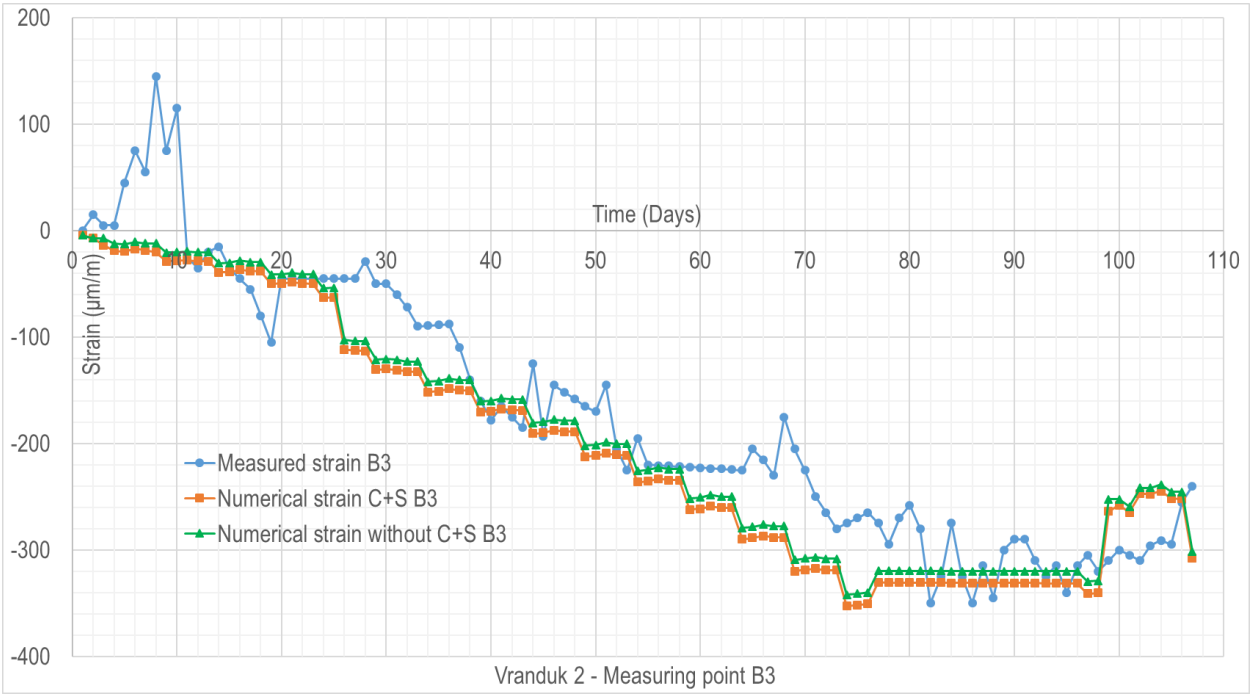


*Figure 71.* Vranduk 2 – measured and numerical strain with and without creep and shrinkage (C+S) – point B3

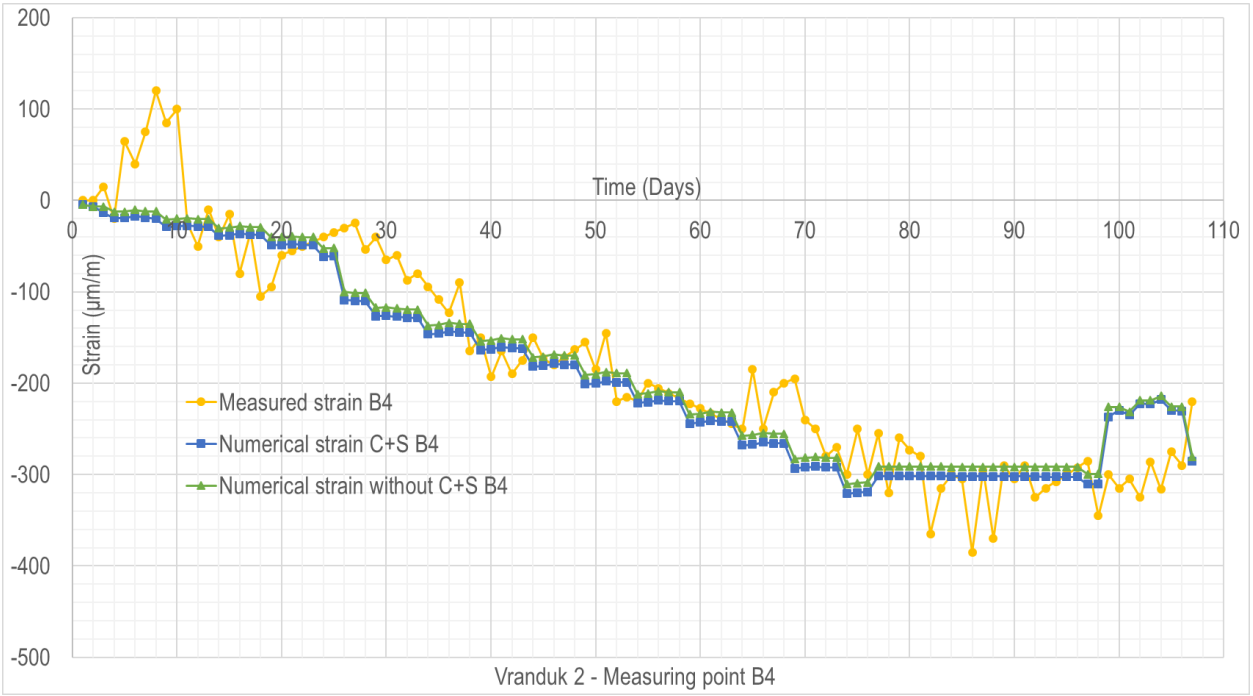


*Figure 72.* Vranduk 2 – measured and numerical strain with and without creep and shrinkage (C+S) – point B4

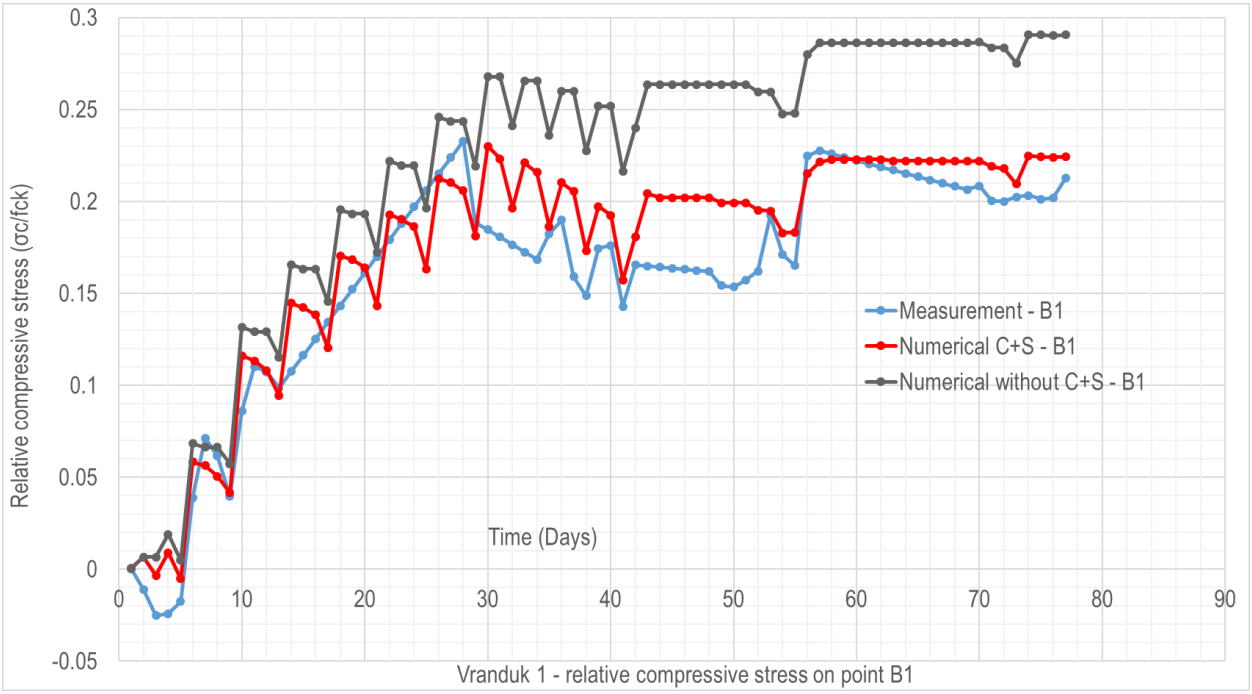


*Figure 73.* Vranduk 1 – relative compressive stress ($\sigma_c/f_{ck}$) – point B1

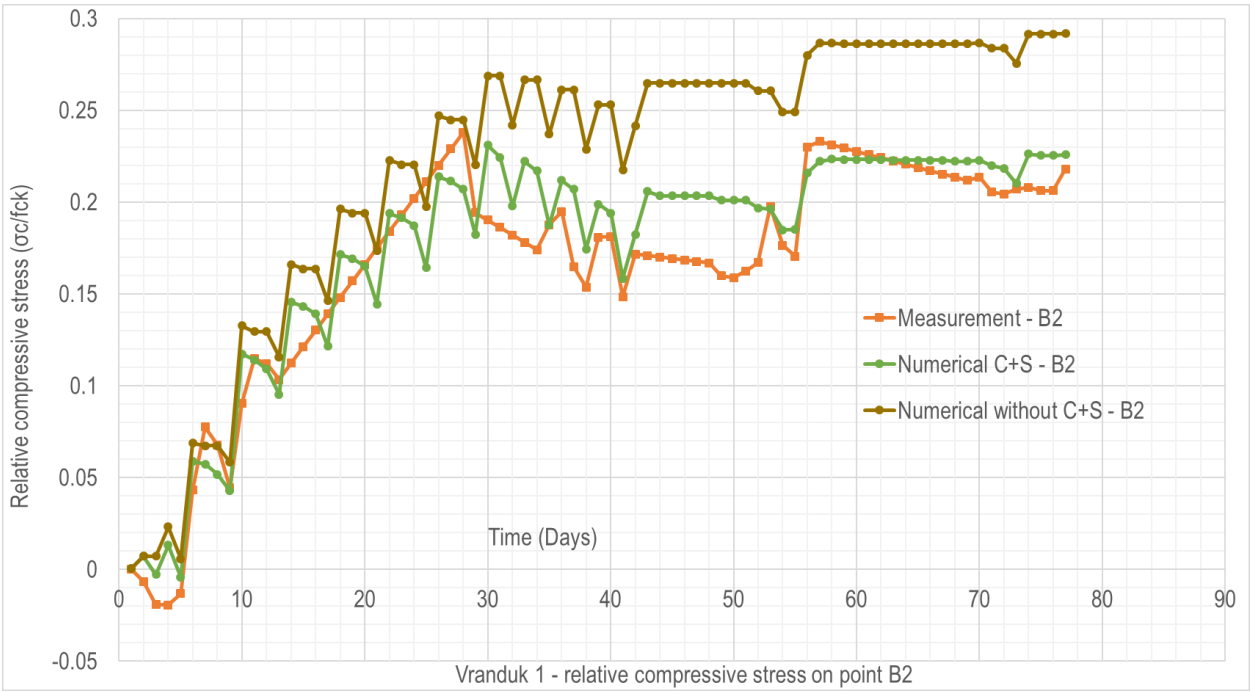


*Figure 74.* Vranduk 1 – relative compressive stress ($\sigma_c/f_{ck}$) – point B2

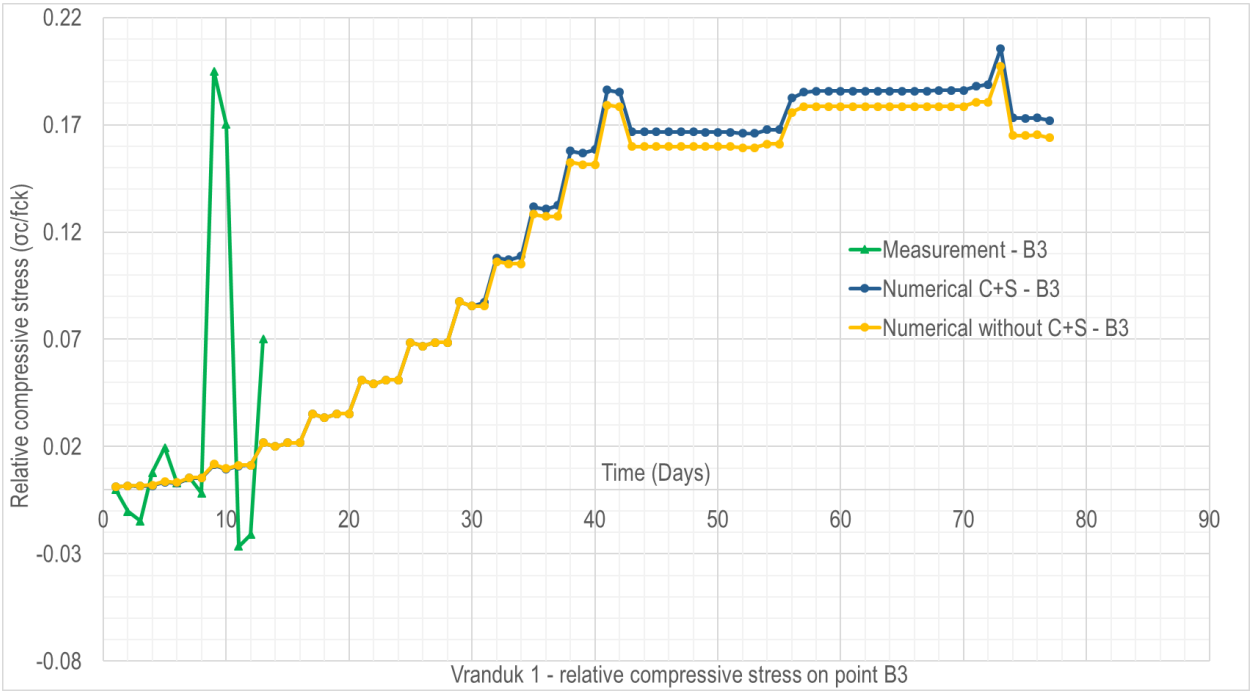


*Figure 75.* Vranduk 1 – relative compressive stress ($\sigma_c/f_{ck}$) – point B3

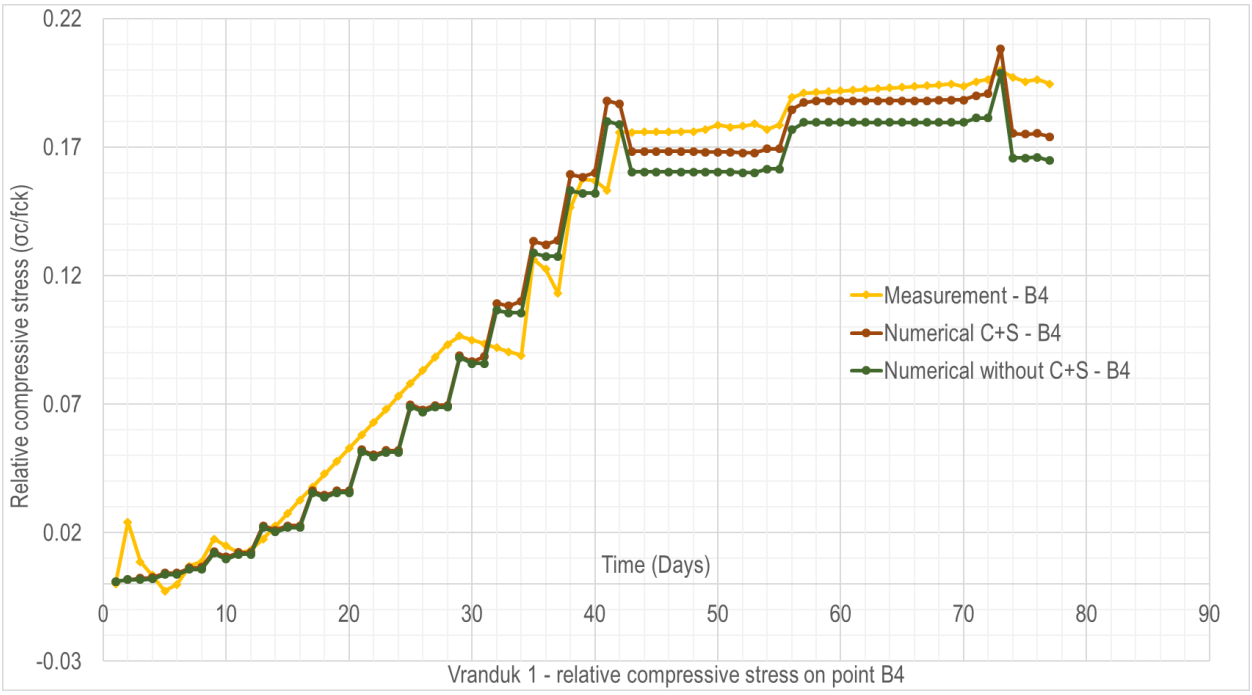


*Figure 76.* Vranduk 1 – relative compressive stress ($\sigma_c/f_{ck}$) – point B4

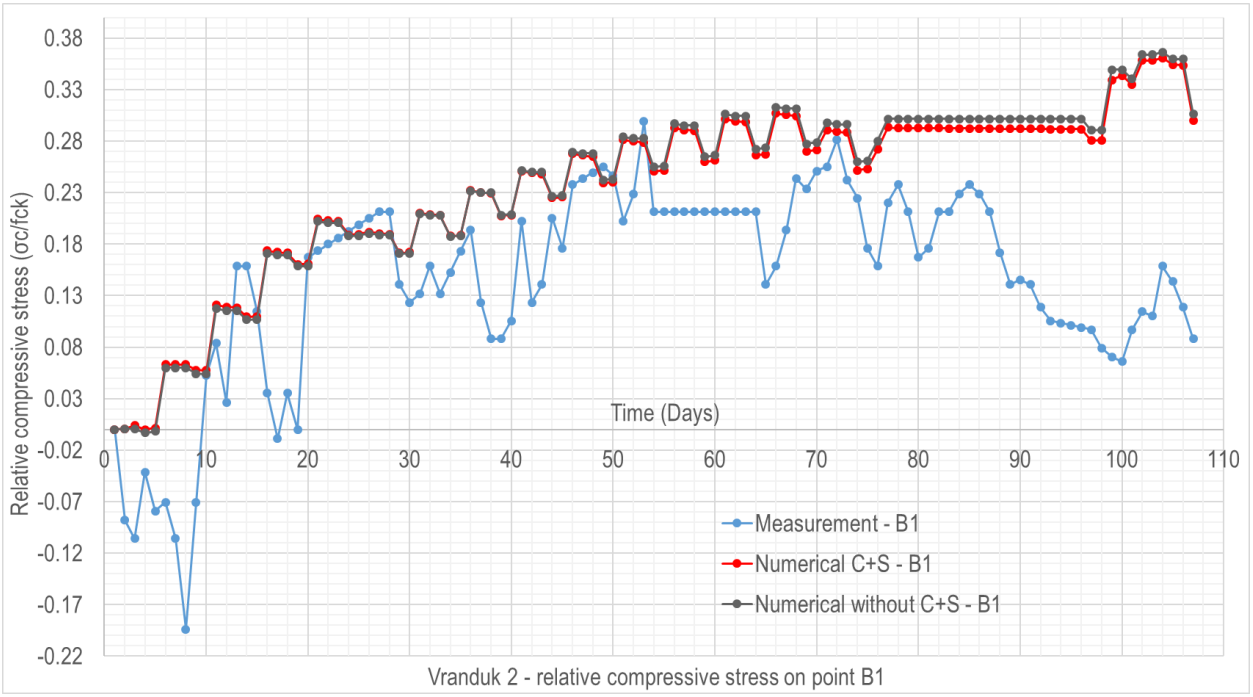


*Figure 77.* Vranduk 2 – relative compressive stress ($\sigma_c/f_{ck}$) – point B1

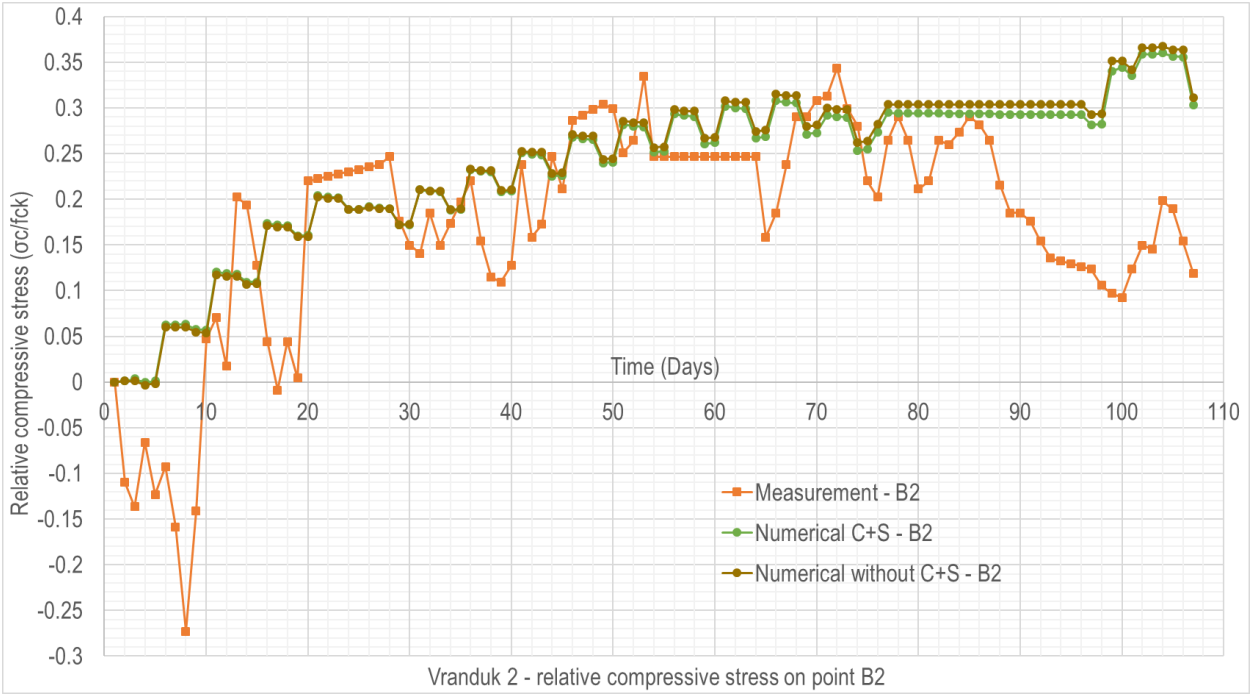


*Figure 78.* Vranduk 2 – relative compressive stress ($\sigma_c/f_{ck}$) – point B2

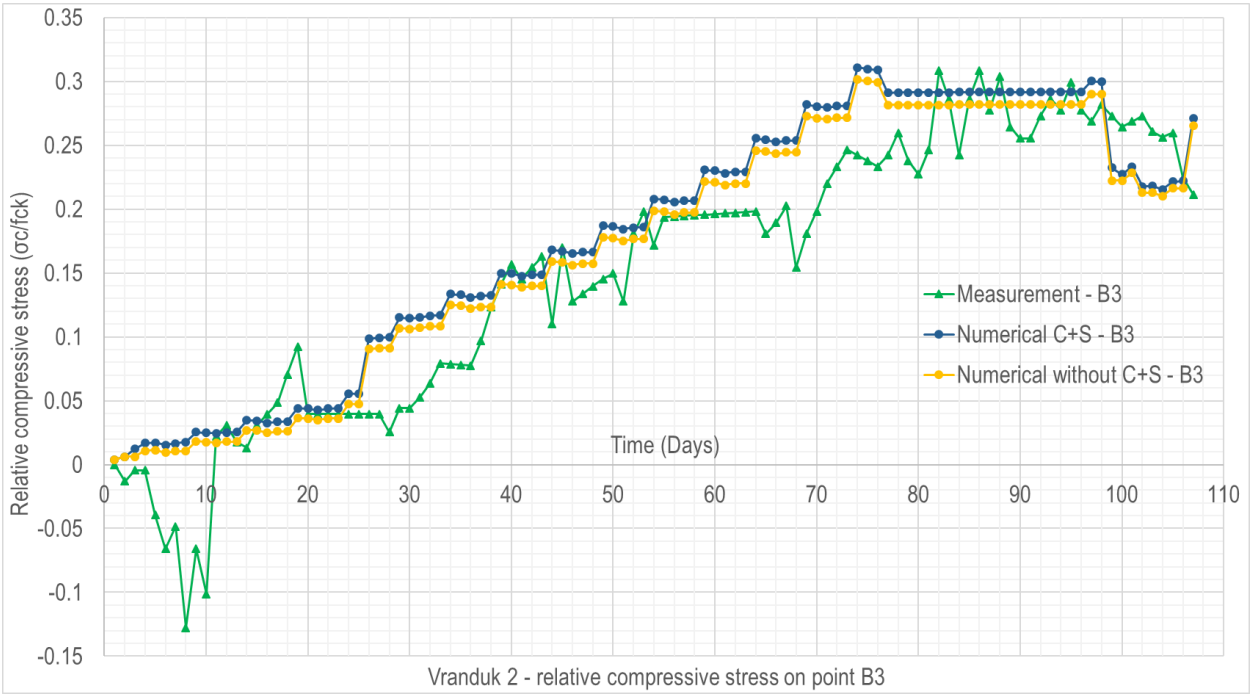


*Figure 79.* Vranduk 2 – relative compressive stress ($\sigma_c/f_{ck}$) – point B3

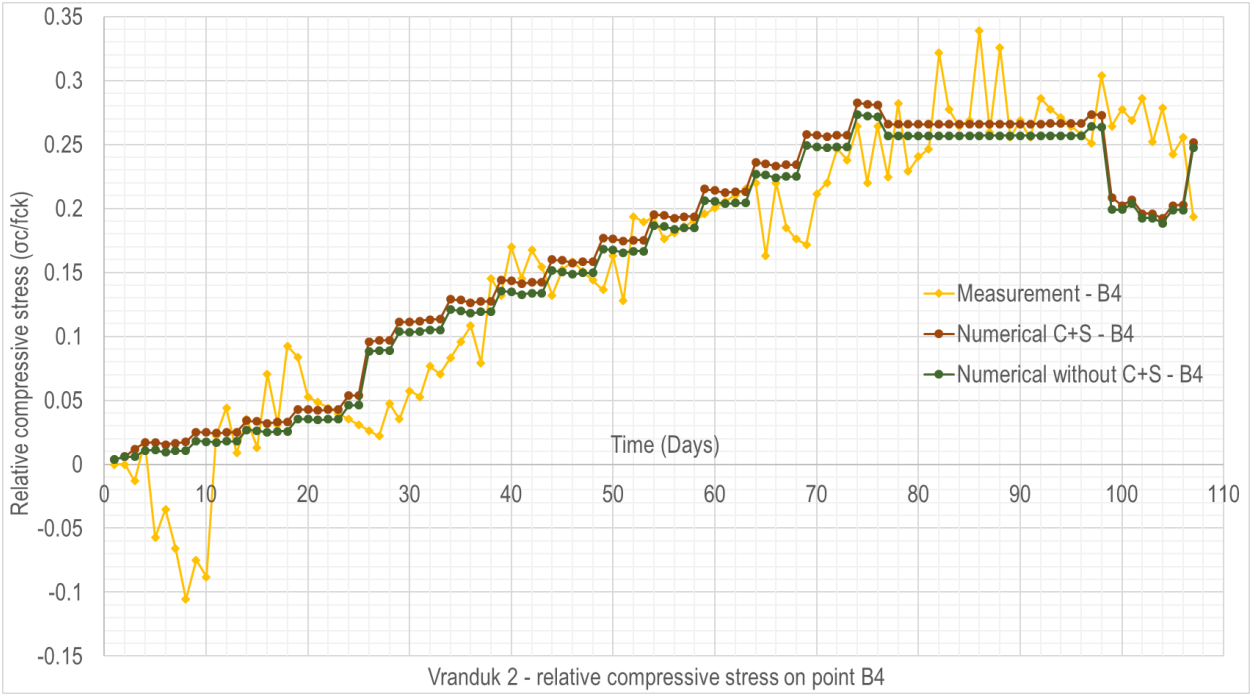


*Figure 80.* Vranduk 2 – relative compressive stress ($\sigma_c/f_{ck}$) – point B4

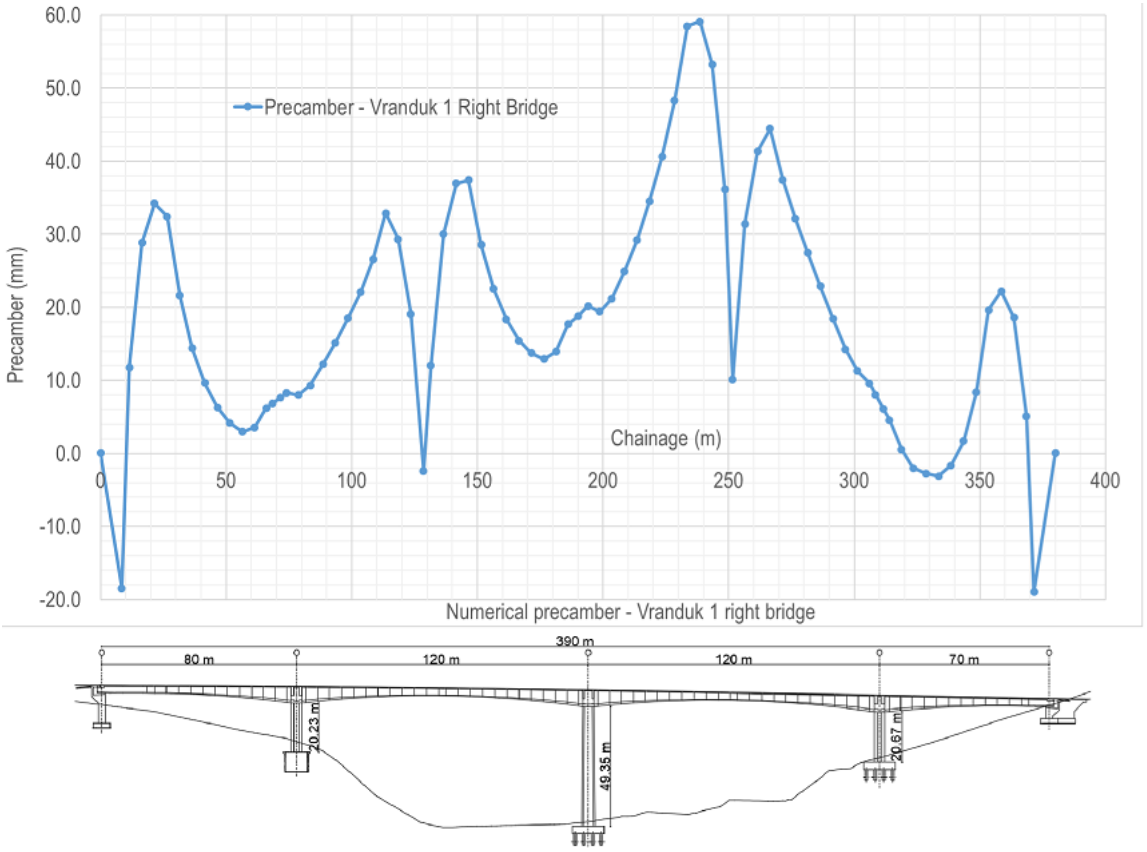


*Figure 81.* Vranduk 1 – numerical precamber

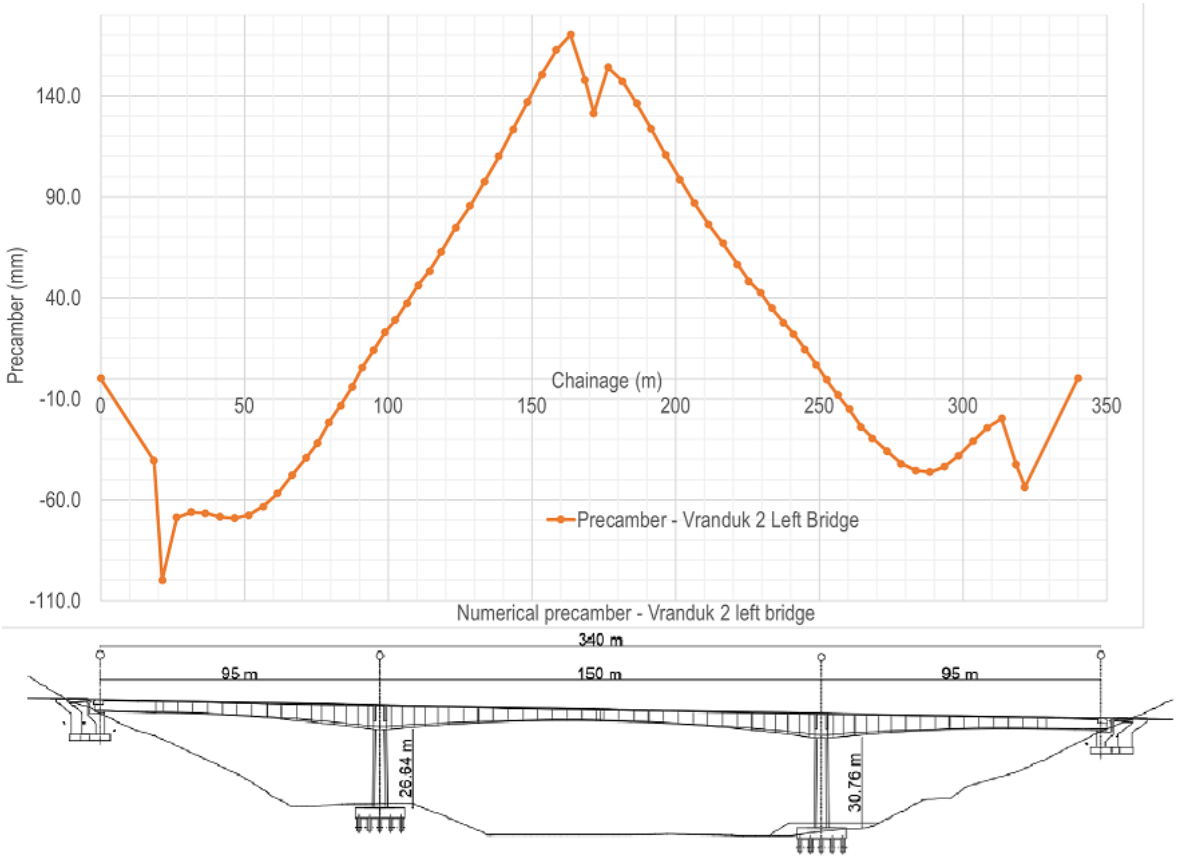


*Figure 82.* Vranduk 2 – numerical precamber

As expected, bridge monitoring results show that all points of the cross section (B1-B4) are in compression due to cantilever construction process and prestressing. Self-weight causes compressive strain in the lower slab and tensile strain in the upper slab initially. Prestressing of balanced cantilever cables used for construction stages which are located in the upper part of the superstructure causes large increase in compressive strain of the upper slab, and minor or no increase in compressive strain in the lower slab. With this repeating process compressive strain is expected on the entire cross section.

On Vranduk 1 (120 m main span) several gaps in measurement occurred, with the largest between days 13-27, missing some segment construction stages. Measured point B3 shows unrealistic strain values, likely due to damage during installation of strain gauges. Nevertheless, remaining strain gauges show reliable results. Points B1 and B2 on upper slab show a stepped increase in compressive strain up to 270.25 μm/m (roughly 9.5 MPa) on day 28 when segment 7 was prestressed. Each stepped increase in strain represents prestressing of a segment with cantilever construction cables located in the upper part of the superstructure. Since all segments after segment 3 have 4 cables per segment, after segment 7 the weight of the cantilever becomes greater than prestressing force moment and the compressive strain in the upper slab starts lowering. On day 42 last prestressing step is visible with the completion of the 11th segment where points B1 and B2 have a compressive strain of around 199.56 μm/m (roughly 7.0 MPa). On day 56 lower slab prestressing cables in the span are prestressed which causes the compressive strain in the top slab to increase to around 261.26 μm/m (about 9.2 MPa) in B1 and B2 points. Compressive strain in the top slab continues to slowly decrease to around 247.67 μm/m (roughly 8.5 MPa) on day 77, likely because of the gradually adding additional dead load of concrete barriers.

Point B4 shows a stepped increase in strain, with each step representing the addition of a dead load of the next segment. Unlike points B1 and B2, point B4 has a constant increase in compressive strain up to 199.56 μm/m (about 7.03 MPa) on day 42 when the last segment was activated with prestressing. On day 56 point B4 gains some compressive strain (up to 214.88 μm/m, roughly 7.57 MPa) due to lower slab cables in the span being prestressed. Compressive strain in the lower slab continues to slowly increase up to 220.88 μm/m (around 7.78 MPa) due to already mentioned additional dead load.

Vranduk 2 bridge (150 m main span) shows similar results with a more jagged strain diagram due to lack of temperature compensation. Points B1 and B2 on the upper slab have a stepped increase in strain up to 320 μm/m (roughly 11.3 MPa) and 390 μm/m (about 13.7 MPa) on day 72. Last segment (15th) was prestressed on day 78 with 270 μm/m (around 9.5 MPa) and 330 μm/m (roughly 11.6 MPa) compressive strain. On days 102 and 104 lower slab prestressing was done with B1 and B2 having 180 μm/m (about 6.3 MPa) and 225 μm/m (around 7.9 MPa) of compressive strain.

As with the previous bridge, points B3 and B4 show stepped increase in compressive strain each time a new segments dead weight was added (with deviations due to temperature change and construction stage loads), reaching 295 μm/m (roughly 10.39 MPa) and 320 μm/m (about 11.27 MPa) on day 78 when the last segment was activated. The maximum measured strain is 350 μm/m (around 12.3 MPa) and 385 μm/m (about 13.6 MPa) on day 86, likely due to uncompensated temperature strain and construction stage loads. When the lower slab cables in the span were prestressed points B3 and B4 had 290 μm/m (roughly 10.3 MPa) and 315 μm/m (about 11.1 MPa) of compressive strain.

In relation to the characteristic concrete strength $f_{ck}$, stresses on Vranduk 1 reach up to 0.238 (9.52 MPa) relative compressive stress in the upper slab and up to 0.20 (8 MPa) relative compressive stress in the lower slab. After the bridge is connected both upper and lower slab have roughly 0.20 (8 MPa) relative compressive stress. On Vranduk 2 relative compressive stress in the upper slab goes up to 0.343 (13.72 MPa) which is a local maximum, while the relative compressive stress in the lower slab reaches 0.339 (13.56 MPa).

Numerical models were used to obtain the necessary precamber of the structure so the bridges would maintain the correct geometry after construction and a 30-year period of exploitation. As expected, Vranduk 1 bridge shows much lower necessary precamber with a maximum of 59.50 mm, while Vranduk 2 bridge shows a greater necessary precamber of 170 mm.

## 3.3. Discussion

During the monitoring process for both bridges power outages were common across the entire construction site. Even though the equipment was connected to an uninterrupted power supply to protect from power surges and outages, it was only enough for 20-30 minutes. The outages usually lasted longer than that which would cause the data acquisition system to shut down, saving all data up to that point. As soon as the problem was detected, the system was turned back on as soon as possible. The system also suffered some accidental mechanical damage due to the construction process, severing several extension cables which were replaced as soon as the damage was noticed. The missing data was interpolated during data processing, losing some construction stage phases, but retaining the general trend that was also confirmed by numerical results.

Strain values on calculated models correspond well with the measured values on bridges Vranduk 1 and Vranduk 2 with minor differences. The jagged parts of measured stress diagrams are due to construction processes and different loads during execution beside the form traveller that could not be taken into account in the numerical model such as working personnel, staff and visitors, possibly with hand tools or other small site equipment, storage of movable items like building and construction materials, precast elements and equipment, or various movable heavy machinery and equipment. The minor differences in calculated and measured stress could be due to a number of reasons, firstly the numerical model is a hybrid between line and area elements to keep the system manageable. Better results could be obtained with 3D brick elements, but due to the large size and specific calculation requirements of balanced cantilever bridges each construction phase would have to be considered and calculated and that would require large amounts of computing power.

Furthermore, the material stress-strain laws are simplified and uniform on the entire structure, while in reality the material (especially concrete) can vary from segment to segment as it is installed. Accidental deviations during construction are not taken into account in the numerical model. Numerous accidental construction stage loads (workers, equipment and material storage), as well as nonlinear temperature change during construction is not taken into account in the numerical model. Specifically, on Vranduk 2 bridge, temperature strain was not compensated which in turn shows large deviations in measured strain values.

Considering the coefficient of linear thermal expansion of concrete is 10-5 $K^{-1}$ the difference could be up to 300 μm/m (10.57 MPa) if we consider a 30 K temperature change. At times the measurements were interrupted and the results during the interruptions were interpolated. As a result, the numerical values give a more detailed overview of bridge behaviour during each stage of construction (showing the construction process for each segment, including form traveller positioning, formwork and reinforcement installation, concreting and prestressing), but the general stress trend is following the measured values. As expected, creep and shrinkage are reducing compressive stresses in upper slab, and increasing compressive stresses in the lower slab of the cross section.

When comparing measured and numerical values the diagrams show that the calculated numerical results including creep and shrinkage correspond very well with the measured values on both bridges. On points B1 and B2 Vranduk 1 shows differences of roughly 50 μm/m (1.76 MPa) on days 42 to 52, with very close results before and after when taking creep and shrinkage into account. The difference is very likely due to an unknown load during construction stages, since the values match very well after this period. The results excluding creep and shrinkage match very well in the beginning, but as expected almost linearly gain the strain difference of 70 μm/m (2.65 MPa) at the end of 77 days, showing how creep and shrinkage expectedly lower the compressive stress in the upper slab.

Point B3 shows unrealistic results with signal loss on day 13, likely due to unintentional measuring cable damage during construction. Numerical results however show that creep and shrinkage increase the compressive strain in the lower slab up to 10.79 μm/m (0.38 MPa). Point B4 shows good correlation of numerical results considering creep and shrinkage with measured strains, and similarly to B3 show that creep and shrinkage increase compressive strain in the lower slab up to 10.51 μm/m (0.37 MPa).

On Vranduk 2 bridge, when looking at points B1 and B2, the diagram represents good correlation with larger local discrepancies of about 141.96 μm/m (5.01 MPa) and 245.47 μm/m (8.64 MPa) at the end. The differences are most likely due to a lack of temperature compensation in the measurements which show unrealistic strain that includes temperature strain. The numerical results show that creep and shrinkage decrease compressive strain in the upper slab by roughly 11.35 μm/m (0.40 MPa).

Diagram for points B3 and B4 shows even better correspondence of numerical and measured results, maintaining the larger local differences from lack of temperature compensation, but also maintaining the same strain trend through construction stages. Average local differences considering creep and shrinkage are about 38.61 μm/m (1.36 MPa), while creep and shrinkage increase the compressive strain in the lower slab by 11.37 μm/m (0.40 MPa).

# 4. CONCLUSION AND DIRECTIONS FOR FURTHER RESEARCH

## 4.1. Conclusion

The balanced cantilever bridges sustain high compressive strains and stresses in concrete during construction and exploitation. The general behaviour of all these structures are similar, but due to the different spans, the superstructure characteristics (self-weight, cross section properties, number and position of balanced cantilever pre-stressing cables) are different, which causes differences.

It is clearly shown that during construction stage, the maximum compressive strain in the upper slab in the 120 m span bridge Vranduk 1 is 270.25 μm/m (roughly 9.5 MPa), while 150 m span Vranduk 2 has a maximum compressive strain of 390 μm/m (about 13.7 MPa) which is a difference of 119.75 μm/m (around 4.2 MPa) or roughly 30%. In the lower slab, Vranduk 1 has a maximum compressive strain of 226.86 μm/m (roughly 8.0 MPa), while Vranduk 2 has 385 μm/m (around 13.6 MPa), which is a difference of 158.14 μm/m (about 5.6 MPa) or roughly 40%. Even if we take into account the lack of temperature compensation on Vranduk 2 bridge and compare the average values, Vranduk 2 still has a higher compressive strain of around 283.93 μm/m (roughly 10.0 MPa). This is expected, as longer spans require more robust superstructure which generally sustains a higher load.

Creep and shrinkage have a considerable effect on balanced cantilever bridges in terms of deflections that have to be taken into account so the segments get the proper precamber. This is especially important on stitch segments where two cantilevers are joined with an end goal of correct road geometry. This research shows the effect of creep and shrinkage on strains in the construction phases.

On Vranduk 1 maximum difference is 70 μm/m (2.65 MPa) in the upper slab which is roughly 28% of the maximum compression strain. On Vranduk 2 the maximum local difference is 245.47 μm/m (8.64 MPa), around 63% of the maximum compression strain. Excluding the maximum values, creep and shrinkage make a difference of around 11 μm/m (0.40 MPa) which is 4.2% of maximum on Vranduk 1 and 2.94% of maximum on Vranduk 2. The small differences are probably due to stress fluctuations between box cross section slabs and webs.

The results also show the importance of temperature compensation when monitoring strain and stress for a longer period of time since the Vranduk 1 bridge results have a better correlation with numerical results due to temperature compensation. Most importantly, the strain differences and trend in all measured points is similar in measured and numerical results which represents a very good match on strain results and confirms the expected bridge behaviour through the entire cantilever construction stage including stitch segment and bridge monolitization.

Relative compressive stresses show that Vranduk 1 bridge is less stressed than Vranduk 2 compared to the characteristic concrete strength, with a ratio of 0.238. On the other hand, Vranduk 2 bridge has a higher stress level, with a ratio of 0.343. Precamber calculations show that the maximum precamber of Vranduk 1 is significantly lower compared to Vranduk 2 with only 35% of its value.

At the end, a recommendation is given to design and build 120 m span bridges if the site conditions allow it and the piers are not too high. The 120 m span superstructure will generally have lower strain and stress levels, as well as lower self-weight. The real benefit is that the superstructure will have a lower cross section (in this case the difference is 1.60 m on the piers, and 0.80 m in the central part of the span) which is much simpler and safer to build. A smaller structure has lower chances of encountering issues during construction inherent to the construction method (less prestressing cables to install, easier cable placement and control, smaller forces for local tendon radial force issues and cracking on lower slab, blisters or through the web due to large prestressing forces). Smaller stress levels, smaller necessary precamber and a leaner structure has less uncertainty during the construction period, and is more feasible.

As the final conclusion of this work, it can be stated that the dissertation sheds light on a crucial aspect of bridge engineering and offers valuable insights for construction professionals and researchers alike. This comprehensive research delves into the intricate details of strain analysis, specifically focusing on cast-in-place balanced cantilever prestressed concrete bridges. The research provides a deep understanding of the behaviour and performance of these bridges during the construction and exploitation phase. The presented findings offer practical implications for engineers, contractors, and project managers involved in the construction of prestressed concrete bridges. It equips professionals with valuable knowledge to optimize construction methods and enhance the safety and efficiency of bridge projects.

By examining strain analysis in cast-in-place balanced cantilever prestressed concrete bridges, the dissertation contributes to the optimization of bridge design. The insights gained from this research can guide future projects, resulting in more robust and structurally sound bridges. It adds to the body of knowledge in the field of bridge engineering and construction. It serves as a valuable resource for researchers, enabling them to build upon the findings and explore new avenues of inquiry.

## 4.2. Directions for further research

This dissertation covers the construction aspect of prestressed concrete bridges built by balanced cantilever construction method on site. Further research should aim to monitor other cast-in-place post-tensioned concrete bridges constructed by the cantilever method with different spans and different superstructures (wide superstructures, boxes with multiple webs, boxes with slanted webs and similar). It would be preferable to install measuring equipment in several cross-sections, and to have at least 8 measuring points in each cross section, including a measuring point on the middle of cross-section. The results obtained from these measurements could be analysed and compared to numerical models, which should provide a comprehensive and robust understanding of the structural behaviour covering many different aspects of these bridges.

# 5. LITERATURE

[1] Mathivat, J. The cantilever construction of prestressed concrete bridges; Editions Eyrolles: 61, boulevard Saint-Germain, 75005 Paris, France, 1979

[2] Group of authors Design guide – Prestressed concrete bridges built using the cantilever method; Setra, 2003

[3] DuBois, A. J. The mechanics of engineering; John Wiley & Sons, 1902

[4] Bender, C. Discussion on Cantilever Bridges by C.F. Findlay; Canadian Society of Civil Engineers, 1890

[5] DeLony, E. Context for world heritage bridges; International Council on Monuments and Sites, 1996

[6] Schneider, C. C. Quebec bridge inquiry report; S. E. Dawson, 1908

[7] Middleton, W. D. The bridge at Quebec; Indiana University Press, 2001

[8] Pilz, M. The Collapse of the K-B Bridge in 1996; London, 1997

[9] Pilz, M., L. G. Continuity in Prestressed Concrete Structures, Time-Dependent Responses; 22nd Conference on Our World in Concrete & Structures, Singapore, 1997

[10] Pilz, M. The Koror-Babeldaob Bridge in the Republic of Palau, History and Time Dependent Stress and Deflection Analysis; Dissertation Imperial College London, Department of Civil Engineering, 1997

[11] Skrinar, M.; Strukelj, A. Eigen frequency monitoring during bridge erection. SEI 1996, 6(3), 191-194.

[12] Strommen, E.; Hjort-Hansen, E.; Kaspersen, J. H. Dynamic loading effects of a rectangular box girder bridge. J. Wind. Eng. Ind. Aerodyn. 2001, 89(14–15), 1607–1618.

[13] Schmidt, S.; Solari, G. 3-D wind-induced effects on bridges during balanced cantilever erection stages. Wind Struct. 2003, 6(1), 1–22.

[14] Morassi, A.; Tonon S. Dynamic testing for structural identification of a bridge. J. Bridge Eng. 2008, 13, 573–585.

[15] Gentile, C.; Bernardini, G. Output-only modal identification of a reinforced concrete bridge from radar-based measurements. Nondectruct. Test. Evaluation 2008, 41, 544–553.

[16] Bayraktar, A.; Altuşnişık, A. C.; Sevim, B.; Domaniç, A.; Taş, Y. Vibration characteristics of Kömürhan highway bridge constructed with balanced cantilever method. J. Perform. Constr. Facil. 2009, 23(2), 90–99.

[17] Liu, C.; DeWolf, J. T.; Kim J. Development of a baseline for structural health monitoring for a curved post-tensioned concrete box girder bridge. Eng. Struct. 2009, 31, 3107–3115.

[18] Stathopoulos, S.; Seifried, G.; Kotsanopoulos, P.; Haug, H.; Spyropoulos, I.; Stathopoulos, K. The Metsovo bridge, Greece. SEI 2010, 20(1), 49–53.

[19] Altuşnişık, A. C.; Bayraktar, A.; Sevim, B.; Ates, S. Ambient vibration based seismic evaluation of isolated Gülburnu Highway Bridge. Soil Dyn. Earthq. Eng. 2010, 31(11), 1496–1510.

[20] Turan, F. N. Determination of dynamic characteristics of balanced cantilever reinforced concrete bridges using ambient vibration data; MSc Thesis, Karadeniz Technical University, Trabzon, Türkiye (in Turkish), 2012

[21] Kudu, F. N.; Bayraktar, A.; Bakir, P. G.; Türker, T.; Altuşnişık, A. C. Ambient vibration testing of Berta Highway Bridge with post-tension tendons. Steel Compos. 2014, 16(1), 23–46.

[22] Sumerkan, S.; Bayraktar, A.; Türker, T.; Akkose, M. A simplified frequency formula for post-tensioned balanced cantilever bridges. Asian J. Civ. Eng. 2019, 20, 983–997.

[23] Bayraktar, A.; Kudu, F. N.; Sumerkan, S.; Demirtas, B., Akkose, M. Near-fault vertical ground motion effects on the response of balanced cantilever bridges. Proc. Inst. Civ. 2020, 173, 17-33.

[24] Casas, J. R. Reliability-based partial safety factors in cantilever construction of concrete bridges. J. Struct. Eng. 1997, 123(3), 305-312.

[25] Manjure, P. J. Rehabilitation of balanced cantilever bridges. Indian Concr. J. 2001, 75(1), 76-82.

[26] Vonganan, B. The second Mekong international bridge, Thailand. SEI 2009, 19(1), 67–68.

[27] Pimanmas, A.; Imsombat, S.; Neilsen, K. Hj. New Phra- Nangklao bridge—A balanced cantilever prestressed concrete bridge in Thailand. SEI 2009, 19(1), 38–40.

[28] Ates, S.; Atmaca, B.; Yildirim, E.; Demiroz, N. A. Effects of soil-structure interaction on construction stage analysis of highway bridges. Comput. Concr. 2013, 12(2), 169–186.

[29] Chen, X.; Omenzetter, P.; Beskhyroun, S. Dynamic testing and long term monitoring of a twelve span viaduct. Key Eng. Mater. 2013, 569–570, 342–349.

[30] Pimentel, M.; Figueiras, J. Assessment of an existing fully prestressed box-girder bridge. Proc. Inst. Civ. 2017, 170(1), 42–53.

[31] Caner, A.; Apaydin, N.; Cinar, M.; Peker, E., Kilic, M. Reconstruction of Partially Collapsed Post-tensioned Begendik Bridge During Balanced Cantilever Construction. Developments in International Bridge Engineering 2021, 17-33.

[32] Kwak, H. G.; Son, J. K. Span ratios in bridges constructed using a balanced cantilever method. Constr Build Mater. 2004, 18(10), 767–779.

[33] Kwak, H. G.; Son, J. K. Design moment variations in bridges constructed using a balanced cantilever method. Constr Build Mater. 2004, 18(10), 753-766.

[34] Hewson, N. Balanced cantilever bridges. Concrete (London) 2007, 41(10), 59-60.

[35] Marzouk, M.; Said, H.; El-Said, M. Special-purpose simulation model for balanced cantilever bridges. J. Bridge Eng. 2008, 13(2), 122–131.

[36] Ates, S. Numerical modelling of continuous concrete box girder bridges considering construction stages. Appl. Math. Model. 2011, 35(8), 3809–3820.

[37] Bravo, J.; Benjumea, J.; Consuegra, F. A. Parametric Study to Estimate Seismic Displacement Demands of Balanced Cantilever Bridges in Service and Construction Conditions; Conference: fib Symposium 2021 - Concrete Structures: New Trends for Eco-Efficiency and Performance, 2021

[38] Pimanmas, A. The effect of long-term creep and prestressing on moment redistribution of balanced cantilever cast-in-place segmental bridge. SJST 2007, 29(1), 205–216.

[39] Hedjazi, S.; Rahai, A.; Sennah, K. Evaluation of creep effects on the time-dependent deflections and stresses in prestressed concrete bridges. Bridge Structures 2007, 3(2), 119-132.

[40] Altuşnişık, A. C.; Bayraktar, A.; Sevim, B.; Adanur, S.; Domaniç, A. Construction stage analysis of Kömürhan highway bridge using time dependent material properties. Struct. Eng. Mech. 2010, 36(2), 207–223.

[41] Malm, R.; Sundquist, H. Time-dependent analyses of segmentally constructed balanced cantilever bridges. Eng Struct. 2010, 32(4), 1038–1045.

[42] Akbar, S.; Carlie, M. Long-term deformation of balanced cantilever bridges due to non-uniform creep and shrinkage; KTH Royal Institute of Technology, School of Architecture and the Built Environment, 2021

[43] McDonald, B.; Saraf, V.; Ross, B. A spectacular collapse: Koror-Babeldaob (Palau) balanced cantilever prestressed, posttensioned bridge. Indian Concr. J. 2003, 77(3), 955–962.

[44] Radić, J.; Gukov, I.; Meštrović, D. A new approach to deflection analysis of cantilever beam bridges. in Proc of the 2nd International Conference IABMAS − Bridge Maintenance, Safety, Management and Cost. Ed. by Watanabe, E.; Frangopol, D. M.; Utsunomiya, T. 18−22 Oct, Kyoto, Japan. Leiden: A. A. Balkema Publishers. 8 p. ISBN 04 1536 336 X, 2004

[45] Jung, S.; Ghaboussi, J.; Marulanda, C. Field calibration of time-dependent behavior in segmental bridges using self-learning simulation. Eng. Struct. 2007, 29(10), 2692–2700.

[46] Kronenberg, J. Continous concrete placing during balanced cantilever construction of a bridge. Concr. Eng. Int. 2008, 12(3), 38–39.

[47] Kamaitis, Z. Field investigation of joints in precast post-tensioned segmental concrete bridges. Balt. J. Road Bridge Eng. 2008, 3(4), 198–205.

[48] Starossek, U. Shin Chon Bridge Korea. SEI 2009, 19(1), 79-84.

[49] Furunes, E. W. Trysfjord bridge, parametric analysis and modelling for drawingless construction of a concrete balanced cantilever bridge; IABSE Congress: Structural Engineering for Future Societal Needs, Ghent, Belgium, 1999-2004, 2021

[50] Integra Ltd. Mostar Preparation of main design and related studies for motorway section in the Corridor Vc, Group F – Structures (Engineering Structures), Book: F 2100 – Civil design of the Vranduk 1 bridge, textual part and drawings, 2018

[51] Integra Ltd. Mostar Preparation of main design and related studies for motorway section in the Corridor Vc, Group F – Structures (Engineering Structures), Book: F 2200 – Civil design of the Vranduk 2 bridge, textual part and drawings, 2018

[52] EN 1992-1-1:2004+AC:2010: Eurocode 2: Design of concrete structures – Part 1-1: General rules and rules for buildings, 2004

[53] CEB-FIP MODEL CODE 1990, Thomas Telford Ltd., London, 1993

**List of figures:**

# PAPER I

# STUDENČICA BRIDGE TESTING

**Marino Jurišić**
*University of Mostar, Faculty of Civil Engineering, Bosnia and Herzegovina, student*
*Corresponding author: jurisicmarino@hotmail.com*
**Marko Cvitković**
*University of Mostar, Faculty of Civil Engineering, Bosnia and Herzegovina, student*

**Abstract:** Studenčica bridge is located at Donji Studenci, to the southwest of Mostar in Bosnia and Herzegovina. The bridge is a great feat of engineering. It is built at a height of 88 m above the valley and is 555 m long, with main spans of 120 m. Before the bridge was opened for traffic, it was subjected to a series of tests to verify whether the construction satisfied the criteria regulated by law. Static and dynamic tests were conducted to confirm the safety of the bridge. Before the tests commenced, a numerical model of the bridge was developed and calculated by using a computer program (TOWER), and the calculation results were later compared with the measured values. The static tests comprised measurement of vertical deformation and stress in the construction, and the dynamic test involved measurement of the oscillation frequencies of the bridge. The results were analyzed to check whether the bridge performs as expected and whether it can be opened for traffic.

**Keywords**: construction performance, static tests, dynamic tests, result analysis, structural testing

# ISPITIVANJE MOSTA STUDENČICA

**Sažetak**: Most Studenčica nalazi se u Donjim Studencima, jugozapadno od Mostara u Bosni i Hercegovini. Most je veliki inženjerski pothvat. Napravljen je na visini od 88 m iznad doline i dug je 555 m, s glavnim rasponima od 120 m. Prije nego što je most otvoren za promet, morao je proći niz provjera radi potvrde zadovoljava li konstrukcija uvjete propisane zakonom. Provedeni su statički i dinamički testovi da se potvrdi sigurnost mosta. Prije nego su testiranja započela, izrađen je i izračunat numerički model mosta u računalnom programu (TOWER), a rezultati su kasnije uspoređeni s izmjerenim vrijednostima. Statički testovi sastojali su se od mjerenja vertikalnih deformacija i naprezanja u konstrukciji, a dinamički testovi su mjerili frekvencije osciliranja mosta. Rezultati su analizirani radi provjere ponaša li se most prema očekivanjima i smije li se otvoriti za promet.

**Ključne riječi**: ponašanje konstrukcije, statički testovi, dinamički testovi, analiza rezultata, ispitivanje konstrukcija

# 1 INTRODUCTION

Bridge testing (numerical and load tests) is an essential part of modern bridge construction. Just like every building, a constructed bridge must be subjected to a series of tests to check whether it complies with the specific demands and requirements so it can be certified as safe and ready for use. Unfortunately, throughout history, some constructions have collapsed; such accidents provide an insight into problems and help researchers learn from past mistakes. Modern technology provides the means to prevent such mistakes and confirm the safety and stability of a construction before it is put to use. The methods and sequences of the tests and interpretation of the test results are determined by the standards that are precisely regulated by law in every country or region (in this case, "Pravilnik za ispitivanje mostova probnim opterećenjem," the current standards in Bosnia and Herzegovina) [1]. Different equipment is used to measure different factors that are compared to the results obtained while testing. As such, it is possible to assess whether the construction is performing as expected. Before the tests commence, the material (concrete, steel) is investigated to confirm that the properties of the material are as described in the project. In this study, bridge samples of built-in concrete and steel were tested in the laboratory, and concrete quality was determined by static tests. This paper describes certain ways of bridge testing that were employed for the Trebižat and Studenčica bridges and provides an interpretation of the results. These bridges are located to the southwest of Mostar in Bosnia and Herzegovina and are named after the rivers that flow under them. The Faculty of Civil Engineering, University of Mostar, tested these bridges with different equipment commonly used for bridge testing. Since similar procedures were used for both bridges, only Studenčica (longer bridge) is reviewed in this paper, considering that the same applies to the other bridge.

# 2 CHARACTERISTICS OF STUDENČICA BRIDGE

The bridge is located at Donji Studenci and is a part of highway corridor Vc, section Počitelj, along the border of the Republic of Croatia. It spans over the Studenčica river and is built at a height of 88 m. The bridge supports a full highway profile, and therefore, it was designed as a dual construction where each one served for a different highway direction. The highway profile (one direction) consists of two lanes 3.75 m wide, one emergency lane 2.5 m wide, and a protective strip of pavement 0.5 m wide. The Jersey barrier is 0.46 m wide. Thus, the complete width of one bridge is 0.46 + 0.50 + 2.50 + 2*3.75 + 2*0.50 + 0.46 = 12.42 m. The bridge has six spans of lengths 70, 120, 120, 120, 80, and 45 m, and thus, its complete length is 555 m. The static system is a frame that consists of a horizontal girder and vertical piers. The cross section of the girder is a box made of pre-stressed concrete. The quality of the concrete is C40/50 (C50/60) with B 500B reinforcement bars and Y 1860 S7 pre-stressing steel. The cross section of the girder box varies; over the abutment and in the middle of the spans, the bridge is 3.1 m high, and over the piers, it is 6.5 m high. The main part of the bridge was built using a balanced cantilever construction method; however, the spans closest to the abutments were built on a scaffolding [2].
Figure 1 is presenting Studenčica bridge under construction and completed bridge.

**Figure 1 Bridge under construction and completed bridge**

# 3 STANDARDS AND REGULATIONS USED IN TESTING

Testing was conducted in accordance with “Pravilnik za ispitivanje mostova probnim opterećenjem” (“Standards for test load bridge testing”) [3]. These regulations require that every road bridge with a span greater than 15 m be subjected to both static and dynamic test loads. They also require that the test load should be between 0.5 and 1.0 of the load used for designing the bridge (coefficient U) [3]. In this case, the test load was four to six vehicles placed according to the calculation such that they had the biggest impact on the bridge. The deformations and stress in the bridge were calculated before the test, and the measured results should be lesser than the calculated ones. Stress diagrams were plotted for the characteristic cross sections where the strains were measured. The frequency in the vertical direction was also measured. Calculation was conducted using Tower 7 Radimpex Beograd program [4].

# 4 TESTS AND RESULTS

As stated earlier, the bridge has to be confirmed safe before it is put to use. For a bridge to be declared safe, it should pass the static and dynamic tests conducted by the authorized personnel. The ability of the bridge to withstand certain (predicted) amounts of load with acceptable deformations is demonstrated through these tests [5]. The results are interpreted by competent engineers; based on the quality of the results, the engineers determine whether the bridge satisfies the criteria set up at the beginning of the testing.

## 4.1 Static tests

Static tests of the bridge are conducted by applying load on bridge spans and above piers to cause deformations and stresses in the construction. In the present case, the load was six trucks weighing 30–50 tons. The weight of the trucks was distributed on their axles and was used as such in the calculation. Appropriate positioning of the trucks on the bridge (Figures 2, 3 and 4) resulted in the desired stress and deformation in the construction, and different positions were used to test the three spans and two piers. The test load was 56% of the live load (coefficient U = 0.56).

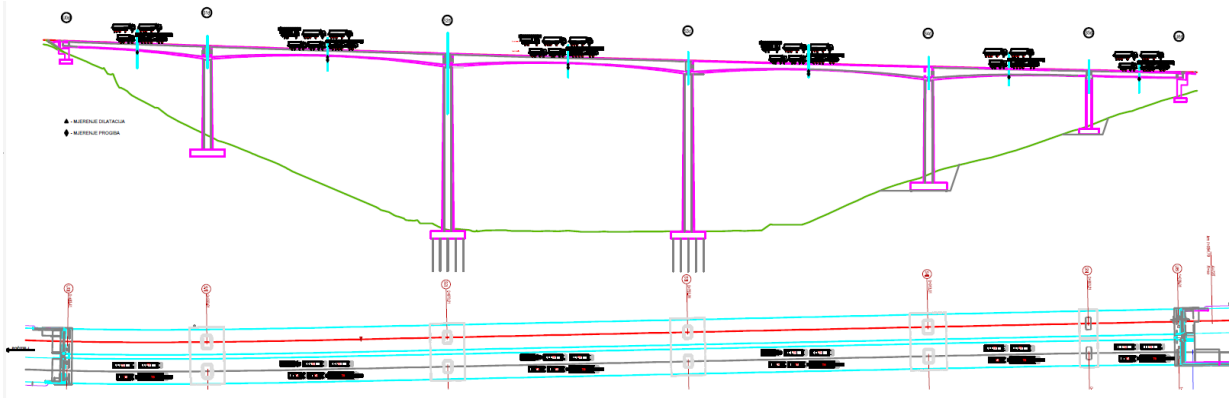

**Figure 2 Illustration of span testing [6]**

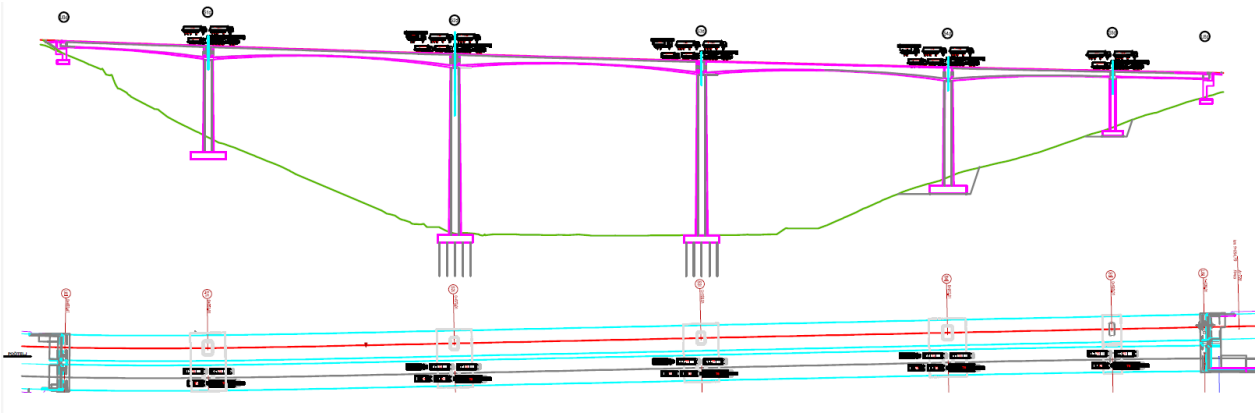

**Figure 3 Illustration of pier testing [6]**

**Figure 4 Test load on the bridge [6]**

S 1

| fck | 64,89 | 57,64 | 61,98 | 58,23 | 54,56 | 53,81 | 54,31 | 60,56 | 54,56 | 62,23 | 59,98 | 59,64 | | 62,56 | 59,98 | 60,73 | 55,39 | 60,31 | 54,39 | 53,81 | 54,56 | 51,56 | 61,23 | 56,64 | 58,14 |
|---|---|---|---|---|---|---|---|---|---|---|---|---|---|---|---|---|---|---|---|---|---|---|---|---|---|
| U0L-XII10L | SPOJNI | XI10L | X10L | IX10L | VIII10L | VII10L | VI10L | V10L | IV10L | III10L | II10L | I10L | BAZNI | II12L | III12L | III12L | IV12L | V12L | VI12L | VII12L | VIII12L | IX12L | X12L | XI12L | SPOJNI |
| G.P. 77,90 | | | | | | | | | | | | | G.P. 67,60 | | | | | | | | | | | | |
| REBRA 71,11 | 77,9 | 69,2 | 74,4 | 69,9 | 65,5 | 64,6 | 65,2 | 72,7 | 65,5 | 74,7 | 72 | 71,6 | REBRA 61 | 75,1 | 72 | 72,9 | 66,5 | 72,4 | 65,3 | 64,6 | 65,5 | 61,9 | 73,5 | 68 | 69,8 |
| D.P. 71,11 | | | | | | | | | | | | | D.P. 75,30 | | | | | | | | | | | | |
| 48,44 Mpa | | | | | | | | | | | | 1 | 64,3 | | 53,56 | | | | | | | | | | |
| 58,4 Mpa | | | | | | | | | | | | 2 | 66,7 | | 55,56 | | | | | | | | | | |
| | | | | | | | | | | | | 3 | 68,4 | | 56,98 | | | | | | | | | | |
| | | | | | | | | | | | | 4 | 62,7 | | 52,23 | | | | | | | | | | |
| | | | | | | | | | | | | 5 | 58,1 | | 48,4 | | | | | | | | | | |
| | | | | | | | | | | | | 6 | 61,6 | | 51,31 | | | | | | | | | | |
| | | | | | | | | | | | | 7 | 67,3 | | 56,06 | | | | | | | | | | |
| | | | | | | | | | | | | 8 | 65,8 | | 54,81 | | | | | | | | | | |
| | | | | | | | | | | | | 9 | 56 | | 46,65 | | | | | | | | | | |
| | | | | | | | | | | | | 53 Mpa | | | | | | | | | | | | | |
| | | | | | | | | | | | | 52,9 Mpa | | fck | | | | | | | | | | | |

**Figure 5 Built-in concrete strength [6]**

The rest of the bridge has similar concrete strengths; therefore, in the model, the quality of pier concrete was C40/50 and that of span concrete was C50/60 (Figure 5).

Vertical deformation of the bridge was measured at every span by using geodetic instruments with an accuracy of ½ mm [6]. The regulations state that no additional load may be on the bridge and no works can be performed while the vertical deformations are being determined because in such situations, the results may be

affected causing false readings [3]. The position of every truck was controlled, and hence, the possible locations of maximum deformations were known. With these measures, it was possible to check whether the construction underwent any plastic deformations. The absence of plastic deformations indicated that the bridge remained in the elastic state (stress and strain were proportional) and that the stress could be calculated if the Young's modulus for concrete and relative longitudinal deformation were known [7]. Table 1 lists the vertical deformations during and after the load was applied. The piers did not undergo any longitudinal deformations, and every deformation that existed in the middle of the spans when the bridge was loaded disappeared when the load was removed; this means that every span returned to its original position with no plastic deformation.

**Table 1 Geodetic measurements [6]**

| Measured points | A (starting state) (m) | B (loaded state) (m) | A-B (m) | C (unloaded state) (m) | A-C (m) |
|---|---|---|---|---|---|
| U0 | | | | | |
| 1/2 | 105.896 | 105.888 | -0.008 | 105.896 | 0.00 |
| S1 | 104.708 | 104.708 | 0.00 | 104.708 | 0.00 |
| 1/2 | 1.343 | 1.363 | -0.020 | 1.343 | 0.00 |
| S2 | 3.278 | 3.278 | 0.00 | 3.278 | 0.00 |
| 1/2 | 1.450 | 1.475 | -0.025 | 1.450 | 0.00 |
| S3 | 3.163 | 3.163 | 0.00 | 3.163 | 0.00 |
| 1/2 | 1.569 | 1.591 | -0.022 | 1.569 | 0.00 |
| S4 | 3.084 | 3.084 | 0.00 | 3.084 | 0.00 |
| 1/2 | 106.886 | 106.877 | -0.009 | 106.886 | 0.00 |
| S5 | 105.985 | 105.985 | 0.00 | 105.985 | 0.00 |
| 1/2 | 106.190 | 106.185 | -0.005 | 106.190 | 0.00 |
| U6 | | | | | |

Relative deformation of the concrete was measured at four locations in the cross section, and it was controlled within the second, third, and fourth span and also above S2 and S3 piers. For this test, electrical strain gages, namely, HBM type K-LY41 100/120, were used [8]. These strain gages can determine the strain in the concrete by measuring the electrical resistance before and after load is applied. Here, the bridge was assumed to be elastic under the test load; this assumption was verified by using the geodetic measurements. This is very important because if the concrete is elastic, its stresses can be easily calculated. In each cross section of the bridge, four strain gages were connected (Figure 6) to the central MGC plus system where the strain data were collected using the Catman AP program package [8]. The system run time was sufficient for observing the starting state, loaded state, and the unloaded state, and it was controlled by the personnel testing the bridge. The software then plotted a diagram showing the strain in the concrete in the given time period (Figures 7 and 8). Results of stress and strain measurement are presented in Tables 2 and 3.

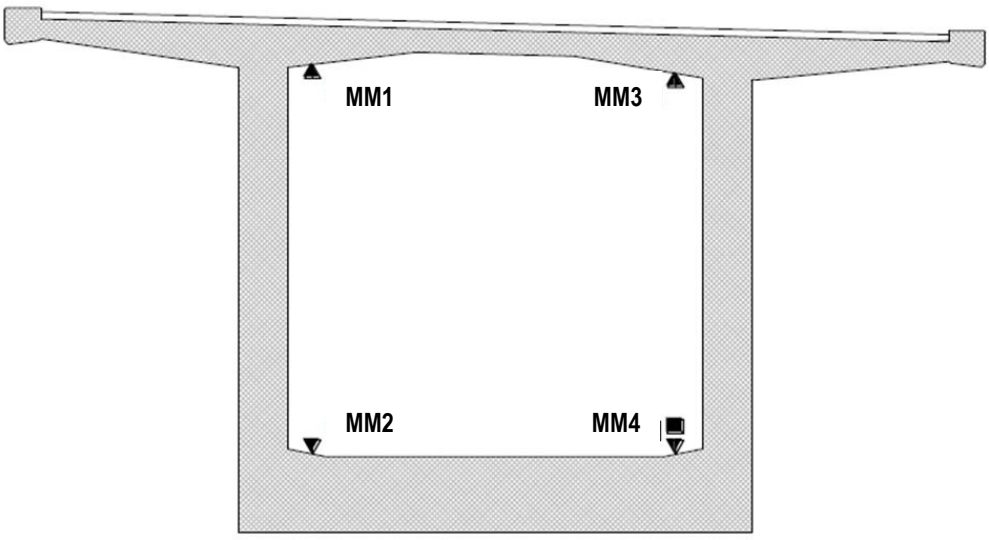


**Figure 6 Position of strain gages [6]**

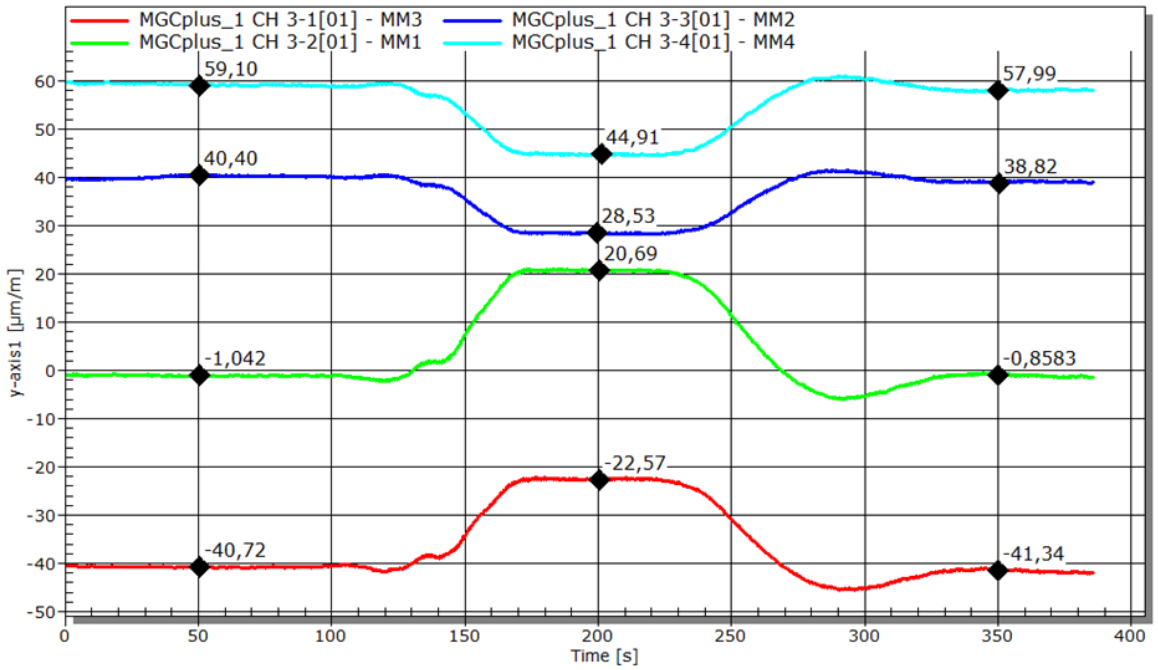


**Figure 7 Example of strain diagram for the region over a pier (S3) in Catman AP [6]**

**Table 2 Strain and stress over a pier (S3) [6]**

| | Strain MM1 (µm/m) | Strain MM2 (µm/m) | Strain MM3 (µm/m) | Strain MM4 (µm/m) |
|---|---|---|---|---|
| Starting state | -1.04 | 40.40 | -40.72 | 59.10 |
| Loaded state | 20.69 | 28.53 | -22.57 | 44.91 |
| Unloaded state | -0.85 | 38,82 | -41.34 | 57.99 |
| Strain | +21.73 µm/m | -11.87 µm/m | +18.15 µm/m | -14.19 µm/m |
| Stress | +0.82 MPa | -0.45 MPa | +0.68 MPa | -0.53 MPa |

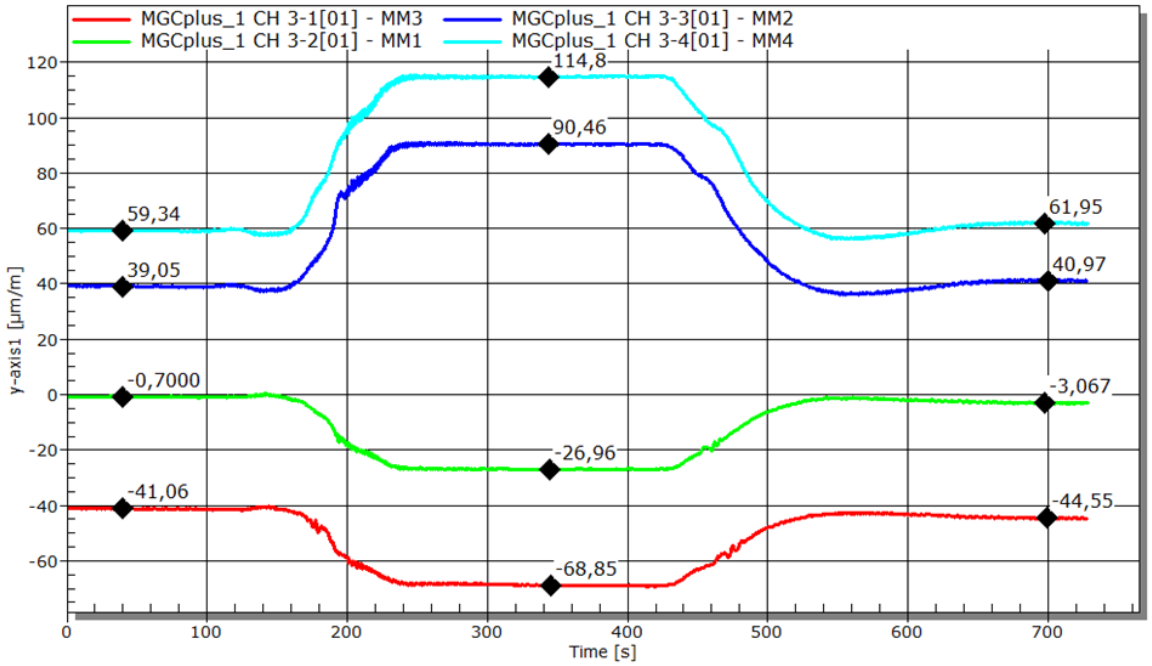


**Figure 8 Example of a strain diagram (third span) in Catman AP [6]**

**Table 3 Strain and stress over the third span [6]**

| | Strain MM1 (μm/m) | Strain MM2 (μm/m) | Strain MM3 (μm/m) | Strain MM4 (μm/m) |
|---|---|---|---|---|
| Starting state | -0.07 | 39.05 | -41.06 | 59.34 |
| Loaded state | -26.96 | 90.46 | -68.85 | 114.80 |
| Unloaded state | -3.06 | 40.97 | -44.55 | 61.95 |
| Strain | -26.89 μm/m | +51.41 μm/m | -27.79 μm/m | +55.46 μm/m |
| Stress | -1.02 MPa | +1.95 MPa | -1.05 MPa | +2.10 MPa |

## 4.2 Dynamic test

Dynamic testing of a construction involves measuring the oscillations of the bridge under dynamic load [5]. The dynamic load is actually the force applied on the bridge when a truck moving at a certain speed goes over a plank. It has an impact on the construction, thus triggering oscillations. The acceleration resulting from such impacts, as in the case of earthquakes, can be measured to plot a graph for the duration when the dynamic force was applied. In this test, T3 truck passed over a 5-cm-thick board at a speed of 40 km/h. The test was conducted only on the central (third) span. The accelerations were measured by HBM acceleration transducers, type B12/500, and the data were collected by the MGC plus system [6]. Frequency diagrams were plotted using the obtained accelerations (Figure 9).

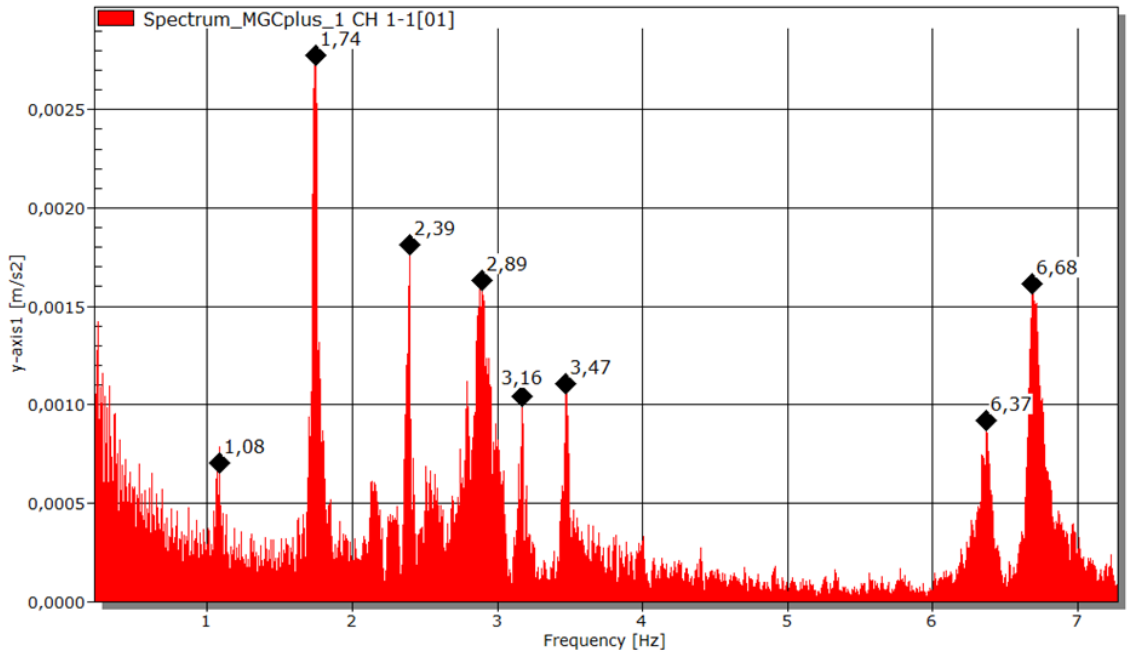


**Figure 9 Frequency diagram [6]**

# 5 COMPARISON OF MEASUREMENT RESULTS WITH MODEL CALCULATIONS

In order to confirm that the bridge is safe and ready for use, it must be proved that the bridge endured the static and dynamic load as predicted. For this purpose, the measured values are compared with the calculated ones (Table 4). For the static test, the geodetic measurements after and before the load was applied should be the same. It is also very important that the readings above the piers remain constant because this is an indicator of foundation settling (piers have great longitudinal stiffness; hence, the piers are considered rigid bodies, and this means that any readings above the piers while the load is applied indicate foundation settling). The stresses measured by the stress gages should be close to our calculated values because the material had elastic properties (Table 5). Concrete strength was investigated in situ. In the dynamic load test, the frequencies measured on the bridge should be close to the calculated values for the dynamic model of the bridge (Table 6). During the tests, the bridge should also be checked visually for cracks to confirm the quality of the material used.

**Table 4 Comparison of measured and calculated vertical deformations [6]**

| Measured points | A (calculated values) (mm) | B (measured values) (mm) | Relative error | A-B (mm) |
|---|---|---|---|---|
| U0 | | | | |
| 1/2 | -8 | -7 | 0.125 | -1 |
| S1 | 0 | 0 | 0 | 0 |
| 1/2 | -20 | -22 | 0.1 | 2 |
| S2 | 0 | 0 | 0 | 0 |
| 1/2 | -25 | -24 | 0.04 | -1 |
| S3 | 0 | 0 | 0 | 0 |
| 1/2 | -22 | -22 | 0 | 0 |
| S4 | 0 | 0 | 0 | 0 |
| 1/2 | -9 | -11 | 0.22 | 2 |
| S5 | 0 | 0 | 0 | 0 |
| 1/2 | -5 | -4 | 0.2 | -1 |
| U6 | | | | |

**Table 5 Comparison of controlled and calculated stress [6]**

| | | Calculated stress (MPa) | Controlled stress (MPa) | Relative error | Difference (MPa) |
|---|---|---|---|---|---|
| Second span | MM1 | -1.08 | -0.80 | 0.259 | -0.28 |
| | MM2 | 2.29 | +1.87 | 0.183 | 0.42 |
| | MM3 | -1.08 | -0.94 | 0.130 | -0.14 |
| | MM4 | 2.28 | +2.10 | -0.079 | -0.18 |
| Second pier | MM1 | 0.81 | +0,71 | 0.123 | 0.10 |
| | MM2 | -1.06 | -0.53 | 0.500 | -0.53 |
| | MM3 | 0.84 | +0.67 | 0.202 | 0.17 |
| | MM4 | -1.10 | -0.54 | 0.418 | -0.46 |
| Third span | MM1 | -1.06 | -1.02 | 0.038 | -0.04 |
| | MM2 | 2.35 | +1.95 | 0.170 | 0.40 |
| | MM3 | -1.05 | -1.05 | 0.000 | -0.00 |
| | MM4 | 2.36 | +2.10 | 0.110 | 0.26 |
| Third pier | MM1 | 0.88 | +0.82 | 0.068 | 0.06 |
| | MM2 | -1.10 | -0.45 | 0.591 | -0.65 |
| | MM3 | 0.89 | +0.68 | 0.236 | 0.21 |
| | MM4 | -1.02 | -0.53 | 0.480 | -0.49 |
| Fourth span | MM1 | -1.05 | -1.03 | 0.019 | -0.02 |
| | MM2 | 2.23 | - | - | - |
| | MM3 | -1.05 | -0.93 | 0.124 | -0.13 |
| | MM4 | 2.23 | +2.15 | 0.036 | 0.08 |

**Table 6 Comparison of calculated and measured frequencies [6]**

| Frequency | Value 1 | Value 2 | Value 3 | Value 4 | Value 5 | Value 6 | Value 7 |
|---|---|---|---|---|---|---|---|
| Calculated values (Hz) | 1.16 | 1.78 | 2.17 | 2.47 | 3.12 | 3.64 | 3.99 |
| Measured values (Hz) | 1.08 | 1.74 | 2.39 | 2.89 | 3.16 | 3.47 | 6.68 |
| Difference (Hz) | 0.08 | 0.04 | -0.22 | -0.47 | -0.04 | 0.17 | -2.69 |

## 6 CONCLUSION

In conclusion, Studenčica was a very challenging construction project. It is the highest bridge in Bosnia and Herzegovina. The tests showed that the designers and builders completed their task successfully. The vertical deformation measurement showed that the bridge is performing as expected and that its vertical deformations are close to the model calculations. Plastic vertical deformations are nonexistent, and thus, the regulations (plastic vertical deformations for pre-stressed constructions should not exceed 20% of the measured ones when the load is removed) are satisfied [3]. All deformations disappeared once the load was removed; in other words, the construction exhibits elastic properties. In addition, there were no deformations (measurements) on the piers; this

implies that there was no differential settling of the foundation. Stresses in the construction were measured indirectly over the strain because the material retained its elastic properties. The stress in the construction was always lesser than the calculated values, thus meeting the criteria [3]. Some bigger deviations were allowed for concrete on the safety side because it is a non-homogeneous material. Visual inspection proved that there were no cracks in the bridge; this implies that the pre-stressing was done successfully and that enough compressive force was applied to the construction. The dynamic tests showed that the measured oscillation frequencies are very similar to the calculated ones and that the bridge performed as expected. All tests showed that the construction satisfied the criteria set as per the regulations and that the bridge can be opened for traffic. The bridge is now in operation, and it carries the Vc highway corridor towards the border with Croatia, connecting Bosnia and Herzegovina with the European highway network.

## ACKNOWLEDGEMENTS

The authors would like to thank the expert team of Faculty of Civil Engineering for the permission to accompany the team on Studenčica bridge and for teaching the authors bridge testing firsthand. The authors also thank Hering d.d. for permission to participate in this work. Special thanks are due to the professors at the Faculty of Civil Engineering, Ivana Domljan, Mladen Glibić, and Mladen Kustura, for their guidance and patience and for providing the material necessary for this paper. Last but not the least, thanks are due to Mr. Denis Stranjak who was kind enough to check the paper for any language errors.

### References

[1] Đuranović N.; Popović J., Aktuelne metode ispitivanja mostovskih konstrukcija
[2] Hering d.d. 2014: Građevinski projekt mosta Studenčica – faza izvedbeni projekt, Široki Brijeg.
[3] Pravilnik za ispitivanje mostova probnim opterećenjem, JUS U.M1.046, Pravilnik br. 50-14233/1, Službeni list SFRJ, br. 60/84, 1984.
[4] Radimpex software, www.radimpex.rs, 14.04.2015.
[5] Abdunur C. 1992: Stress monitoring and re-adjustment in concrete structures. 1st European Conference on Smart Structures and Materials, Glasgow.
[6] Glibić M.; Kustura M. 2014: Izvješće o ispitivanju mosta Studenčica – "Lijevi most" (LOT 7, Dionica Počitelj-Bijača, poddionica 2) probnim opterećenjem.
[7] Abdunur C. 1996: Stress redistribution and structural reserves in prestressed concrete bridges. 3rd International Conference on Bridge Management, Guildford.
[8] HBM test and measurement, http://www.hbm.com/, 14.04.2015.

# PAPER II

applied sciences

MDPI

*Review*

# Long-Term Effects in Structures: Background and Recent Developments

**Alen Harapin [1], Marino Jurišić [2,*], Neda Bebek [3] and Marina Sunara [1]**

[1] Faculty of Civil Engineering, Architecture and Geodesy, University of Split, Matice Hrvatske 15, 21000 Split, Croatia; alen.harapin@gradst.hr (A.H.); marina.sunara@gradst.hr (M.S.)
[2] Faculty of Civil Engineering, Architecture and Geodesy, University of Mostar, Matice Hrvatske bb, 88000 Mostar, Bosnia and Herzegovina
[3] HERING d.d. for Design and Construction, Provo bb, 88220 Široki Brijeg, Bosnia and Herzegovina; nbebek@hering.ba
* Correspondence: marino.jurisic@fgag.sum.ba; Tel.: +387-63-434-119

**Abstract:** This article addresses the often overlooked but critical long-term factors of creep, shrinkage, ageing and corrosion in civil engineering structures. The paper emphasizes their substantial impact on structural mechanical resistance and safety, drawing attention to key examples like the Civic Tower in Pavia, the Koror-Babeldaob Bridge and dams in the USA. By exploring the challenges faced in modern engineering, the article sheds light on the need to consider these effects. Various models for predicting creep and shrinkage in concrete structures are introduced as potential solutions. In conclusion, the paper highlights the necessity for engineers to navigate the intricacies of material behaviour for successful construction amidst evolving challenges.

**Keywords:** concrete; creep; shrinkage; long-term effects; ageing; corrosion

check for updates

**Citation:** Harapin, A.; Jurišić, M.; Bebek, N.; Sunara, M. Long-Term Effects in Structures: Background and Recent Developments. *Appl. Sci.* **2024**, *14*, 2352. https://doi.org/10.3390/app14062352

Academic Editors: Luca Susmel and Kang Su Kim

Received: 31 January 2024
Revised: 28 February 2024
Accepted: 6 March 2024
Published: 11 March 2024



## 1. Introduction

Material parameters are generally time-dependent; that is, they change their properties over period of time. In some cases, this change is positive (for example, concrete increases its strength over time), but in some cases, change can induce the weakening of material and overall structure. That kind of negative change can lead to structural collapse.

When discussing long-term effects on masonry and concrete structures, considerations include creep, shrinkage, aging and corrosion. The goal of this paper is to provide insight into these processes, accompanied by examples that underscore their significance and the potential consequences of neglecting them. Concrete is a mixture of cement, aggregate and water with additives. Cement is a mixture of calcium silicates and aluminates. After adding water in dry mixture of cement and aggregate, a number of exothermic chemical reactions start simultaneously. This process is commonly denoted with the term hydration. Hydration begins immediately after the cement comes in contact with water, but lasts for a very long period of time. During prolonged hydration, concrete increases its strength and modulus of elasticity and this process is called aging.

Over time, concrete can be affected by reactive liquids and gases which can cause chemical, physical–chemical or colloidal deterioration and disintegration of concrete components. This process is known as concrete corrosion. Also, there is another type of corrosion—corrosion of reinforcement—which will not be discussed in this paper. Creep is the process of structure deformation under long-term (sustained) load.

It is well established that body deforms under the influence of force. When a force is applied, the change is immediate. In addition, if the force is applied over an extended period, the material attempts to adapt, changing its shape and volume to redistribute stress.

Generally, creep in concrete is defined as a time-dependent deformation due to long-term actions [1,2]. These definitions imply that creep will lead to an increase in initial

deformation over time, while in the absence of creep, the initial deformation will decrease as a function of aging, shrinkage of concrete and relaxation of steel [3]. Structure stability can be seriously threatened if progression of shrinkage and creep deformation is neglected. Thus, the obligation to take creep into account when designing and dimensioning reinforced and prestressed structures is even more important. Therefore, considering creep is crucial when designing and dimensioning reinforced and prestressed structures, as it can cause stress redistribution in structures, which leads to a reduction in the load-bearing capacity.

Concrete shrinkage can be described by defining a decreasing function of volume concerning moisture change in the concrete mixture. In the case of restrained deformations of concrete, shrinkage will initiate further stresses in the concrete, which will be accounted for by reinforcement. Therefore, reinforcement accounts for the reduction in shrinkage deformation [4,5]. Displacement decreases over time [3] if shrinkage is present. Also, the influence of creep diminishes with time.

The change in the strain in concrete over time is illustrated below (Figure 1). Shrinkage starts immediately after concrete mixture is prepared. At time $t_0$, the structure is loaded, causing immediate strain ($\varepsilon_m$). Subsequently, creep develops, a process that gradually diminishes over time (Figure 1). Upon unloading, the structure immediately recovers a part of the strain, while another part recovers over a more extended period. The irreversible part of the strain is impossible to recover.

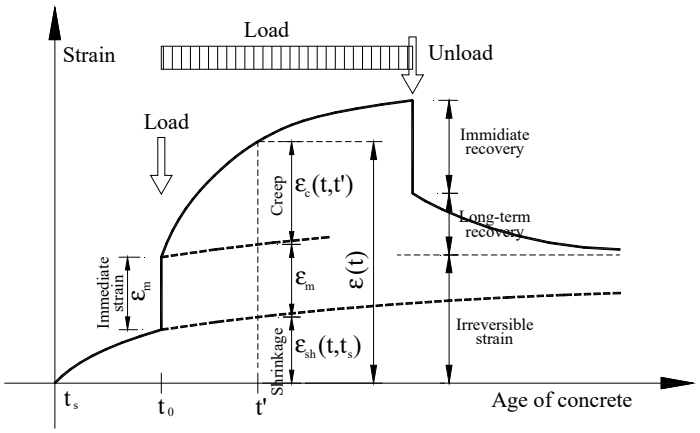


**Figure 1.** Age-dependent strain change in concrete.

As mentioned earlier, concrete aging contributes to the improvement of strength as well as other mechanical properties which are considered positive. On the other side, concrete corrosion occurs only in direct contact with water.

## 2. Motivation

As mentioned in the Introduction, in most cases, long-term effects such as corrosion, aging, shrinkage and creep can be neglected. In the design of simple residential buildings, using approximate solutions (or completely neglecting mentioned effects) is a common practice. However, the neglect of the long-term effects in more complex structures can lead to reduction in mechanical resistance and stability. Three illustrative cases will be mentioned, with structures that had failed due to one or more already mentioned long-term effects.

### *2.1. The Civic Tower in Pavia, Italy*

The Civic Tower (city of Pavia, Italy) was built near Pavia Cathedral in 11th century, from brickwork masonry (Figure 2). The tower had a rectangular footprint, and its height was 72 m.

**Figure 2.** Civic Tower in Pavia, Italy, before the collapse [6].

The Civic Tower suddenly collapsed on 17 March 1989 killing four and injuring fifteen people. All that was left of the tower was 8000 cubic meters of brick, sand and granite rubble (Figure 3) [7,8].

**Figure 3.** Remains of the Civic Tower in Pavia after the collapse [8].

The collapse stunned engineering community and officials. The tower was solidly built, there was not an indication of chemical–physical damage of the bricks (main building material), or the settlement. The collapse of the tower made the Italian government close the Leaning Tower of Pisa over concerns that the popular tourist site might also be at risk of collapse [7,8].

To fully understand the cause of the collapse numerous experimental and numerical investigations were conducted, leading to several identified factors [7,8]:

- The tower was built in several phases, starting from 1060. The steeple, built with granite blocks, was added 500–600 years later;
- The thick bearing walls (2.8 m) were made of two thin external faces in regular brickwork and the internal core was made (filled with) with some kind of soft concrete containing mixture of broken bricks and stone pebbles with thick layers of mortar;

- The total estimated mass of the tower was 12,000 tons, with the steeple alone weighing 3000 tons.

An investigation showed that the bottom part of the tower was under very high compression stresses caused by its own weight: maximum values of 1.7 to 2.0 MPa were found according to the FE elastic model, and between 1.8 and 3.5 MPa according to experimental measurements. These values are significantly high compared to the material's compressive strength [7,8]. This likely resulted in the gradual development of tiny fissures, which, over centuries, might have contributed to the sudden collapse of the material without any obvious immediate cause or evident warning signs, such as significant cracks or spalling, even in the days leading up to the collapse. A careful review of the photographs captured by archaeologists for the Civic Museums in 1968 indicates that, even then, there were fine vertical cracks spread widely across the exterior surface of the tower wall. These cracks were exceptionally challenging to observe and resembled those observed on the specimens during testing [9].

Identifying the sole cause of the collapse proved challenging, but the elevated compressive stress induced by the dead load of the tower was undoubtedly one of the main contributing factors to the disaster.

### 2.2. The Koror-Babeldaob Bridge, Palau

The Koror-Babeldaob Bridge was a bridge in Palau that was connecting islands Koror and Babeldaob. The bridge was a balanced cantilever prestressed concrete box girder bridge with a total length of 385.6 m and a main span of 240.8 m. It was primarily constructed for carrying traffic, but it also carried water-supply piping and electrical conduits [10].

Sagging in the bridge's centre began almost immediately after its completion. After a decade of use, concrete creep led to a sag of approximately 1.2 m in the main span's middle section, causing driver anxiety and government concern (Figure 4). Therefore, the Palau government commissioned two independent studies to determine if the bridge was safe to use. Both studies concluded that the safety of the bridge was sufficient, despite an expected additional sag of 1 m. Encouraged by these studies, the government decided to take only a couple of cosmetic interventions with resurfacing and reinforcement of the bridge.

**Figure 4.** The Koror-Babeldaob Bridge, sagging of the middle point [10].

The bridge collapsed abruptly and catastrophically on 26 September 1996 during the nice weather and practically unloaded (Figure 5). This disaster occurred only 18 years after

construction, 6 years after engineers declared the bridge safe, and less than 3 months after all the reinforcements were made to address the escalating sagging [10].

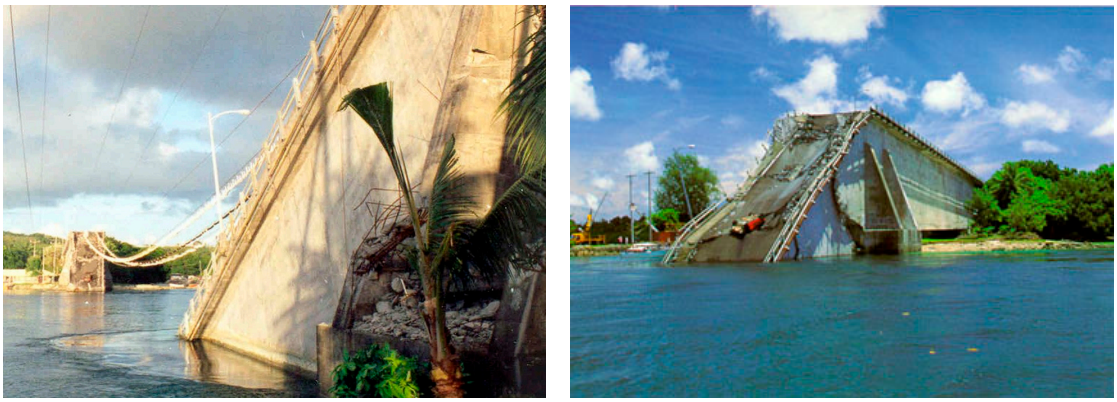

(a) (b)

**Figure 5.** (**a**,**b**) The Koror-Babeldaob Bridge collapse [11].

The main cause of the collapse of Koror-Babeldaob Bridge remains unexplained, despite various studies having been conducted. The most likely theory is that the collapse occurred due to excessive long-time deflections of the prestressed box girders [12]. This could be due to factors such as inadequate design assumptions, material properties, construction practices, or environmental conditions, leading to unexpected deformation and ultimately structural failure. However, as the lawsuit regarding the demolition was settled out of court, the final cause has never been disclosed [10,11].

### *2.3. Concrete Dams in the USA*

In the design and construction of the first modern concrete dams, relatively little attention had been paid to the materials and their behaviour over time. However, even the engineers at the time were aware of certain shortcomings and attempted to solve them. The works of Abrams [13] from 1918 on concrete mixture and determination of water–cement factor are likely among the earliest in this field. Understanding the processes created by hydration of cement was encouraged in the late 1920s, when engineers tried to understand the phenomenon of hydration heat that creates unwanted cracks in massive concrete dams.

The design and construction of the Hoover Dam in the 1930s (Figure 6), the largest dam in the world at that time, with an extremely large amount of concrete, led to advancement in concrete mix design, transportation, installation and cooling of concrete. Strict controls of the installed concrete enabled the reduction in the water–cement factor, which led to significantly better quality of the concrete. Low hydration heat concrete, originally developed for the Hoover Dam, also showed very high resistance to the sulphate environment. At the same time, these successes encouraged researchers into further development of the concrete resistant to all types of degradation [14,15].

In the years that followed, various concrete mixes with different additives were proposed for concrete dams. Some concrete dams met expectations, and some did not. Comparing the results on individual dams has proven highly beneficial in designing durable and resistant concrete mixture. For example, concrete in direct contact with water at the Arrowrock Dam (Boise River, ID, USA) and the Lahontan Dam (Carson River, NV, USA) required significant repairs after 20 years of use, with concrete on the overflows proving particularly sensitive. In contrast, the Elephant Butte Dam (Elephant Butte, NM, USA) remained completely undamaged (Figure 7) [14,15].

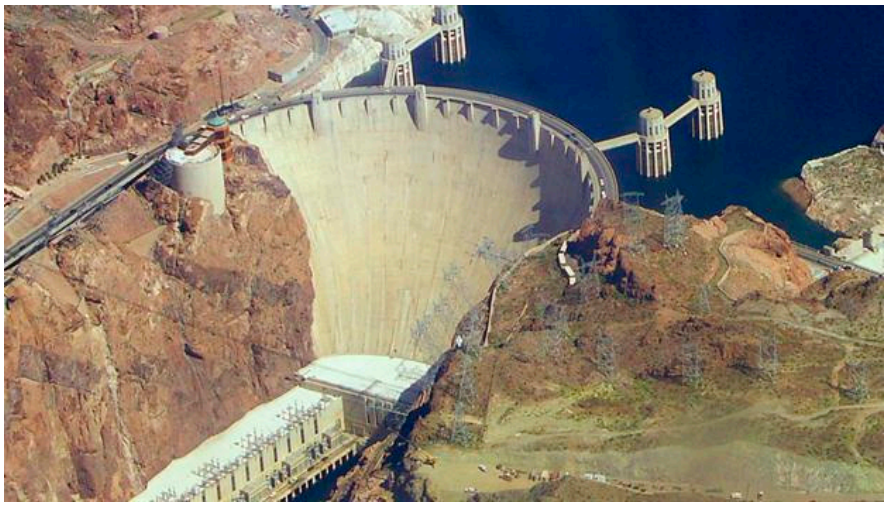

**Figure 6.** The Hoover Dam on Colorado river, USA [16].

(**a**) (**b**) (**c**)

**Figure 7.** Dams in the USA: (**a**) Arrowrock; (**b**) Lahontan; (**c**) Elephant Butte [17–19].

One extreme example is the American Falls Dam, built in 1927, which exhibited significant signs of degradation and had to be replaced in 1977.

Systematic studies of the physical properties of dams, considering chemical changes in the concrete over time, have provided invaluable insights into estimating changes in compressive strength and modulus of elasticity of the concrete in contact with water.

Various improvements in the concrete durability over time are evident: from the first concrete with a reduced water–cement factor, through concrete with additives such as pozzolani, to the concrete with the addition of polymer and silicate dust (silica fume) (Figure 8) [14]. This development continues to this day.

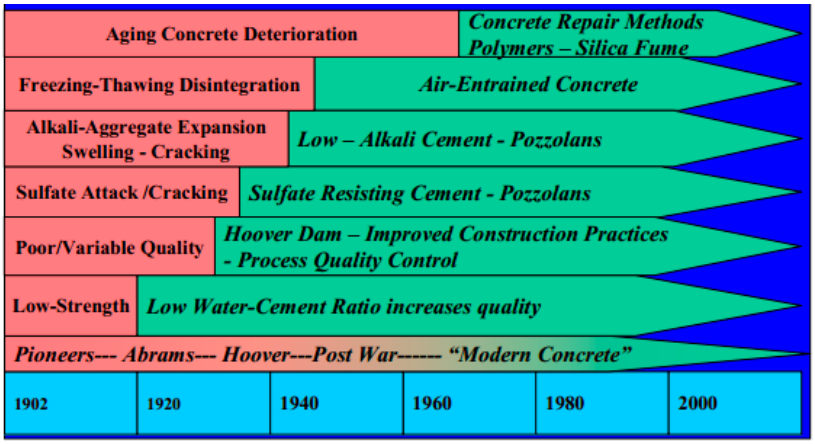


**Figure 8.** Timeline of various improvements in concrete durability [12].

## 3. Long-Term Effects in Concrete

In the Introduction, the effects of creep, shrinkage, ageing and corrosion on concrete are highlighted.

Observing creep and shrinkage separately is the simplest and most convenient approach. The disadvantage of this approach is evident since mentioned effects are not independent from one another [20,21].

It should also be noted that a number of different alternating external influences make it impossible for the model calculations to completely coincide with the measured results. The coefficient of variation for laboratory-measured shrinkage on samples from a single concrete mix was approximately 8% [22–29]. Hence, it is unrealistic to expect that the predicted and experimental results will be in the range of less than 20%. For creep, deviation is even greater. In structures where creep and shrinkage might cause critical deformation or stresses, conducting test specimens and extrapolating the results is advisable.

### *3.1. Concrete Shrinkage*

Concrete shrinkage occurs during the process of concrete hardening due to hydration of cement, as well as the process of drying concrete due to loss of moisture to the environment. The volume of hardened concrete decreases. Shrinkage obtains its maximum on surfaces of the element exposed to drying and decreases towards the inside of the element. The main factors affecting shrinkage are as follows [28–31]:

(1) Mechanical effects from temperature changes;
(2) Thermal effects of cement hydration;
(3) Hydrological effects related to hydration;
(4) Hydrological effects related to climate;
(5) Compressive strength of concrete;
(6) Consistency of the fresh mix;
(7) Type and content of cement;
(8) Water–cement (w/c) factor;
(9) Ratio of fine aggregate according to the total amount of aggregate;
(10) Air content;
(11) Effective element thickness.

According to the literature [32,33], shrinkage can be divided into four main types:

- Autogenous shrinkage—reduction in volume of the mixture of water and cement during hydration;
- Plastic shrinkage—created by the vacuum which occurs when water evaporates from the pores of the capillaries;
- Drying shrinkage—due to the loss of moisture from the concrete, i.e., the release of water from the concrete into the environment; this occurs with hardened concrete;
- Carbonization shrinkage—a reduction in volume by carbonization as a consequence of chemical reactions in cement stone caused by carbon dioxide from the environment.

Each type of shrinkage is schematically illustrated concerning concrete age (Figure 9), along with ratios between each type of shrinkage [34].

A large number of factors affecting shrinkage makes it impossible to generalize one universal model. Researchers have adopted a phenomenological approach, collecting data over long period of time. A contribution in this area was made by numerous authors, some of whom are listed below [21].

One of the earliest models describing concrete shrinkage originates from Michaelis and Menten [5] (1913). It explains the phenomenon of shrinkage by physical-chemical processes at the beginning of the hardening of concrete. After World War II, research on concrete shrinkage intensified. Several models were proposed, based on the phenomenological parameters: Miller (1958), Branson (1977) and Corley & Sozen (1978) [21].

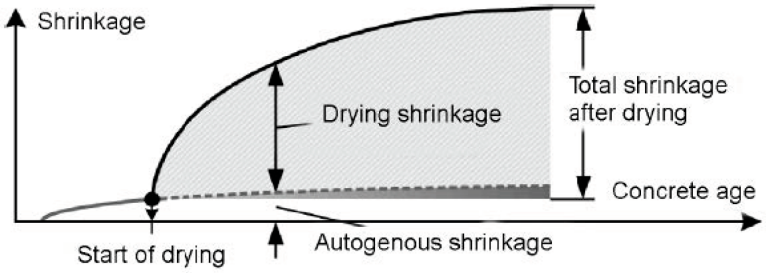


**Figure 9.** Shrinkage strain components for normal concrete [34].

From the mid-1990s, several significant studies were conducted. Hua, Erlacher and Acker (1995) proposed a macroscopic-scale analytical model of autogenous shrinkage and two years later improved this model. Koenders and Breugel (1997) used thermodynamic approach to determine autogenous shrinkage of hardening cement paste. Ishida et al. (1998) proposed a model which is based on micro-mechanical influence of water in pore structure of the concrete [21,31].

It can be shown that reduction in the shrinkage strain would substantially diminish initials cracks too [35–38]. Achieving this could involve replacing Portland cement with Sulfoaluminate cement (SAC), which can be combined with shrinkage-reducing admixture. Assuming regular concrete strength, autogenous shrinkage as well as the early-age strength of concrete, will decrease with the addition of fly ash [39,40]. Conversely, high-strength concrete will exhibit increased shrinkage under the same conditions [41].

Current research on shrinkage primarily focuses on a deeper understanding of autogenous and drying shrinkage [31], particularly in construction stages [42], using new types of cement [43], or with different types of concrete mixtures with different admixtures: various types of aggregate, fibres, etc. [44].

Despite numerous theories, shrinkage remains incompletely explored, and not all causes of this physical phenomenon have been explained. Over the last 5 years, Web of Science has registered over 80 papers dedicated specially to concrete shrinkage.

### *3.2. Concrete Creep*

Creep is a time-dependent deformation of concrete under constant load, which can be several times greater than the initial deformation [1,2]. Concrete creep can be divided into two components:

(1) Basic creep occurs in conditions without movement of moisture;
(2) Creep by drying: the part of creep that occurs when there is movement of moisture from or into the environment.

For the purpose of practical design, it is not necessary to distinguish between basic creep and creep by drying [3]. Creep by drying, in addition to opening cracks, has the most significant impact on the nonlinear behaviour of structures, while the impact of basic creep on nonlinearity is almost negligible [45].

According to [2], there are three main groups of factors affect the occurrence of creep:

(1) The composition of the concrete mix;
(2) The impact of the environment in which the observed structure is located;
(3) The design of the system.

Although the mechanism of creep is still not fully known, it can be said that creep depends on the properties and amount of cement paste and on the properties of the aggregate within the concrete mix. Generally, a concrete mix with a larger volume of aggregate (and a corresponding reduction in the content of cement paste) will lead to less creep deformation in contrast to a mix with a larger volume of cement paste. Also, the "stiffer" unit will try to "restrain" more time-dependent deformation behaviour, and thus reduce the creep effect. If aggregate is (partly) made from recycled concrete, its increasing in the concrete mix will lead to an increase in creep and shrinkage [46,47]. It has also been

observed that the creep deformation is inversely proportional to the degree of cement hardening [48]. It is also known that an increase in water content [48] and air in the concrete mix causes an increase in creep deformation, which is approximately proportional to the square of the water–cement factor [48,49]. Fresh concrete with better properties ensures a lower degree of creep and shrinkage development. A study in the literature [49] deals with this issue and proposes a new numerical approach to predict time-dependent flow of fresh concrete based on the discrete element method.

The next group of factors influencing creep behaviour are the environmental conditions in which the concrete is prepared, installed and loaded. The creep size is particularly sensitive to the relative humidity conditions of the concrete sample. An increase in relative humidity causes a slower creep development and thus decline in the final amount of creep. The development of concrete creep over time also depends on the duration and type of curing of the concrete. Thus, increasing the curing period of wetting concrete is directly related to lower creep development, while curing concrete reduces the size of the final creep deformation up to 30% [2]. Creep is also very sensitive to temperature conditions; an increase in the degree of creep development is related to higher temperatures.

An important factor influencing the development of creep deformation is the adopted design solution. The magnitude of the stress in the concrete element is linearly related to the creep deformation for stress values up to approximately 40 to 60% of the compressive strength [2]. The creep deformation is inversely proportional to the strength of the concrete at the moment of loading [48]. The size and the shape of the concrete element is another key factor. Thinner concrete elements will more easily allow the loss of moisture to the environment, and will thus experience greater creep deformation than thicker concrete elements [48]. Also, load time is very important. Concrete loaded in the later period is exposed to less total creep deformation. For instance, the same concrete loaded on the first day has an 18% higher creep deformation than concrete loaded on the third day [50].

Numerous researchers, including Z.P. Bažant [22–27], have studied the phenomena of shrinkage and creep of concrete over the years. Despite many proposed models, none provide a complete description of the creep phenomenon, each having advantages, disadvantages and specific applications. More recently, many articles [51–53] have focused on the time-dependent behaviour of fibre-reinforced concrete or artificial materials such as AFRP (aramid fibre-reinforced polymer), CFRP (carbon fibre-reinforced polymer), or GFRP (glass fibre-reinforced polymer), although the time-dependent behaviour of "normal" concrete has not been fully tested and defined.

### *3.3. The Models for Prediction of Creep and Shrinkage*

Over the past three decades, numerous models have been proposed to estimate the creep and shrinkage. In the majority of cases, those two phenomena are treated together. These models aim to strike a balance between reliability and ease of use, and they mainly differ in the number and type of parameters they take into account. The reliance of the engineering community, which typically possesses limited knowledge of concrete creep and shrinkage, on simplified models underscores the importance of such models in the field.

Despite a level of uncertainty such simplifications bring into the model, the right choice of parameters can much accelerate the calculations while preserving model predictions.

Some of the most commonly used models in engineering practice are as follows:

- ACI-92 (American Concrete Institute) [2];
- The Eurocode-2 model, based on Fib Model Code 1990 with its revision in 1999;
- Australian Standard AS 3600 Model Code of 1988 [7];
- South African Standard SABS 0100 2000 [54];
- The model of British Standard BS 8110 from 1985 [5];
- The new Fib Model Code Model, from 2010;
- The model of the Japanese Society of Civil Engineers.

Some engineers use strictly scientific models, such as the Gardner–Lockman model GL2000 and the B3 or B4 models suggested by Bažant and his co-workers and approved

by Recommendation of RILEM (The International Union of Laboratories and Experts in Construction Materials, Systems and Structures).

With the exception of the last three models (GL2000, B3 and B4), all others are based on norms for structures design and express creep strain as the product of the concrete elastic deformation and the creep coefficient. The creep coefficient can be calculated according to several intrinsic and/or extrinsic variables [55]. Some of the mentioned codes with factors which were accounted for in calculations are listed below (Table 1) [55].

**Table 1.** Models of creep and shrinkage predictions and factors accounted for [55].

| | FACTOR ACCOUNTED FOR DIFFERENT PREDICTION METHODS | ACI 209 (1992) [2] | AS 3600 (1988) [7] | BS 8110 (1985) [5] | CEB-FIP (1978) [56] | CEB-FIP (1990) [57] | SABS 0100 (1992) [54] | RILEM B3 (1995) [58] |
|---|---|---|---|---|---|---|---|---|
| Intrinsic factors | Aggregate type | | | | | | ✓ | |
| | A/C ratio | | | | | | | ✓ |
| | Air Content | | | | | | | |
| | Cement Content | | | | ✓ | ✓ | | |
| | Cement Type | | | | | ✓ | | ✓ |
| | Concrete Density | | ✓ | | | | | |
| | Fine Total Agreggate Ratio | ✓ | | | | | | |
| | W/C Ratio | ✓ | | | | ✓ | | ✓ |
| | Water Content | | | | | | | ✓ |
| Extrinsic Factors | Age at First Loading | ✓ | ✓ | ✓ | ✓ | ✓ | ✓ | ✓ |
| | Age of Sample | | | | | | | ✓ |
| | Applied Stress | ✓ | ✓ | ✓ | ✓ | ✓ | ✓ | ✓ |
| | Characteristic Strength at Loading | | | ✓ | | | ✓ | |
| | Cross-sectional Shape | | | | | | | ✓ |
| | Duration of Loading | ✓ | ✓ | | ✓ | ✓ | | ✓ |
| | Effective Thickness | ✓ | ✓ | ✓ | ✓ | ✓ | ✓ | ✓ |
| | Elastic Modulus at Age of Loading | | | ✓ | | | ✓ | ✓ |
| | Relative Humidity | ✓ | ✓ | ✓ | ✓ | ✓ | ✓ | ✓ |
| | Temperature | | | | | ✓ | | ✓ |
| | Time Drying Commences | | | | | | | ✓ |

All mentioned models would give significant differences in determining the creep coefficient and the relative shrinkage, so one has to be very careful in which cases to use them. A comparative study about model usage can be found in [55].

### *3.4. Aging of the Concrete*

Concrete, widely utilized in infrastructure such as buildings, bridges and dams, is subjected to various environmental and mechanical factors that contribute to its deterioration over time. As concrete ages, it undergoes changes in mechanical and physical properties that can impact its structural integrity. Over time, factors such as moisture ingress, chemical reactions and mechanical loading contribute to deterioration. Creep, a gradual deformation under sustained loads, increases with age, leading to potential structural deformation. Shrinkage, caused by moisture loss, can result in cracking and reduced durability. Additionally, the porosity of concrete may increase over time, making it more susceptible to moisture penetration and chemical attacks. These changes in mechanical and physical

properties highlight the importance of proactive maintenance and rehabilitation efforts to ensure the long-term performance of concrete structures [59–61].

While aging can lead to some deterioration in concrete structures, there are indeed positive aspects as well. With proper curing and aging, concrete can experience improvements in strength and modulus of elasticity over time. This phenomenon is often attributed to the ongoing hydration process, which continues even after the initial setting of the concrete. As hydration progresses, the cementitious matrix becomes more compact and dense, resulting in enhanced mechanical properties. Additionally, chemical reactions within the concrete can contribute to the development of additional bonding between particles, further increasing strength and stiffness. Therefore, aging can have beneficial effects on the mechanical properties of concrete under certain conditions.

The existing evaluations on the influence of and aging on the mechanical properties focus on compressive strength, along with elastic modulus and splitting tensile strength. Estimating the elastic modulus and splitting tensile strength is crucial since stress calculations rely on the elastic modulus, while the initiation of cracks is assessed based on the tensile strength. Often, these models take temperature into account in addition to concrete ageing [62]. Prediction models for aging concrete, like most, exhibit several shortcomings: simplified assumptions, lack of validation, limited accuracy, difficulty in accounting for combined effects, and sensitivity to input parameters.

Nowadays, many methods have been developed which involves establishing a functional relationship between concrete's mechanical properties and its age through data fitting from early experimental data. This method aims to derive a functional equation that enables the calculation of concrete's mechanical parameters at any given time [63].

### *3.5. Corrosion*

The corrosion of embedded steel stands as a primary cause behind the premature deterioration of reinforced concrete structures globally [64].

The causes of corrosion in reinforced concrete (RC) structures can be attributed to several factors, including the following:

- Carbonation: Carbon dioxide ($CO_2$) from the atmosphere reacts with calcium hydroxide in concrete, reducing its pH and neutralizing its alkalinity. As the pH level decreases to a critical point, the passive layer becomes unstable, leading to potential steel corrosion. Throughout the propagation stage, the corrosion rate is contingent upon various factors, including the presence of water and oxygen. Carbonation-induced corrosion results in general corrosion of steel when it comes into contact with carbonated concrete [65].
- Chloride Attack: Chloride ions, often present in seawater, or marine environments, can penetrate concrete and reach the embedded steel reinforcement. Chloride attack can initiate and accelerate corrosion by breaking down the passive film on the steel surface.
- Moisture and Oxygen: Corrosion of steel reinforcement in concrete requires the presence of moisture and oxygen. Water ingress through cracks or pores in the concrete provides the necessary electrolyte for the electrochemical corrosion process, while oxygen facilitates the oxidation of iron in the steel.
- Cracks and Poor Concrete Cover: Cracks in concrete structures can provide pathways for aggressive substances such as chlorides and carbon dioxide to reach the embedded steel reinforcement, accelerating corrosion. Inadequate concrete cover over the reinforcement also increases the risk of corrosion by reducing the protective barrier between the steel and external corrosive agents [66].
- Microorganisms (bacteria): Microbiologically influenced corrosion occurs when microorganisms, such as colonize the concrete surface and create conditions conducive to corrosion. These microorganisms produce metabolic by products that can degrade the protective passive film on embedded steel reinforcement and promote localized corrosion.

With respect to the abovementioned factors, carbonation and chloride attack are the most common cause of corrosion [67]. Various analytical methods for predicting basic corrosion mechanisms in reinforced concrete are proposed. Estimating the depth of carbonation in concrete can be accomplished using classical approach from CEB [68] and modified [69] diffusion models. The composition of concrete plays a significant role in the diffusion of $CO_2$, while humidity strongly influences the rate of carbonation. Surface materials with high compactness and impermeability can noticeably delay the carbonation process of concrete. Similarly, chloride concentration within the concrete can be determined using diffusion models [69]. Various models have been proposed to incorporate the time-dependent diffusion coefficient for concretes [70–73]. It is important to account for variations in the diffusion coefficient due to concrete cracking and changes in the water-to-cement ratio. Detailed discussions on models are provided in [74].

## 4. Discussion

The history of engineering in the construction of permanent structures goes back to ancient civilizations, where marvels such as the pyramids in Egypt, the Great Wall of China, Roman bridges and the intricate urban planning of Macedonian and Aztec cities demonstrated early engineering prowess. From grand temples to revered churches and mosques, these structures stand as tangible testaments to the enduring ambition of engineers throughout history. The initial impetus for the development of concrete stemmed from the desire to emulate the longevity associated with natural stone while simultaneously achieving cost-effectiveness and ease of use. However, this ambitious vision has encountered challenges in its realization.

Since its inception, concrete has presented engineers with certain limitations. In response, the field has witnessed a continuous quest for innovation, leading to transformative technologies such as reinforced concrete, pre-stressed concrete, high-strength concrete, self-compacting concrete and various additive-enhanced concretes. While these advancements may not always provide cost-efficient or simplified solutions, they undeniably represent a significant advance in the field of civil engineering and push the boundaries of what is feasible. Today's engineering is grappling with a variety of complex challenges, from the construction of towering skyscrapers and expansive bridges to the engineering of tunnels beneath the sea. Moreover, the prospect of constructing futuristic projects in space and on other planets looms on the horizon. In this landscape, understanding material behaviour, particularly under extreme loading conditions, is no longer a luxury but an essential requirement for engineers. Aspects of concrete behaviour that were once overlooked in common engineering practice, such as temperature variations, creep, shrinkage, ageing, corrosion and distinct performance phases, have now become key considerations in the planning and execution of construction projects.

## 5. Conclusions

Concrete, which started as a simple mix of cement, water and aggregates, has transformed into a versatile, high-tech material with the addition of fibres and other substances. This evolution demonstrates its ability to tackle various challenges. Understanding how these new materials behave is now crucial for researchers, emphasizing the importance of grasping how materials react in today's complex construction environments.

In the modern lexicon, an "Engineer" is defined as a "skilful contriver or originator of something". In today's era, engineers are tasked with embodying this definition, serving as adept contrivers who can navigate and address the intricate demands posed by contemporary construction challenges. The evolution of concrete and the corresponding innovations in engineering practices reflect the dynamic nature of the field, where continual adaptation and ingenuity are indispensable to meet the evolving requirements of construction in the modern world.

**Funding:** This research is partially supported through project KK.01.1.1.02.0027, a project co-financed by the Croatian Government and the European Union through the European Regional Development Fund—the Competitiveness and Cohesion Operational Programme.

**Data Availability Statement:** Not applicable.

**Conflicts of Interest:** Author Neda Bebekwas employed by the company HERING d.d. for Design and Construction. The remaining authors declare that the re-search was conducted in the absence of any commercial or financial relationships that could be construed as a potential conflict of interest.

## References

1. Naaman, A.E. *Prestressed Concrete Analysis and Design: Fundamentals*, 2nd ed.; Techno Press 3000: Ann Arbor, MI, USA, 2004.
2. ACI Committee 209. *Guide for Modeling and Calculating Shrinkage and Creep of Concrete (ACI 209.2R-08)*; American Concrete Institute: Farmington Hills, MI, USA, 2008.
3. Mante, D.M. Improving Camber Predictions for Precast, Prestressed Concrete Bridge Girders. Ph.D. Thesis, Auburn University, Auburn, AL, USA, 2016.
4. Chow, C.O.; Hinton, E.; Abdel Rahman, H.H. Analysis of Creep and Shrinkage Effect in Reinforced Concrete Beams. In Proceedings of the International Conference on Computer-Aided Analysis and Design of Concrete Structures, Split, Yugoslavia, 17–21 September 1984.
5. Ghali, A.; Favre, R.; Elbadry, M. *Concrete Structures: Stresses and Deformations*, 3rd ed.; Spon Press: London, UK, 2002.
6. Available online: https://en.wikipedia.org/wiki/Civic_Tower_(Pavia) (accessed on 31 January 2024).
7. Binda, L.; Anzani, A.; Saisi, A. Failures due to long-term behaviour of heavy structures: The Pavia Civic Tower and the Noto Cathedral. *Trans. Built Environ.* **2003**, *66*, 99–108.
8. Binda, L.; Saisi, A.; Tiraboschi, C. Investigation procedures for the diagnosis of historic masonries. *Constr. Build. Mater.* **2000**, *14*, 199–233. [CrossRef]
9. Binda, L. *Learning from Failure Long-Term Behaviour of Heavy Masonry Structures*; WIT Press: Southampton, UK; Boston, MA, USA, 2008; ISBN 9781845640576.
10. Koror–Babeldaob Bridge—Wikipedia. Available online: https://en.wikipedia.org/wiki/Koror%E2%80%93Babeldaob_Bridge (accessed on 31 January 2024).
11. Koror-Babeldaob Bridge | Koror, Palau | WJE. Available online: https://www.wje.com/projects/detail/koror-babeldaob-bridge (accessed on 31 January 2024).
12. Bažant, Z.P.; Yu, Q.; Li, G.H. Excessive long-time deflection of prestressed boxgirder. I: Record-span bridge in Palau and other paradigms. *J. Struct. Eng. ASCE* **2012**, *138*, 676–686. [CrossRef]
13. Abrams, D.A. *Design of Concrete Mixtures, Structural Materials Research Laboratory*; Lewis Institute: Chicago, IL, USA, 1918.
14. Dolen, T.P. *Materials Properties Model of Aging Concrete*; Report DSO-05-05; U.S. Department of the Interior Bureau of Reclamation, Technical Service Center: Denver, CO, USA, 2005.
15. Dolen, T.P.; Scott, G.; von Fay, K.; Hamilton, R. *The Effects of Concrete Deterioration on Safety of Dams*; Dam Safety Research Report No. DSO-03-05; Dam Safety Office (DSO), US Department of Interior: Washington, DC, USA, 2003.
16. Available online: http://www.history.com/topics/hoover-dam (accessed on 31 January 2024).
17. Available online: http://www.usbr.gov/projects/Facility.jsp?fac_Name=Arrowrock+Dam (accessed on 31 January 2024).
18. Available online: https://en.wikipedia.org/wiki/Lahontan_Dam (accessed on 31 January 2024).
19. Available online: http://elephantbuttelake.net/photos.php (accessed on 31 January 2024).
20. Gribniak, V.; Kaklauskas, G.; Kliukas, R.; Jakubovskis, R. Shrinkage effect on short-term deformation behavior of reinforced concrete—When it should not be neglected. *Mater. Des.* **2013**, *51*, 1060–1070. [CrossRef]
21. Gribniak, V.; Kaklauskas, G.; Bacinskas, D. Shrinkage in Reinforced Concrete Structures: A Computational Aspect. *J. Civ. Eng. Manag.* **2008**, *14*, 49–60. [CrossRef]
22. Bažant, Z.P.; Kim, S.S. Nonlinear creep of concrete—Adaptation and flow. *J. Eng. Mech. Div.* **1979**, *105*, 429–445. [CrossRef]
23. Bažant, Z.P.; Prasannan, S. Solidification theory for concrete creep. Part II: Verification and Application. *J. Eng. Mech.* **1989**, *115*, 1704–1725. [CrossRef]
24. Bažant, Z.P.; Asghari, A.A. Constitutive law for nonlinear creep of concrete. *J. Eng. Mech. Div.* **1977**, *103*, 113–124. [CrossRef]
25. Bažant, Z.P.; Panula, L. Creep and shrinkage characterization for analyzing prestressed concrete structures. *PCI J.* **1980**, *25*, 86–122.
26. Bažant, Z.P.; Chern, J.C. Log-double-power law for concrete creep. *ACI J.* **1985**, *82*, 665–675.
27. Bažant, Z.P.; Kim, J.K. Improved prediction model for time—Dependent deformations of concrete: Part 2—Basic creep. *Mater. Struct.* **1991**, *24*, 409–421. [CrossRef]
28. Bažant, Z.P. Theory of creep and shrinkage in concrete structures: A precise of recent developments. In *Mechanics Today*; Nemat-Nasser, S., Ed.; Pergamon Press: New York, NY, USA, 1975; Volume 2.
29. Bažant, Z.P. Mathematical models for creep and shrinkage of concrete. In *Creep and Shrinkage in Concrete Structures*; Bazant, Z.P., Wittmann, F.H., Eds.; John Wiley and Sons: New York, NY, USA, 1982.
30. Wyffels, T.A.; Frenc, C.E.; Shield, C.K. *Effects of Pre-Release Cracks in High-Strength Prestressed Concrete*; Final Project Report; Minnesota Department of Transportation Office of Research Administration, University of Minnesota: St. Paul, MN, USA, 2000.

31. Kovler, K.; Zhutovsky, S. Overview and future trends of shrinkage research. *Mater. Struct.* **2006**, *39*, 827–847. [CrossRef]
32. Aslani, F. Experimental and Numerical Study of Time Dependet Behaviour of Reinforced Self-Compacting Concrete Slabs. Ph.D. Thesis, School of Civil and Environmental Engineering, University of Technology Sydney, Sydney, Australia, 2014.
33. Gilbert, R.I.; Ranzi, G. *Time-Dependent Behaviour of Concrete Structures*; Spon Press: London, UK; New York, NY, USA, 2011.
34. Sakata, K.; Shimomura, T. Recent progress in research on and evaluation of concrete creep and shrinkage in Japan. *J. Adv. Concr. Technol.* **2004**, *2*, 133–140. [CrossRef]
35. Gilbert, G.I. Shrinkage and early-age temperature induced cracking and crack control in concrete structures. In Proceedings of the Second International Conference on Performance-Based and Life-Cycle Structural Engineering (PLSE 2015), Brisbane, Australia, 9–11 December 2015; Fernando, D., Teng, J.-G., Torero, J.L., Eds.; pp. 591–599.
36. Klemczak, B.; Knoppik-Wrobel, A. Early age thermal and shrinkage cracks in concrete structures—Description of the problem. *Archit. Civ. Eng. Environ.* **2011**, *4*, 35–48.
37. Klemczak, B.; Knoppik-Wrobel, A. Early age thermal and shrinkage cracks in concrete structures—Influence of geometry and dimension of a structure. *Archit. Civ. Eng. Environ.* **2011**, *4*, 55–70.
38. Safiuddin, M.; Amrul Kaish, A.B.M.; Woon, C.N.; Raman, S.N. Early—Age cracking in concrete: Causes, consequence, remedial measures, and recommendations. *Appl. Sci.* **2018**, *8*, 1730. [CrossRef]
39. Biolzi, L.; Cattaneo, S.; Crespi, P.; Giordano, N. Damage in glass-concrete composite panels. *Constr. Build. Mater.* **2016**, *116*, 235–244. [CrossRef]
40. Sarkar, S.; Halder, A.; Bishnoi, S. Shrinkage in concretes containing fly ash. In *Proceeding of the UKIERI Concrete Congress*; Jalandhar: Bella Vista, Australia, 2013; pp. 1–11.
41. Kate, G.K.; Murnal, P.B. Effect of addition of fly ash on shrinkage characteristics in high strength concrete. *Int. J. Adv. Technol. Civ. Eng.* **2013**, *2*, 11–16. [CrossRef]
42. Xia, D.; He, M.; Tang, Y.J.; Shi, L.W. Experimental study on concrete's dry-shrinkage stress in construction stage. In Proceedings of the International Conference on Applied Materials and Electronics Engineering (AMEE), Hong Kong, China, 18–19 January 2012; pp. 200–203.
43. Li, Y.H.; Bai, J.B.; Liu, L.M.; Wang, X.Y.; Yu, Y.; Li, T. Micro and macro experimental study of using the new cement-based self-stress grouting material to solve shrinkage problem. *J. Mater. Res. Technol.* **2022**, *17*, 3118–3137. [CrossRef]
44. Frayyeh Qais, J.; Kamil Mushtaq, H. The Effect of Adding Fibers on Dry Shrinkage of Geopolymer Concrete. *Civ. Eng. J. Tehran* **2021**, *12*, 2099–2108. [CrossRef]
45. Havlasek, P.; Jirasek, M. Multiscale modeling of drying shrinkage and creep of concrete. *Cem. Concr. Res.* **2016**, *85*, 55–74. [CrossRef]
46. Geng, Y.; Wang, Y.; Chen, J. Creep behaviour of concrete using recycled coarse aggregates obtained from source concrete with different strengths. *Constr. Build. Mater.* **2016**, *128*, 199–213. [CrossRef]
47. Seara-Paz, S.; Gonzales-Fonteboa, B.; Martinez-Abella, F.; Gonzales-Taboada, I. Time-dependent behaviour of structural concrete made with recycled coarse aggregates. Creep and shrinkage. *Constr. Build. Mater.* **2016**, *122*, 95–109. [CrossRef]
48. Neville, A.M.; Brooks, J.J. Time-Dependent behaviour of concrete containing a plasticiser. *Concrete* **1975**, *9*, 33–35.
49. Li, Z.; Cao, G.; Tan, Y. Prediction of time-dependent flow behaviors of fresh concrete. *Constr. Build. Mater.* **2016**, *125*, 510–519. [CrossRef]
50. Polivka, M.P. Studies of creep in mass concrete, Paper 12. In *Symposium on Mass Concrete*; ACI Special Publication: Baltimore, MD, USA, 1964; Volume 6.
51. Jeong, Y.; Lee, J.; Kim, W.S. Modeling and Measurement of Sustained Loading and Temperature-Dependent Deformation of Carbon Fiber-Reinforced Polymer Bonded to Concrete. *Materials* **2015**, *8*, 435–450. [CrossRef] [PubMed]
52. Lou, T.; Lopes, S.M.R.; Lopes, A.V. Time-dependent behavior of concrete beams prestressed with bonded AFRP tendons. *Compos. Part B Eng.* **2016**, *97*, 1–8. [CrossRef]
53. Zawam, M.; Soudki, K.; West, J.S. Effect of Prestressing Level on the Time-Dependent Behavior of GFRP Prestressed Concrete Beams. *J. Compos. Constr.* **2017**, *21*, 04017001. [CrossRef]
54. *SABS 0100 2000*; The Structural Use of Concrete Part 1: Design. South African Bureau of Standards: Pretoria, South Africa, 2000.
55. Usibe, B.E.; Iniobong, I.E.; Ushie, E.O.J. Prediction of Creep Deformation in Concrete Using Some Design Code Models. *Lat. Am. J. Phys. Educ.* **2012**, *6*, 375. [CrossRef]
56. CEB-FIP. *Design Manual Application of the CEB-FIP Model Code 1978 for Concrete Structures*; CEB-FIP: Lausanne, Switzerland, 1984.
57. CEB-FIP. *Model Code 1990 Design Code, Thomas Telford*; CEB-FIP: Lausanne, Switzerland, 1999.
58. Bažant, Z.P.; Baweja, S. Creep and shrinkage prediction model for analysis and design of concrete structures—Model B3. *Mater. and Struct.* **1995**, *28*, 357–365, 415–430, 488–495.
59. Pijaudier-Cabot, G.; Haidar, K.; Loukili, A.; Omar, M. Ageing and durability of concrete structures, International Centre for Mechanical Sciences. *CISM* **2017**, *461*, 255–286.
60. Soutsos, M.N. *Concrete Durability: A Practical Guide to the Design of Durable Concrete Structures*; Thomas Telford Ltd.: London, UK, 2009.
61. Wan-Wendner, R. Aging concrete structures: A review of mechanics and concept. *Die Bodenkult. J. Land Manag. Food Environ.* **2018**, *69*, 175–199. [CrossRef]

62. Kim, J.-K.; Han, S.H.; Park, S.K. Effect of temperature and aging on the mechanical properties of concrete: Part II. Prediction model. *Cem. Concr. Res.* **2002**, *32*, 1095–1100. [CrossRef]
63. Yang, Q.; Wang, X.; Peng, X.; Qin, F. General Curve Model for Evaluating Mechanical Properties of Concrete at Different Ages. *Coatings* **2023**, *13*, 2002. [CrossRef]
64. Bamforth, P. Enhancing reinforced concrete durability: Guidance on selecting measures for minimising the risk of corrosion of reinforcement in concrete. In *Concrete Society Technical Report*; Concrete Society: Camberley, UK, 2004; Volume 61.
65. Bertolini, L.; Elsener, B.; Pedeferri, P.; Redaelli, E.; Polder, R. *Corrosion of Steel in Concrete: Prevention, Diagnosis, Repair*, 2nd ed.; Wiley-VCH: Weinheim, Germany, 2013.
66. Wu, J.; He, Y.; Xu, C.; Jia, X.; Huang, Y.; Chen, Q.; Huang, C.; Dadras Eslamlou, A.; Huang, S. Interpretability Analysis of Convolutional Neural Networks for Crack Detection. *Buildings* **2023**, *13*, 3095. [CrossRef]
67. Revert, A.B.; De Weerdt, K.; Hornbostel, K.; Geiker, M.R. *State-of-the-Art Report: Service Life Modelling, Carbonation of Concrete and Corrosion in Carbonated Concrete*; Report No. R-1-2017; Norwegian University of Science and Technology: Trondheim, Norway, 2017.
68. Comité Euro-International du Béton (CEB). *New Approach to Durability Design—An Example for Carbonation Induced Corrosion*; Bulletin No. 238; Comité Euro-International du Béton (CEB): Lausanne, Switzerland, 1997.
69. Yoon, I.-S.; Copuroglu, O.; Park, K.-B. Effect of global climatic change on carbonation progress of concrete. *Atmos. Environ.* **2007**, *41*, 7274–7285. [CrossRef]
70. Roa-Rodriguez, G.; Aperador, W.; Delgado, A. Calculation of chloride penetration profile in concrete structures. *Int. J. Electrochem. Sci.* **2013**, *8*, 5022–5035. [CrossRef]
71. Leber, I.; Blakey, F.A. Some effects of carbon dioxide on mortars and concrete. *ACI Mater. J.* **1956**, *28*, 295–308. [CrossRef]
72. Bentz, E.C.; Thomas, M.D.A. *Life-365 Service Life Prediction Model, Life-365 Consortium III*; The Silica Fume Association: Lovettsville, VA, USA, 2013.
73. Kwon, S.J.; Na, U.J.; Park, S.S.; Jung, S.H. Service life prediction of concrete wharves with early-aged crack: Probabilistic approach for chloride diffusion. *Struct. Saf.* **2009**, *31*, 75–83. [CrossRef]
74. Zhou, Y.; Gencturk, B.; Willam, K.; Attar, A. Carbonation-Induced and Chloride-Induced Corrosion in Reinforced Concrete Structures. *J. Mater. Civ. Eng.* **2014**, *27*, 04014245. [CrossRef]

# PAPER III

*SUBMITTED AND UNDER SECOND ROUND REVIEW IN STRUCTURAL ENGINEERING INTERNATIONAL*

# Balanced cantilever construction method in post-tensioned concrete bridges

**Marino Jurišić [1], Neda Bebek [2], Dragan Ćubela [3] and Alen Harapin [4]**

[1] Faculty of Civil Engineering, Architecture and Geodesy, University of Mostar, Matice hrvatske bb, 88000 Mostar, Bosnia and Herzegovina; marino.jurisic@fgag.sum.ba - corresponding author
[2] HERING d.d. for design and construction, Provo bb, 88220 Široki Brijeg, Bosnia and Herzegovina; nbebek@hering.ba
[3] Faculty of Civil Engineering, Architecture and Geodesy, University of Mostar, Matice hrvatske bb, 88000 Mostar, Bosnia and Herzegovina; dragan.cubela@fgag.sum.ba
[4] Faculty of Civil Engineering, Architecture and Geodesy, University of Split, Matice hrvatske 15, 21000 Split, Croatia; alen.harapin@gradst.hr

**Featured Application: The paper presents an overview of balanced cantilever method used in bridge construction with a focus on post-tensioned concrete bridges, including the historical development and research focusing on post-tensioned concrete bridges, and can be used as a starting point for future research.**

**Abstract:** This paper gives an overview on balanced cantilever construction method history and research, with a focus on post-tensioned concrete bridges. In the introduction the method and the history of cantilever construction in steel, concrete and post-tensioned concrete bridges is presented. Structural failure of two different bridges is shown as a motivation for a more detailed understanding of the performance and force transmission of these bridges. Recent experimental and numerical research on post-tensioned concrete balanced cantilever bridges is introduced. In conclusion, most of the research is done on already completed structures. For a better overview, the need to conduct numerical and experimental research on balanced cantilever bridges during construction is highlighted.

**Keywords:** experimental research; numerical research; balanced cantilever method; prestressed concrete; concrete bridges

## 1. Introduction

Balanced cantilever construction method implies segmentally built superstructures starting from the supports, relying on previously built segments to carry the weight of the following structure segment and all other loads related to the works (scaffolding and construction stage loads). In the inception the method was mostly used to build steel bridges, while today it is often used to build post-tensioned concrete bridges with a variable superstructure height, where every new segment that is integrated in the structure after hardening becomes a starting point for further construction. Prestressing steel cables are installed in the upper slab of the superstructure cross section to increase the load bearing capacity during construction phase and subsequently achieve greater spans. The segments of the superstructure can be built by concreting on the spot, or by installing and integrating already prefabricated segments [1].

### 1.1. History of cantilever construction

Cantilever construction method has been used in ancient times to build bridges worldwide. The first bridges to be constructed with this method were made with wood and some structures can still be found in Tibet, China and India. American engineer Thomas Pope designed a 550 m span wooden bridge with a shallow arch resting on two masonry abutments from where it was supposed to be built by the cantilever method with prefabricated segments [2]. Engineers from 19th century understood that continuous beams have a better moment distribution due to the negative support moment compared to simple beams, and can be used to achieve greater spans [3]. Heinrich Gerber was one of those who patented a hinge in a span of a continuous girder, and is considered to be the first to build such a structure [4]. The hinge creates a statically determinate system which is not subjected to parasitic effects due to loads like temperature, differential settling and creep and shrinkage. Besides that, the calculation of stresses and forces in the structure is simpler [3]. Throughout 19th and 20th century the cantilever construction method is mainly used for building arch and truss metal bridges with suspended central span. The Hassfurt Bridge, which was completed in 1867, is considered the first modern cantilever bridge with a main span of 38 m. Other important bridges are: The High Bridge in Kentucky completed in 1877, the Niagara Railroad Bridge completed in 1883, the Poughkeepsie Bridge completed in 1889, and the most famous cantilever bridge in Scotland, Forth Bridge, that was completed in 1890 and held the record for the longest span in the world (518.16 m) for 29 years (Figure 1) [5].

After the development of reinforced concrete, the cantilever method is used for concrete bridges. In 1928, Freyssinet was already working on the construction of the segments of the arches of the Plougastel bridge with a span of 185 m. In the form in which it exists today, this method was first applied in 1930 on the Herval Bridge over the Rio Peixe River in Brazil, where reinforcing bars were continued with serrated elements. Caquot designed the 100 m span Donzere Bridge in France, but this technique has not been widely adopted on reinforced concrete bridges due to the large amount of reinforcement required to secure the cantilevers and the crack widths in the upper zone of the span structure. After the development of prestressing, which is suitable for cantilever construction, the method receives wide application. Freyssinet used it in 1945-1950. for the construction of the Luzancy Bridge, five bridges over the Marne River and the Caracas Viaduct. In Germany Finsterwalder introduces cantilever construction in 1950 on the Balduinstein and Neckarrens bridges. The contractor company Boussiron used the method for the construction of the la Voulte railway bridge over the Rhône in 1952. From this moment on, the development of cantilever construction accelerated. In the period from 1952-1953. in Germany, the company Dyckerhoff and Widman works on structures with prestressed bars. The first bridge in France where the segments are concreted on site is Chazey. It was made in 1955 using prestressing cables. At the same time cable prestressing starts in Germany, Austria and several other countries. Except for arches and span structures with inclined columns, all structures had a joint in the middle of the span. A new step was taken in 1962 when the joint was removed and the continuity of the span construction was introduced on the Lacroix-Falgarde and Vallon du Moulin a Poudre bridges. Another step forward was made with the introduction of prefabricated elements.

One of the first bridges with prefabricated elements was Choisy-le-Roi built in 1962 in France where the joints were glued and the segments integrated by prestressing. Similar techniques are soon used all over the world and imposing structures such as the Chillon Viaduct and the Rio Niteroi Bridge in Brazil (total length of 8 km) were built. The cantilever construction method was also developed for cable-stayed bridges, for example the Brotonne bridge with a main span of 320 m, which at one time held the record for the longest span made of prestressed concrete [1]. The longest free-cantilever cast-in-place span is currently the Shibanpo Bridge (2006) over the Yangtze River in China with a span of 330 m. It is followed by the Stolma Bridge (1998) in Norway with a span of 301 m.

### *1.2. Post-tensioned concrete balanced cantilever bridges*

The most usual method of balanced cantilever bridge construction is to build a pier on top of which the initial part of the span construction is built (base segment). Then, mobile scaffolding (cantilever form travellers), which will support the formwork of individual bridge segments, are installed. The main load-bearing part of the moving traveller is a rhombus, which is attached to the upper edge of the span structure with anchors through a steel rail. After the formwork is placed, the segment is reinforced and concreted. As soon as the concrete reaches sufficient strength, the cables of the cantilever construction in the upper part of the segment are prestressed. Then the formwork is released and the traveller is pushed forward to get into the position for the next segment. This process is repeated until the bridge cantilever is completed. This process is simultaneous on both sides to keep the cantilever balanced (Figure 2).

The advantages of this type of construction are numerous. First, span structures are made without any contact with the ground, which allows construction over flooded rivers or very deep and steep ravines. This method can also be used to build different geometries. Span structure can be of constant or variable height (linear, parabolic, cubic). The method is flexible with regard to the geometry of the road on the bridge because, unlike the incremental launching method, any horizontal and vertical geometry can be made without major difficulties. Furthermore, construction in segments of 3-5 m is very feasible in terms of the required amount of formwork for span construction, even if the spans are small and of different lengths (Figure 3).

Cantilever post-tensioned concrete bridges with a box cross section superstructure can be built in spans of 60-300 m. However, there are other cost-effective construction methods in this range. Cantilever post-tensioned concrete bridges with spans under 80 m compete with concrete-steel composite bridges. If the geometry of the road is favourable, then they are competing with prestressed incrementally launched bridges in spans of 35-70 m. For spans between 70-120 m, cantilever bridges can have a constant or variable span structure height. Here, they are competing with concrete-steel girder bridges. For aesthetic reasons, cable stayed bridges are also used in these spans. For 100-200 m spans, cantilever bridges usually have a variable height of the span structure and compete with box section composite bridges and cable-stayed bridges. The design with light steel webs can also prove to be economical [1].

The disadvantage of this method is that for equal spans these bridges are much heavier than composite bridges. In the case of prefabricated elements, the shorter length of the segments reduces the total weight of the segment and thus reduces the cost of installation. However, the bigger weight request larger foundations and supports. Another major drawback is the large number of tasks that must be completed in the field for the construction of the span structure and access roads. Although the number of these tasks is reduced if the segments are prefabricated, it is still higher than the incremental launching process.

When the structure crosses the road, safety can be jeopardized which can lead to road closures. From an aesthetic point of view, bridges made with the cantilever construction method often have a high cross section. As a result of segmental construction and segmental concreting, there may be a difference in the colour of the structure in adjacent segments.

## 2. Motivation

The strongest motivation for carrying out research on the behaviour of structures built using balanced cantilever method is to prevent possible disasters due to insufficient knowledge of force transfer and load-bearing capacity. Only two examples will be cited that left a deep mark on the bridge-building community.

One of the earlier notable examples of collapse was a steel bridge in Quebec that collapsed twice during construction. The first collapse took place in 1907 with 75 victims. The collapse occurred due to a wrong calculation of the dead weight of the bridge, which was greater than the bridge under construction could handle [6]. Construction continued in 1916, but during the raising of the central part, there was a problem with the cranes which caused the central part to fall and claimed the lives of 13 workers (Figure 4) [7]. The bridge was finally completed in 1919 and still holds the record for the longest span of a cantilever bridge, at 549 m.

Another example is the Koror-Babeldaob balanced cantilever post-tensioned concrete bridge in Palau built in 1977 (Figure 5). It had a main span of 240.8 m and at the time held the record for the longest span of its type. The bridge had a joint in the middle of the span [8]. Shortly after construction, the bridge developed large vertical deflections. By 1996, the middle of the span had dropped by 1.2 m, which upset the local population who asked the authorities to intervene. Two studies were made (Louis Berger International and Japan International Co-operation Agency) and both concluded that the bridge is safe and that the large displacements are the result of concrete creep and a lower elasticity modulus. A third study was made in 1993 by ABAM, Seattle, which concluded that the bridge would drop an additional 0.84 m in the next 85 years and a rehabilitation with 40 external post-tensioned cables was proposed. Renovation was done between 1995 and 1996, during which the joint in the middle of the bridge was removed and external post-tensioned cables with deviators were installed.

Three months after reconstruction on September 26, 1996. the bridge collapsed suddenly and catastrophically. A subsequent study determined that the cause of the collapse was a change in the bridge's static system and a crack in the top slab, where tensile stress occurred. The calculation of the bridge was made using a linear model, not taking into account the redistribution of forces due to the effects of creep and shrinkage (Figure 6) [9-10].

## 3. Previous research on post-tensioned concrete balanced cantilever bridges

Due to the sudden increase in the application of cantilever construction, from the 1970s onwards, there is an increased need for research into force distribution during construction and exploitation of post-tensioned concrete bridges built with this method. Research intensified especially in the 1990s with the development of experimental testing techniques and computer nonlinear numerical methods.

One topic of research was the dynamic characteristics and response of structures, covering natural oscillation frequencies, response to wind loads, seismic response, ambient vibration and forced vibration tests, all using numerical and/or experimental methods.

Skrinar and Strukelj (1996) carried out measurements to determine the natural oscillation frequencies of a balanced cantilever bridge of variable superstructure height during construction in Slovenia, and the frequencies were measured for each segment [11].

Strommen et al. (2001) investigate the influence of dynamic crosswind loading on vertical oscillations during the construction phase of balanced cantilevered bridges. Research is conducted in a wind tunnel, and based on these experiments, a procedure for predicting the dynamic response of the structure was created [12]. Schmidt and Solari (2003) also investigate the influence of wind on balanced cantilever bridges and provide a procedure for determining the influence of wind on the superstructure and piers. The conclusion is that some wind effects in different bridge configurations should not be ignored in order to obtain realistic impact on the structure [13].

Morassi and Tonon (2008) perform a series of forced vibration tests to determine the dynamic characteristics of the three-span Palu post-tensioned bridge in north-eastern Italy in a seismically active area [14]. Gentile and Bernardini conduct ambient vibration experiments on the Capriate cantilever bridge using radar measurement. The values of natural frequencies and modal shapes that were obtained through accelerometers with a radar sensor matched with the values obtained by conventional accelerometers [15].

Bayraktar et al. (2009) conducted research on the vibration characteristics of the Komurhan bridge [16]. Liu et al. determined the dynamic response of a 235 m long three span bridge through a series of ambient vibration tests that were conducted over 12 months [17]. Stathopoulos investigates the dynamic behaviour of the balanced cantilever Metsovo bridge in Greece [18]. Altunisik et al. (2011) measure the dynamic response of the balance cantilever Gulburn viaduct using ambient vibration tests [19].

In his work, Turan (2012) investigates the dynamic characteristics of balanced cantilever bridges using numerical and experimental methods [20]. Kudu et al. (2014) determine the dynamic characteristics of the Berta balanced cantilever post-tensioned bridge using the finite element method and modal analysis [21].

Sumerkan (2019) gives a simplified expression for frequencies in post-tensioned balanced cantilever bridges [22]. Bayraktar et al. (2020) investigate the influence of vertical displacements in the ground near faults on the seismic behaviour of balanced cantilever bridges. The numerical analysis showed that the vertical movements of the ground significantly affect the seismic behaviour of the bridge [23].

Another topic of research was reliability, behaviour and rehabilitation of structures, mostly determined by experimental tests and onsite analyses. In some cases, long term structural monitoring and numerical analysis were used.

Casas (1997) conducted research to determine the reliability partial safety factor on balanced cantilever concrete bridges. The research is conducted on bridges with a span of 80 to 140 m, and an example was made on a bridge with a span of 120 m [24]. Manjure (2001) works on the rehabilitation of balanced cantilever bridges with suspended central part of the span in India, where problems occur during the exploitation phase due to poor concreting and reinforcement detailing [25].

Vonganan conducts structure behaviour research on the Mekong Bridge in Thailand [26]. Pinmanas et al conduct a study on the Phra-Nangklao post-tensioned balanced cantilever bridge in Thailand [27]. Ates et al. (2013) investigate the structural behaviour of balanced cantilever bridges taking into account the interaction between the structure and the soil [28]. Chen et al. (2013) conducted dynamic tests and long-term monitoring of the 12-span Newmarket (Auckland, New Zealand) viaduct using wireless sensors shortly after the works were completed [29].

Pimentel and Figueiras (2017) present a new methodology for assessing the condition of post-tensioned balanced cantilever bridges including experimental and numerical investigations [30]. Caner (2021) analyses the reconstruction of the partially collapsed balanced cantilever post-tensioned bridge Begendik [31].

One other interesting topic of research was the design of post-tensioned concrete bridges built using the balanced cantilever construction method, which focused on superstructure optimisations, bending moment variations, simulation models as well as material and geometric nonlinearities.

Kwak and Son (2004) work on determining the span ratios of balance cantilever bridges through time analyses, in which the main guideline is that vertical displacement does not occur at the edge of the cantilever due to the action of weight and post-tensioned cables for cantilever construction [32]. They are also working on determining the variation of the bending moment over time taking into account construction phases and concrete creep. On the basis of these researches, they provide an expression to obtain the bending moment and its variation by elastic analysis without taking into account the construction phases and creep [33]. Hewson (2007) conducts a study on the balanced cantilever method of bridge construction [34].

Marzouk et al. (2008) develop a special simulation model for balanced cantilever bridges built both with prefabricated and onsite concreted segments [35]. Ates (2011) works on the numerical modelling of balanced cantilever bridges taking into account the time-dependent characteristics of the material. Analyses have shown that time-dependent material characteristics and geometric nonlinearity should be taken into account in order to obtain the correct behaviour of concrete bridges [36]. Bravo et al. (2021) conduct research to assess the seismic displacement of balanced cantilever bridges in the construction phase and in the exploitation phase [37].

Time-dependant effects such as creep and shrinkage during and after construction is another important topic of research focusing on the influence on force and stress distribution, as well as additional deformations.

Pimanmas (2007) investigates the influence of long-term creep and prestressing on the redistribution of bending moments in balanced cantilever bridges. The analysis shows that creep in these cases can increase the value of the negative moment and that rough estimates of creep can lead to wrong results. The exact phases of construction should be taken into account [38]. In the same year, Hedjazi and colleagues investigated the influence of concrete creep on deflections and stresses in post-tensioned balance cantilever bridges. Three-dimensional models are made out of areas with included material nonlinearity and concrete creep [39].

Altunisik et al. (2010) conduct an analysis of the construction phases of the Komurhan bridge taking into account the time-dependent material characteristics [40]. Malm and Sunquist perform a time-sensitive analysis of segmental balanced cantilever bridges. They concluded that larger than expected deflections and higher stresses in the ribs were obtained due to the prestressing of the bottom slab cables. In addition, they show a significant influence of creep in cantilever construction as well as non-uniform drying shrinkage on the completed bridge [41]. Akbar and Carlie (2021) investigate the effects of creep and shrinkage on the long-term deformations of balanced cantilever bridges [42].

Construction aspects of real bridges are a major research focus, using mostly experimental onsite tests and analyses to cover critical errors, precamber and deflection issues before and after stitch segments, concrete installation and various construction processes.

McDonald et al. (2003) investigate the collapse of the Koror-Babeldaob Bridge in Palau. An analysis of the field inspection was performed and calculations of the bridge before and after reconstruction were made. The result of the analysis shows that the most likely cause of the collapse is damage during the removal of the original concrete road surface [43]. Radić et al. deal with precamber and deflections of balanced cantilever bridges, and provide an expression for the approximate calculation of the required precamber [44].

Jung et al. (2007) work on a simulation that uses field measurements to calibrate the numerical deflection results of balanced cantilevered bridges. The quality of the calibration depends on the experience of the engineer on site, and it is important for the correct joining of the bridge [45]. In the same year, Kronenberg studies the continuous installation of concrete in balanced cantilever bridges. As an example, he cites the Hacka bridge in the Czech Republic, which was completed after only two years of construction [46].

Kamaitis investigates the connections between segments in prefabricated balanced cantilever bridges. The research covers 5 major bridges, classification and statistics of joint problems [47]. Starossek (2009) presents the project of phase I construction of the Shin-Chon balanced cantilever post-tensioned bridge in Korea [48]. Furunes (2021) analyses aspects of the construction of the 260m-span Trysfjord Bridge in Norway using the balanced cantilever process and implementing programming into design [49].

## 4. Conclusions related to previous research and literature

With a few exceptions, the majority of previously mentioned articles show research done on completed post-tensioned concrete bridges. The research yields useful insight into post-tensioned balanced cantilever concrete bridges. Wind experiments produced a procedure for dynamic response predictions, and showed that wind loads can prove critical and must not be ignored in some cases. Numerical analysis of vertical displacements in the ground near faults showed that the vertical movements significantly affect the seismic behaviour of the bridge. Research done on reliability, rehabilitation and behaviour identify common problems like poor concreting and reinforcement detailing, as well as providing insight to the real structural capacity of the bridges. On the topic of design, important span ratios and superstructure optimisation is shown, and an expression to obtain bending moment variations by elastic analysis without creep and construction phases is produced. The importance of time-dependant effects of creep and shrinkage during construction phases and exploitation is emphasized. The research shows that time-dependant effects, as well as material and geometric nonlinearities should be taken into account to properly describe the flow of forces and stresses, deflections, as well as general structural behaviour. Importance of precamber of structure and correct calculation in order to properly join the bridge is highlighted, and an expression to calculate the precamber is given. Different bridges were monitored during construction and various problems and solutions are presented.

The balanced cantilever construction process is complex in terms of stress, strain, deformation, geometry (deflection) and safety changes during its construction and use. Each segment of the bridge has differently aged concrete and thus different rheological characteristics: strength, modulus of elasticity, deformations, shrinkage and creep parameters, etc. These characteristics depend on the type of concrete, segment construction duration and the timing of prestressing, formwork release and form traveller position change.

In addition, a number of previously listed studies show that the behaviour of bridges built using the balanced cantilever method is a continuous topic of research by the academic and professional community. The accelerated construction of road and railway bridges, with greater spans and more demanding geometry, places greater demands on engineers, designers and contractors in terms of saving materials, reducing the cost and speed of construction, while maintaining the same level of mechanical resistance, stability and reliability. Knowing the exact flow of forces in them becomes the primary task of the designer.

As can be seen from recent research, predicting the behaviour of post-tensioned concrete bridges to all the loads that act on them, left the domain of the classic engineer and the usual linear models from commercial computer programs for structural calculations long ago.

Research generally moves in two directions. The first direction is the examination of constructed bridges with the aim of determining their behaviour, which is usually carried out in situ, on real objects. Such research, although not rare, is unfortunately usually carried out on already built structures, where the influence of the construction method and the changes in the flow of forces that arise with it can only be concluded from the final state of stress and deformation.

Another direction is the creation of specific numerical models that are calibrated with data measured in situ, thus creating reliable models that can realistically describe the behaviour of the structure.

## 5. Acknowledgments

This research is partially supported through project KK.01.1.1.02.0027 co-financed by the Croatian Government and the European Union through the European Regional Development Fund — the Competitiveness and Cohesion Operational Programme.

## 6. Disclosure statement

The authors report there are no competing interests to declare.

## 7. Data availability statement

All data, models, or code that support the findings of this study are available from the corresponding author upon reasonable request.

## 8. Figures

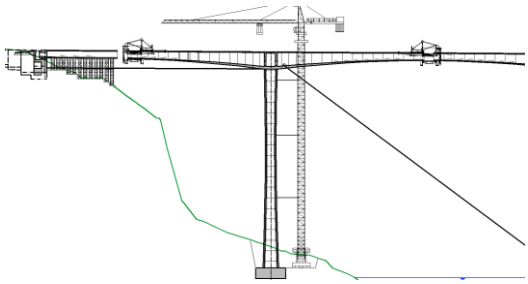

(a)

(b)

| Type | Spans: 35 | 70 | 90 | 120 | 150 | 200 | 300 |
|---|---|---|---|---|---|---|---|
| - Bridges built using the cantilever construction method | | | | | | | |
| - Incrementally launched concrete bridges | | | | | | | |
| - Composite beam bridges | | | | | | | |
| - Composite box girder bridges | | | | | | | |
| - Orthotropic slab box-section bridges | | | | | | | |
| - Cable-stayed bridges | | | | | | | |

(**a**)

(**b**)

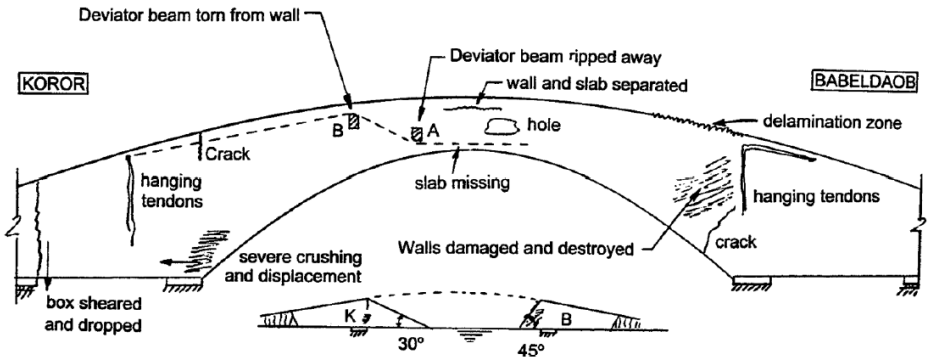


## 9. Figure captions

**Figure 1.** Forth bridge, Scotland (by MrMasterKeyboard - Own work, CC BY-SA 4.0, https://commons.wikimedia.org/w/index.php?curid=121262762)

**Figure 2.** (**a**) Scheme of a balanced cantilever construction process on a post-tensioned concrete bridge (by authors); (**b**) Balanced cantilever construction method on a post-tensioned concrete bridge during construction (by authors)

**Figure 3.** Feasibility of different bridge types by span length (m) – (black – feasible, dark grey – possible and possibly feasible, light grey – possible but not feasible) (by Group of authors Design guide – Prestressed concrete bridges built using the cantilever method; Setra, 2003)

**Figure 4.** Quebec bridge, collapse of the central segment (historical archive, public domain)

**Figure 5.** (**a**) Koror-Babeldaob bridge after construction (public domain); (**b**) Koror-Babeldaob bridge after collapse (by Ed Zeilnhofer, CC BY 3.0, https://commons.wikimedia.org/w/index.php?curid=14637885)

**Figure 6.** Koror-Babeldaob bridge damage overview (by Matthias Pilz, The Koror-Babeldaob Bridge in the Republic of Palau, History and Time Dependent Stress and Deflection Analysis)

## References


1. Mathivat, J. *The cantilever construction of prestressed concrete bridges*; Editions Eyrolles: 61, boulevard Saint-Germain, 75005 Paris, France, 1979
2. Group of authors *Design guide – Prestressed concrete bridges built using the cantilever method*; Setra, 2003
3. DuBois, A. J. *The mechanics of engineering*; John Wiley & Sons, 1902
4. Bender, C. *Discussion on Cantilever Bridges by C.F. Findlay*; Canadian Society of Civil Engineers, 1890
5. DeLony, E. *Context for world heritage bridges*; International Council on Monuments and Sites, 1996
6. Schneider, C. C. *Quebec bridge inquiry report*; S. E. Dawson, 1908
7. Middleton, W. D. *The bridge at Quebec*; Indiana University Press, 2001
8. Pilz, M. *The Collapse of the K-B Bridge in 1996*; London, 1997
9. Pilz, M., L. G. *Continuity in Prestressed Concrete Structures, Time-Dependent Responses*; 22nd Conference on Our World in Concrete & Structures, Singapore, 1997
10. Pilz, M. *The Koror-Babeldaob Bridge in the Republic of Palau, History and Time Dependent Stress and Deflection Analysis*; Dissertation Imperial College London, Department of Civil Engineering, 1997
11. Skrinar, M.; Strukelj, A. Eigen frequency monitoring during bridge erection. *SEI* **1996**, *6(3)*, 191-194.
12. Strommen, E.; Hjort-Hansen, E.; Kaspersen, J. H. Dynamic loading effects of a rectangular box girder bridge. *J. Wind. Eng. Ind. Aerodyn.* **2001**, *89(14–15)*, 1607–1618.
13. Schmidt, S.; Solari, G. 3-D wind-induced effects on bridges during balanced cantilever erection stages. *Wind Struct.* **2003**, *6(1)*, 1–22.
14. Morassi, A.; Tonon S. Dynamic testing for structural identification of a bridge. *J. Bridge Eng.* **2008**, *13*, 573–585.
15. Gentile, C.; Bernardini, G. Output-only modal identification of a reinforced concrete bridge from radar-based measurements. *Nondectruct. Test. Evaluation* **2008**, *41*, 544–553.
16. Bayraktar, A.; Altuşnişık, A. C.; Sevim, B.; Domaniç, A.; Taş, Y. Vibration characteristics of Kömürhan highway bridge constructed with balanced cantilever method. *J. Perform. Constr. Facil.* **2009**, *23(2)*, 90–99.
17. Liu, C.; DeWolf, J. T.; Kim J. Development of a baseline for structural health monitoring for a curved post-tensioned concrete box girder bridge. *Eng. Struct.* **2009**, *31*, 3107–3115.
18. Stathopoulos, S.; Seifried, G.; Kotsanopoulos, P.; Haug, H.; Spyropoulos, I.; Stathopoulos, K. The Metsovo bridge, Greece. *SEI* **2010**, *20(1),* 49–53.
19. Altuşnişık, A. C.; Bayraktar, A.; Sevim, B.; Ates, S. Ambient vibration based seismic evaluation of isolated Gülburnu Highway Bridge. *Soil Dyn. Earthq. Eng.* **2010**, *31(11),* 1496–1510.
20. Turan, F. N. *Determination of dynamic characteristics of balanced cantilever reinforced concrete bridges using ambient vibration data;* MSc Thesis, Karadeniz Technical University, Trabzon, Türkiye (in Turkish), 2012
21. Kudu, F. N.; Bayraktar, A.; Bakir, P. G.; Türker, T.; Altuşnişık, A. C. Ambient vibration testing of Berta Highway Bridge with post-tension tendons. *Steel Compos.* **2014**, *16(1),* 23–46.
22. Sumerkan, S.; Bayraktar, A.; Türker, T.; Akkose, M. A simplified frequency formula for post-tensioned balanced cantilever bridges. *Asian J. Civ. Eng.* **2019**, *20,* 983–997.
23. Bayraktar, A.; Kudu, F. N.; Sumerkan, S.; Demirtas, B., Akkose, M. Near-fault vertical ground motion effects on the response of balanced cantilever bridges. *Proc. Inst. Civ.* **2020**, *173,* 17-33.
24. Casas, J. R. Reliability-based partial safety factors in cantilever construction of concrete bridges. *J. Struct. Eng.* **1997**, *123(3)*, 305-312.
25. Manjure, P. J. Rehabilitation of balanced cantilever bridges. *Indian Concr. J.* **2001**, *75(1)*, 76-82.
26. Vonganan, B. The second Mekong international bridge, Thailand. *SEI* **2009**, *19(1),* 67–68.
27. Pimanmas, A.; Imsombat, S.; Neilsen, K. Hj. New Phra- Nangklao bridge—A balanced cantilever prestressed concrete bridge in Thailand. *SEI* **2009**, *19(1),* 38–40.
28. Ates, S.; Atmaca, B.; Yildirim, E.; Demiroz, N. A. Effects of soil-structure interaction on construction stage analysis of highway bridges. *Comput. Concr.* **2013**, *12(2),* 169–186.
29. Chen, X.; Omenzetter, P.; Beskhyroun, S. Dynamic testing and long term monitoring of a twelve span viaduct. *Key Eng. Mater.* **2013**, *569–570,* 342–349.
30. Pimentel, M.; Figueiras, J. Assessment of an existing fully prestressed box-girder bridge. *Proc. Inst. Civ.* **2017**, *170(1),* 42–53.
31. Caner, A.; Apaydin, N.; Cinar, M.; Peker, E., Kilic, M. Reconstruction of Partially Collapsed Post-tensioned Begendik Bridge During Balanced Cantilever Construction. *Developments in International Bridge Engineering* **2021**, 17-33.
32. Kwak, H. G.; Son, J. K. Span ratios in bridges constructed using a balanced cantilever method. *Constr Build Mater.* **2004**, 18*(10)*, 767–779.
33. Kwak, H. G.; Son, J. K. Design moment variations in bridges constructed using a balanced cantilever method. *Constr Build Mater.* **2004**, 18*(10)*, 753-766.
34. Hewson, N. Balanced cantilever bridges. *Concrete (London)* **2007**, *41(10)*, 59-60.
35. Marzouk, M.; Said, H.; El-Said, M. Special-purpose simulation model for balanced cantilever bridges. *J. Bridge Eng.* **2008**, *13(2)*, 122–131.

36. Ates, S. Numerical modelling of continuous concrete box girder bridges considering construction stages. *Appl. Math. Model.* **2011**, *35(8)*, 3809–3820.
37. Bravo, J.; Benjumea, J.; Consuegra, F. A. *Parametric Study to Estimate Seismic Displacement Demands of Balanced Cantilever Bridges in Service and Construction Conditions;* Conference: fib Symposium 2021 - Concrete Structures: New Trends for Eco-Efficiency and Performance, 2021
38. Pimanmas, A. The effect of long-term creep and prestressing on moment redistribution of balanced cantilever cast-in-place segmental bridge. *SJST* **2007**, *29(1)*, 205–216.
39. Hedjazi, S.; Rahai, A.; Sennah, K. Evaluation of creep effects on the time-dependent deflections and stresses in prestressed concrete bridges. *Bridge Structures* **2007**, *3(2)*, 119-132.
40. Altuşnişık, A. C.; Bayraktar, A.; Sevim, B.; Adanur, S.; Domaniç, A. Construction stage analysis of Kömürhan highway bridge using time dependent material properties. *Struct. Eng. Mech.* **2010**, *36(2)*, 207–223.
41. Malm, R.; Sundquist, H. Time-dependent analyses of segmentally constructed balanced cantilever bridges. *Eng Struct.* **2010**, *32(4)*, 1038–1045.
42. Akbar, S.; Carlie, M. *Long-term deformation of balanced cantilever bridges due to non-uniform creep and shrinkage*; KTH Royal Institute of Technology, School of Architecture and the Built Environment, 2021
43. McDonald, B.; Saraf, V.; Ross, B. A spectacular collapse: Koror-Babeldaob (Palau) balanced cantilever prestressed, posttensioned bridge. *Indian Concr. J.* **2003**, *77(3)*, 955–962.
44. Radić, J.; Gukov, I.; Meštrović, D. A new approach to deflection analysis of cantilever beam bridges. in Proc of the 2nd International Conference IABMAS − Bridge Maintenance, Safety, Management and Cost. Ed. by Watanabe, E.; Frangopol, D. M.; Utsunomiya, T. 18–22 Oct, Kyoto, Japan. Leiden: A. A. Balkema Publishers. 8 p. ISBN 04 1536 336 X, 2004
45. Jung, S.; Ghaboussi, J.; Marulanda, C. Field calibration of time-dependent behavior in segmental bridges using self-learning simulation. *Eng. Struct.* **2007**, *29(10)*, 2692–2700.
46. Kronenberg, J. Continous concrete placing during balanced cantilever construction of a bridge. *Concr. Eng. Int.* **2008**, *12(3)*, 38–39.
47. Kamaitis, Z. Field investigation of joints in precast post-tensioned segmental concrete bridges. *Balt. J. Road Bridge Eng.* **2008**, *3(4)*, 198–205.
48. Starossek, U. Shin Chon Bridge Korea. *SEI* **2009**, *19(1)*, 79-84.
49. Furunes, E. W. *Trysfjord bridge, parametric analysis and modelling for drawingless construction of a concrete balanced cantilever bridge;* IABSE Congress: Structural Engineering for Future Societal Needs, Ghent, Belgium, 1999-2004, 2021

# PAPER IV


Taylor & Francis
Taylor & Francis Group

Structural Engineering International

ISSN: (Print) (Online) Journal homepage: www.tandfonline.com/journals/tsei20

# Strain Analysis on Cast-In-Place Balanced Cantilever Prestressed Concrete Bridges During Construction

**Marino Jurišić (Ph.D Student), Neda Bebek (Ph.D Student), Dragan Ćubela (Assoc. Prof.) & Alen Harapin (Prof.)**

**To cite this article:** Marino Jurišić (Ph.D Student), Neda Bebek (Ph.D Student), Dragan Ćubela (Assoc. Prof.) & Alen Harapin (Prof.) (02 Feb 2024): Strain Analysis on Cast-In-Place Balanced Cantilever Prestressed Concrete Bridges During Construction, Structural Engineering International, DOI: 10.1080/10168664.2023.2296979

**To link to this article:** https://doi.org/10.1080/10168664.2023.2296979

# Strain Analysis on Cast-In-Place Balanced Cantilever Prestressed Concrete Bridges During Construction*

**Marino Jurišić,** Ph.D Student, Faculty of Civil Engineering, Architecture and Geodesy, University of Mostar, Mostar, Bosnia and Herzegovina; **Neda Bebek,** Ph.D Student, HERING Inc. for Design and Construction, Široki Brijeg, Bosnia and Herzegovina; **Dragan Ćubela,** Assoc. Prof., Faculty of Civil Engineering, Architecture and Geodesy, University of Mostar, Mostar, Bosnia and Herzegovina; **Alen Harapin,** Prof., Faculty of Civil Engineering, Architecture and Geodesy, University of Split, Split, Croatia.
Contact marino.jurisic@fgag.sum.ba
DOI: 10.1080/10168664.2023.2296979

## Abstract

This article shows the strain analysis on two cantilever cast-in-place prestressed concrete bridges during construction. Strain gauges, measuring strain based on the change in electrical resistance, were installed on both structures in order to obtain strain results during and after construction. Nonlinear numerical models were made to simulate the realistic behaviour of the structure and show the effect of creep and shrinkage during the construction phases. The numerical model taking into account creep and shrinkage is validated and shows good overlap with the measured results. Relative compressive stresses as well as the necessary precamber are shown. The effects of creep and shrinkage are analysed. Finally, the data can be used to analyse and compare other similar bridges and validate different numerical models. A recommendation for the design of future prestressed concrete balanced cantilever bridges is given.

**Keywords:** experimental research; balanced cantilever; prestressed concrete; concrete bridges; strain analysis; monitoring; numerical modelling

## Introduction

Balanced cantilever construction method wimplies segmentally built superstructures starting from the supports, relying on previously built segments to carry the weight of the following structure segment and all other loads related to the works (scaffolding and construction stage loads). In the nineteenth century, the method was mostly used to build steel bridges, while today it is often used to build prestressed concrete bridges with a variable superstructure height, where every new segment that is integrated into the structure after hardening becomes a starting point for further construction. Prestressing steel cables are installed in the upper slab of the superstructure cross section to increase the load bearing capacity during the construction phase and subsequently achieve greater spans. The segments of the superstructure can be built by concreting on the spot, or by installing and integrating already prefabricated segments.[1]

The most usual method of balanced cantilever bridge construction is first to build a column on top of which the initial part of the span construction is built, often referred to as the base segment or the pier head. Then, mobile scaffolding called the cantilever forming travellers, which will support the formwork of individual bridge segments, are installed. The main load-bearing part of the moving traveller is a rhombus, which is attached to the upper edge of the span structure with anchors through a steel rail. After the formwork is placed, the segment is reinforced and concreted. As soon as the concrete reaches sufficient strength, the cables of the cantilever construction in the upper part of the segment are pre-tensioned in order to activate the segment. Then the formwork is released and the traveller is pushed forward over the rails to get into the position for the next segment. This process is repeated until the bridge cantilever is completed. It is important to emphasize that this process with balanced cantilevered bridges takes place simultaneously on the left and right sides of the cantilever, so that the structure remains stable during construction.

The advantages of this type of construction are numerous. First, span structures are made without any contact with the ground, which allows construction over flooded rivers or very deep and steep ravines. This method can also be used to build different geometries. Span structures can be of constant or variable height (linear, parabolic, cubic). The method is flexible with regard to the geometry of the road on the bridge because, unlike the incremental launching method, any horizontal and vertical geometry can be made without major difficulty. Furthermore, construction in segments of 3–5 m is very feasible in terms of the required amount of formwork for span construction, even if the spans are small and of different lengths.

Owing to the sudden increase in the application of cantilever construction, and in order to prevent unwanted consequences such as excessive deflections and cracking resulting from underestimating creep and shrinkage and local prestressing effects, from the 1970s onwards, there was an increased need for research into force distribution during construction and use of bridges built with this method. Research intensified especially in the 1990s with the development of experimental testing techniques and computer nonlinear numerical methods.

Reference [2] carried out measurements to determine the natural

*__Featured Application.__ This work provides strain measurement results on prestressed concrete bridges built by the balanced cantilever method during construction, as well as a numerical model that is validated by the measurements and shows the impact of creep and shrinkage strain during construction. Relative concrete compressive stresses, as well as numerical precamber are shown and analysed. The research provides valuable insight on the behaviour of prestressed balanced cantilever concrete bridges during construction and can help calibrate and validate different numerical models.

oscillation frequencies of a balanced cantilever bridge of variable superstructure height during construction in Slovenia.[2] Reference [3] conducted research to determine the reliability partial safety factor on balanced cantilever concrete bridges. Reference [4] worked on the rehabilitation of balanced cantilever bridges with suspended central part of the span in India. Reference [5] investigated the collapse of the Koror-Babeldaob Bridge in Palau. Reference [6] worked on determining the span ratios of balance cantilever bridges through time analyses. They are also working on determining the variation of the bending moment over time taking into account construction phases and concrete creep.[7] Reference [8] dealt with the precamber and deflections of balanced cantilever bridges, and provided an expression for the approximate calculation of the required precamber. Reference [9] investigates the influence of long-term creep and prestressing on the redistribution of bending moments in balanced cantilever bridges. Reference [10] worked on a simulation that used field measurements to calibrate the numerical deflection results of balanced cantilevered bridges. Reference [11] conducted a study on the balanced cantilever method of bridge construction. In the same year, Hedjazi and colleagues investigated the influence of concrete creep on deflections and stresses in prestressed balance cantilever bridges [12].

Reference [13] developed a special simulation model for balanced cantilever bridges built both with prefabricated and onsite concreted segments. In the same year, Kronenberg studied the continuous installation of concrete in balanced cantilever bridges.[14] Reference [15] investigated the connections between segments in prefabricated balanced cantilever bridges.

Reference [16] conducted structure behaviour research on the Mekong Bridge in Thailand. Reference [17] conducted a study on the Phra-Nangklao prestressed balanced cantilever bridge in Thailand.

Reference [18] presented the project of phase I construction of the ShinChon balanced cantilever prestressed bridge in Korea. Reference [19] conducted an analysis of the construction phases of the Komurhan bridge taking into account the time-dependent material characteristics. Reference [20] performed a time-sensitive analysis of segmental balanced cantilever bridges. Reference [21] investigated the dynamic behaviour of the balanced cantilever Metsovo bridge in Greece.

Reference [22] worked on the numerical modelling of balanced cantilever bridges taking into account the time-dependent characteristics of the material.

Reference [23] investigated the structural behaviour of balanced cantilever bridges taking into account the interaction between the structure and the soil.

Reference [24] presented a new methodology for assessing the condition of prestressed balanced cantilever bridges including experimental and numerical investigations. Reference [25] gave a simplified expression for frequencies in prestressed balanced cantilever bridges. Reference [26] investigated the influence of vertical displacements in the ground near faults on the seismic behaviour of balanced cantilever bridges.

Reference [27] analysed the reconstruction of the partially collapsed balanced cantilever prestressed bridge at Begendik. Reference [28] conducted research to assess the seismic displacement of balanced cantilever bridges in the construction phase and in the use phase. Reference [29] analysed aspects of the construction of the 260 m-span Trysfjord Bridge in Norway using the balanced cantilever process and implementing programming into design. Reference [30] investigated the effects of creep and shrinkage on the long-term deformations of balanced cantilever bridges.

The majority of the previously mentioned articles show research done on completed bridges, with few exceptions where research is conducted during construction. The balanced cantilever construction process is simple, yet complex in terms of stress, strain, deformation, geometry (deflection) and statical system changes during its construction and use. Furthermore, each segment of the bridge has differently aged concrete at a given point in time and thus different essential rheological characteristics: strength, modulus of elasticity, deformations, shrinkage and creep parameters, etc. These characteristics depend on the type of concrete, segment construction duration and the timing of prestressing, formwork release and form traveller position change.

On the other hand, the mechanical characteristics of the concrete depend on the prestressing force losses during and after the construction of the bridge. In addition, a number of the previously listed studies show that the behaviour of bridges built using the balanced cantilever method is a continuous topic of research by the academic and professional community. The accelerated construction of road and railway bridges, with greater spans and more demanding geometry, places greater demands on engineers, designers and contractors in terms of saving materials and reducing the cost and speed of construction, while maintaining the same level of mechanical resistance, stability and reliability.

Extreme weather conditions, earthquakes, ice, torrents, hurricane winds and the like, which we have been witnessing more and more recently, place greater demands on bridge structures. Knowing the exact flow of forces in them becomes the primary task of the designer.

As can be seen from recent research, predicting the behaviour of such bridges to all the loads that act on them, long ago left the domain of the classical engineer and the usual linear models from commercial computer programs for structural calculations.

Research generally moves in two directions. The first direction is the examination of constructed bridges with the aim of determining their behaviour, which is usually carried out *in situ*, on real objects. Such research, although not rare, is unfortunately usually carried out on already built structures, where the influence of the construction method and the changes in the flow of forces that arise with it can only be concluded from the final state of stress and deformation.

Another direction is the creation of specific numerical models that are calibrated with data measured *in situ*, thus creating reliable models that can realistically describe the behaviour of the structure.

## Overview of the Tested Bridges

The research was conducted on Vranduk 1 and Vranduk 2 Bridges,

which are located in Bosnia and Herzegovina on motorway corridor Vc, section Zenica Municipality Northern Administrative Border (Nemila) to Zenica North (Donja Gračanica), subsection Vranduk–Ponirak. The route of the subsection is bound to the Bosna river valley as much as the technical elements and terrain conditions allow it, since the river valley is almost entirely occupied by the existing Doboj–Zenica road and Vrhpolje/Šamac–Sarajevo railroad with several local roads. The Bosna river makes an S turn in the area and both bridges cross the river. Each motorway direction has its own construction, so there are left and right Vranduk 1 and Vranduk 2 Bridges. The measuring instruments are placed on the right of Vranduk 1 Bridge and the left of Vranduk 2 Bridge on superstructure base segments above the S1 piers (*Fig. 1*).

Vranduk 1 Right Bridge starts at station km 1 + 280.00 (meaning that particular station is 1.28 kilometers from the start point of this motorway's chainage) to km 1 + 670.00. Starting at station 1 + 280.00, the length 76.292 m to station 1 + 356.292 is a constant left curve of 755.75 m radius, which continues in a transition curve 92.5 m long to 1 + 448.792. After that, there is a transient curve 86 m long to 1 + 546.049, which passes into a constant right curve of 694 m radius with a length of 123.951 m to the end of the bridge at the station 1 + 670.00. Warping is carried out on a 50 m length, 25 m left and right from the crossing of slope 2.5% to the left to a crossing slope 2.5% to the right. Vertical alignment in the beginning is almost 0% and gradually falls to 1.89%. The width of the roadway is 12.00 m, and the width of the protective barriers is 0.46 m. Total bridge width is 0.46 + 1.00 + 2.50 + 3.75 + 3.75 + 0.25 + 0.75 + 0.46 = 12.92 m.

The bridge has a prestressed concrete superstructure with spans of 80.00 + 120.00 + 120.00 + 70.00 = 390.00 m.
The span construction has a box cross section of variable height in the main spans and constant height in the rest of the bridge (parts of spans are built on scaffolding near the abutments). The height of the section changes parabolically from 6.80 m on the main piers to 3.20 m in the middle of the span, while the height on the rest of the bridge towards the abutments is a constant 3.20 m.

The top slab and box cantilevers have the same shape along the entire bridge, with a thickness of 0.55 m on joints with the webs, 0.25 m at the ends of cantilevers and 0.30 in the centre of the box. The box webs are 0.50 m thick with a thicknesses of 0.65 m above the piers. Thickening of the webs is done on a slope, 11.25 m from the edge of the piers. The bottom slab is 0.30 m thick.

The edges of the bottom slab are thickened in length from 0.60 to 0.42 m. The bottom slab is thicker on the supports, so above the abutments the thickness increases in length from 5.00 up to 0.50 m, while at the connection with the main piers it has a thickness of 1.00 m, which changes at a length of 36.25 m from the edge of the pier. Above the piers in the span construction there are two transverse diaphragms of 0.70 and 0.60 m thickness, which are mapped out by the outer contours of the pillar, with openings at the bottom 2.00 m high and 1.20 m wide. Above the abutment bearing diaphragm, the thickness is 3.00, height 1.70 and width 1.20 m. The middle piers are monolithically connected to the span structure, while the abutments have two bearings.

Pier S2D has a box cross section of 6.80 × 4.50 m in contact with the span construction that follows a 100:1 widening slope to ground contact. The middle pier (S2D) has a wall thickness of 0.70 m, while piers S1D and S3D consist of two parallel walls. The walls on S1D are 1.20 m thick and the walls on S3D are 1.40 m thick. The pier S1D is based on a round well foundation with a diameter of 9.00 m and a well depth of 8.00 m. The S2D pier is placed on 16 piles that are 1.20 m in diameter and 9 m long and are connected to a 13.00 × 13.00 × 3.00 m base slab. The S3D pier is placed on 16 piles that are 1.20 m in diameter and 19 m long and are connected to a 13.00 × 13.00 × 3.00 m base slab.

The U1D and U2D abutments are located on the embankment and are placed on shallow foundations. The U1D abutment has a side wing wall that is founded on a 8.00 × 3.50 × 2.00 m foundation. The main wall foundation is 13.92 × 7.00 × 2.00 m. The wall thickness is 3.00 m and there are two bearings on which the structure will be supported. On the left side there is no side wing wall. The U2D abutment foundation has a base dimension of 13.92 × 7.00 × 2.00 m with a 4.40 m high main wall which is 3.00 m thick and on which two bearings will be placed. There is a right-wing wall, founded on a 7.23 × 3.50 × 2.00 m foundation. There is no right-side wing wall. The abutments have approach slabs 4.00 m in length at an incline of 10%.

The bridge has been designed according to EN rules for a design life of 100 years. The superstructure and piers are made with C40/50 concrete, and the rest of the structure (piles, pile slabs, well, abutments) are made with C30/37. The reinforcing steel is B 500B and the prestressing steel is Y1860.[31]

Vranduk 2 Left Bridge starts at station km 1 + 816.00 to km 2 + 156.00. The bridge starts with a straight part, from station 1 + 816.00 to 1 + 840.75, and is 24.75 m long. After that comes a transition curve (chlothoid) 197.00 m long to 2 + 019.75, which becomes a constant left curve to the end of the bridge with a radius of 987.50, 136.24 m long to 2 + 156.00. The cross slope of the bridge on abutment U1L is 2.5% and is gradually increased to 4.0% on the end of the transition curve and it stays constant to the end of the bridge. The width of the roadway is 12.00 m, and the width of protective barriers is 0.46 m. The total bridge width is 0.46 + 1.00 + 2.50 + 3.75 + 3.75 + 0.25 + 0.75 + 0.46 = 12.92 m.

The bridge has a prestressed concrete superstructure with spans of 95.00 + 150.00 + 95.00 = 340.00 m. The span construction has a box cross section of variable height on the main spans and a constant height on the rest of the bridge (parts of the spans are built on scaffolding near the abutments). The height of the section changes parabolically from 8.40 m on the main piers to 4.00 m in the

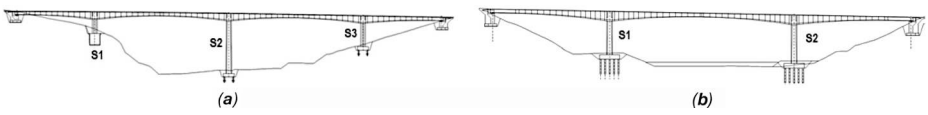


*Fig. 1: (a) Vranduk 1 Bridge longitudinal section. (b) Vranduk 2 Bridge longitudinal section*

middle of the span, while the height on the rest of the bridge towards abutments is a constant 4.00 m.

The top slabs and box cantilevers have the same shape along the bridge, with a thickness 0.55 m on joints with the webs, 0.25 m on the ends of cantilevers and 0.30 m in the middle of the box. The webs are 0.50 m thick and are thickened to 0.65 m above the piers. Web thickening is done 13.25 m from the edge of the pier. The top slab is 0.30 m thick with thickenings in length of 1.75–1.90 m to the web where it is 0.55 m.

The bottom slab is thickened at the supports, above the abutment in a 5.00 m length of slab it is thickened to 0.50 m, while on piers it is 1.00 m, changing in a length of 31.25 m. Two diaphragms stand above piers 0.70 m thick and follow the outer contours of the pier. The diaphragms have 2.00 × 1.00 openings. Above the abutment bearings, the diaphragms are 3.00 m thick with an opening of 1.85 × 1.00. The centre piers are monolithically connected to the span structure, and each abutment has two bearings.

Piers have a 6.80 × 4.50 m box cross section on the intersection with the span construction and the dimensions are widened in an inclination of 100:1 to ground level. All piers have walls that are 0.70 m thick. The piers are built on 20 piles that are 1.20 m in diameter and have lengths of 12 m for S1L and 12 m for S2L. They are connected to 16.60 × 13.00 × 3.50 m pile slabs.

Abutments U1L and U2L are situated next to an embankment and have shallow foundations. Abutment U1L has a 13.92 × 7.00 × 2.00 m foundation with a main wall 7.28 m high and 3.00 m thick. Bearings will be placed on top of the wall. Abutment wings have a 3.00 and 6.74 m long foundation with the same dimensions as the abutment wall foundation. The side wing walls are partly founded. Abutment U2L has a 13.92 × 7.00 × 2.00 m foundation with a wall 5.24 m high and 3.00 m thick. Bearings will be placed on top of the wall. Abutment wings have a 3.00 m long foundation with the same dimensions as the abutment wall foundation. Side wing walls are partly founded. The abutments have approach slabs 4.00 m in length at an incline of 10%.

The bridge has been designed according to EN rules for a design life of 100 years. The superstructure is made with C40/50 concrete, and the rest of the structure (piers, piles, pile slabs, well, abutments) are made with C30/37. The reinforcing steel is B 500B and the prestressing steel is Y1860.[32]

## Monitoring Plan and Measuring Equipment Installation

The monitoring on both bridges was done on the base segments of the first piers. Only two strain monitoring devices were available, each with a total of eight measuring points. Because of this, the bridges are monitored in only one section on the base segment, which allows the construction process to be followed through all phases and the strain changes in the concrete and prestressing steel to be measured. The monitoring began on 25 March 2021 and ended on 17 September 2021. The goal was to have a continuous strain data acquisition throughout the construction phase of the cantilevers on the S1 piers, as well as after the cantilevers had been connected and the span tendons prestressed. Following Hooke's law, the stress in the materials can be assumed using the strain and Young's modulus of elasticity.

Data acquisition systems and strain gauges were used, in this case electrical strain gauges that consist of carriers, covering foils, measuring grids and connections. The gauge was fixed to the structure with strong adhesives to ensure equal deformations. A weak electrical current was passed through the measuring grid, which gave the reference resistance. Deforming the grid by stretching or compressing changes its resistance.

If the gauge sensitivity factor is known (the relation between strain and resistance differences) the strain can be calculated through the resistance difference. All the gauges used measured strain in one direction (linear gauges) and had a nominal resistance of 120 Ω. For concrete, gauges with a 50 mm measuring grid were used because of the heterogeneous nature of the material. For the prestressing steel, gauges with a 3 mm measuring grid were used because the material was homogenous and a gauge this size can fit on a prestressing steel wire. The device used for the data acquisition system has eight input channels (via 15-pin connectors) and supports half and full Wheatstone bridge configurations for multiple measuring purposes. In this case, a quarter Wheatstone bridge configuration was used with special adapters. Precise 120 Ω metal-film resistors were connected in the 15-pin connectors to form a full Wheatstone bridge configuration with the strain gauge. The adapter was located near the strain gauge (15–20 cm) to reduce measuring deviations due to additional resistance in cables that lead from the strain gauge to the adapter.

All of the strain gauges have been prepared in advance. Depending on the measuring point, eight extension cables with lengths of 17.00 to 24.00 m were made with a male 15-pin connector on one end and a female 15-pin connector on the other.

The strain gauges were soldered on one end of the adapters and were connected to the data acquisition system, which has an accuracy of 0.05% and can measure up to 40,000 samples per second through extension cables. The universal amplifier was connected to a computer through a LAN cable and utilised computer software for data acquisition, storage and analysis.

Both the computer and the universal amplifier were connected to an uninterruptable power supply that was protected from short term power disruptions. The UPS was connected to a 220 V power network.

The strain gauges for both bridges were applied on concrete and prestressing steel in the same cross section of the superstructure. The section was moved 0.50 m from the edge of diaphragms towards the span to lessen its effect on strain. A total of 16 strain gauges were installed.

On Vranduk 2 Bridge, four strain gauges were installed on concrete, specifically in the inner corners of the superstructure box cross section. The gauges were offset 0.50 m from the webs of the cross section. Four strain gauges were installed on prestressing steel wires, two on prestressing tendons for the construction stage of segment 1, and two on the prestressing tendons for the construction stage of segment 7. The gauges did not compensate for temperature change strain.

On Vranduk 1 Bridge, four strain gauges were installed on concrete in

the corners of the cross section, two gauges on the prestressing steel used for the construction stage of the first segment, and two gauges, one on the unloaded concrete sample positioned near the upper slab and one on the unloaded prestressing wire sample placed next to the prestressing cable, for temperature compensation (*Fig. 2*).

The procedure for installing strain gauges on concrete was identical for both bridges. Firstly, the concrete surface in the area where the gauge is fixed was ground with a fine grinder to get a good surface for the adhesive. This is especially important on the bottom slab because of the coarse concrete surface. On the top slab, the concrete was already very smooth because of the formwork.

After grinding, a steel hook was anchored near the ground area to hold the adapter and gauge before fixing, as well as to prevent accidental damage or disconnection during monitoring. The adapter was fixed to the hook with plastic zip ties. The next step was to clean the area with alcohol to remove leftover dust. Two-component adhesive was mixed and applied to the concrete surface, and the strain gauge was put in the adhesive. Excessive adhesive was pushed out manually with the help of a plastic film to avoid sticking, and the adhesive was left to harden. After hardening, a protective aluminium foil with a kneading compound was put over the strain gauge and lead wires to protect from weather and smaller impacts. The edge of the aluminium foil was covered with silicone to completely isolate the strain gauge. The resistance of the gauge was checked through the adapter to ensure the installation was correct and the gauge worked.

For strain gauges installed on prestressing steel, alcohol was used to clean the area of the wire where the gauge would be applied. The strain gauges and adapters were fixed to the surrounding steel reinforcement bars with plastic zip ties. Cyanoacrylate super glue was applied to the gauge and the gauge was positioned on the wire and held in place with a thin plastic film. After hardening, a protective aluminium foil with kneading compound was put over the strain gauge and lead wires to protect from water. The resistance was checked to confirm that no damage had occurred during installation.

After strain gauge installation, the adapters were connected to the data acquisition system inside the pier head through extension cables that passed through openings in the diaphragm for gauges on concrete, and through plastic tubes left next to prestressing ducts for gauges on prestressing steel.

## Numerical Models of the Bridges

Hybrid 3D FEM numerical models of Vranduk 1 and Vranduk 2 Bridges have been made to obtain and compare results with measured stress/strain values. All modelling was carried out in a computer software with robust capabilities, with respect to realistic bridge dimensions and construction stages. Two models were made for each bridge (four models in total), one model considering creep and shrinkage calculations between construction stages and the other one without creep or shrinkage. The goal was to determine the effect of creep and shrinkage on the stress/strain values for these balanced cantilever bridges. A hybrid model consisting of structural lines and structural areas was adopted for both bridges to get a better overview of results. Most of the bridge was modelled with structural lines that are given proper cross sections, while the pier head and S1 piers where the strains were measured were modelled with area elements to obtain accurate results (*Fig. 3*).

The general layout of the bridges was taken from design drawings.[31,32] A maximum longitudinal slope of 1.89% on both Vranduk 1 and Vranduk 2 Bridges was omitted since it had a negligible effect on the structure. Horizontal curves were not insignificant and were taken into account when modelling the bridges for two reasons. On balanced cantilever bridges, creep and shrinkage play an important part in segment precamber calculations during construction and big bends will affect cable positioning, creep and shrinkage. The other reason is that the pier and its superstructure are a cantilever during construction. For concrete bridges, self-weight is a dominant load and the eccentricity of such a load due to road bends and its effect on piers and foundations cannot be ignored. After inspecting the design drawings, a graphical input program was used to input the correct axis geometry. Placements (planes linked to a certain chainage on the axis) were input on the axes so segments of the bridge with different cross sections and prestressing cables could the defined. Horizontal curves were also linked to chainage on the axis.

After the layout had been set, pier and superstructure cross sections were simplified and input. Pier cross sections remained the same since they were already simple. Superstructure sections had been modified so the box top slab is horizontal and has no cross slope since it has little effect on the structure and would require more time for input. The parapet had been simplified so that the top slab extended to the end of the parapet and the missing self-weight was added to additional weight in loads.

The superstructure was highest on piers and lowest in the middle of the spans. The upper box slab followed the longitudinal slope and was horizontal in the model, while the lower slab followed a parabolic trajectory. This means that every segment of the

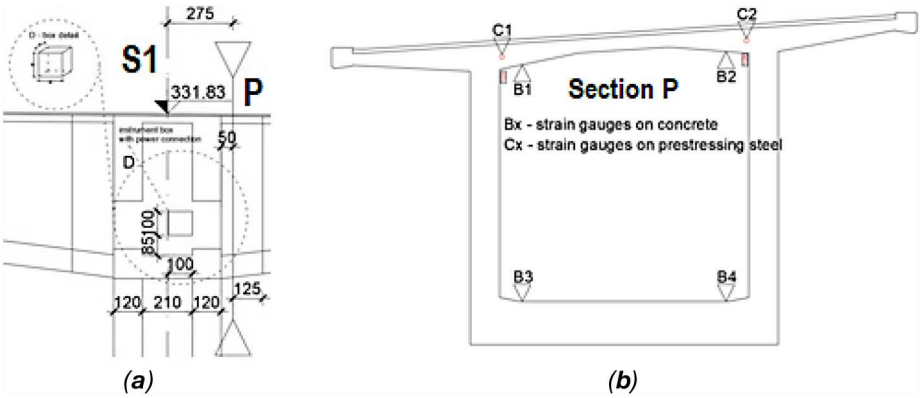


*Fig. 2: (a) Vranduk 1 longitudinal strain gauge section position. (b) Vranduk 1 strain gauge position in the cross section*

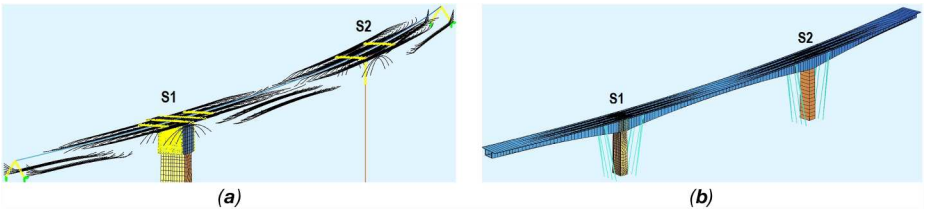


*Fig. 3: (a) Vranduk 2 numerical model tendon layout. (b) Vranduk 2 numerical model*

bridge cantilever had different start and end cross sections. In total, 13 superstructure cross sections were input for Vranduk 1 Bridge, and 17 for Vranduk 2 Bridge. Vranduk 1 superstructure and piers were input with C40/50 concrete and B500B reinforcement, while on Vranduk 2 the superstructure was input with C40/50 concrete and piers were input with C30/37 concrete. The reinforcement was B500B. Prestressing cables for both bridges were input with Y1860 prestressing steel.

After the cross sections were input, the segments of the superstructure and piers were formed as construction lines with start and end cross sections. When forming the finite element mesh, the software interpolated cross sections between segment ends. Piers and abutments were connected to the superstructure with constraints. Bridge models were mostly line elements and in those sections connections were made with point constraints. On piers S1 for both bridges, the pier and pier head were modelled with area elements and those sections were connected to the rest of the superstructure with point-to-line constraints.

Structural areas were modelled with realistic geometry and slab thickness with the finite element mesh automatically generated and mostly regular. The abutments and foundations were not modelled since they had little effect on the structure, point and line supports were used to represent foundations. The piers had fixed supports and the abutments had roller supports that allowed longitudinal movement and moment.

All prestressing cables were modelled individually for both bridges as post tensioned cables embedded in the concrete and grouted immediately after prestressing, whereas in reality the grouting was done a day or two after prestressing. Each cable had 19 strands of 1.5 $cm^2$ area (each cable was 28.5 $cm^2$). All cables had a low relaxation value of 2.5% after 1000 h stressed at $0.7 \times f_{pk}$.

Vranduk 1 Bridge has a total of 168 prestressing cables, 120 cables for the balanced cantilevering construction stages in the top slab of the superstructure cross section and 48 cables for the use phase in the bottom slab in spans. Above each pier head there are 40 construction stage cables (20 per web) that are anchored on each finished segment of the structure. Six cables are anchored on the first and second segments, four cables on segments three to seven, and two cables on segments eight to eleven. In the main spans, there are sixteen cables in the lower slab (eight per web). These cables are anchored on segments five to eight with four cables per segment. There are eight cables in end spans (four per web) with four cables anchored on two segments.[31]

Vranduk 2 Bridge has a total of 174 prestressing cables, 124 cables for balanced cantilevering construction stages in the top slab of the superstructure cross section and 50 cables for the use phase in the bottom slab in spans. Above each pier head there are 62 construction stage cables (31 per web) that are anchored on each finished segment of the structure. Six cables are anchored on segments one to three, four cables on segments four to thirteen, and two cables on segments fourteen to fifteen. In the main span, there are 20 cables in the lower slab (10 per web). These cables are anchored on segments eight to twelve with four cables per segment. There are fourteen cables in end spans (seven per web) with four cables anchored on three segments and two cables anchored on one segment. In the main span, there are two cables in the upper slab used for the closing segment in case of sudden temperature change or other accidental loading.[32]

The following loads that affect the bridge structures during and immediately after construction are taken into account: dead load of the structure segments, additional dead load per design drawing (parapets, concrete barriers, asphalt, waterproofing, drainage, installations), prestressing, creep and shrinkage, and form traveller construction loads.

Construction stages are the most important part of a balanced cantilever bridge calculation since they determine the behaviour of the bridge before and after closing segments. Before the work can begin on the superstructure, the pier and pier head are constructed. Then, the real construction stages for the superstructure segments are input into the program in the following general repeating order:

XX10 S1-SEG1–segment dead load and stiffness activated
XX11 S1-SEG1 prestressing–prestressing of a previously activated segment
XX14 S1-SEG2 form traveller–the form traveller is moved for the next segment
XX15 C+S–the creep and shrinkage step
XX17 S1-SEG2 fresh concrete–the concrete weight of the next segment, no stiffness
XX20 S1-SEG2–the next segment dead load and stiffness are activated

Loads such as the form traveller and fresh concrete are artificially moved by activating and deactivating the load for each segment as the construction stages progress. Vranduk 1 Bridge has a total of 322 construction phases and Vranduk 2 has a total of 312 construction phases.

Construction stages are calculated using a full geometrical nonlinear analysis with nonlinear material properties (the serviceability limit state (SLS) material curve is used in the calculations, which gives realistic results). Creep and shrinkage are calculated according to EN 1992-1-1:2004 +AC:2010.[33] For each time step, the correct duration has been provided as well as values for humidity (70%) and temperature (20°). For longer periods, more time steps are defined. Creep values are calculated individually for each load part, so backward creeping is taken into account. Furthermore, each new segment is positioned tangentially on existing structure, so the segment positions

and deflections are calculated correctly. The time of first loading is input separately for every activated part of the structure because of different construction durations. Losses in prestressing cable forces due to the relaxation of prestressing steel as well as the creep and shrinkage of concrete are calculated and taken into account. The stiffness development of concrete is taken into account by calculating the temperature adjusted concrete age T1 according to CEB-FIP model code 1990.[34]

## Results

Vranduk 1 Bridge was monitored for a total of 77 days, while Vranduk 2 Bridge was monitored for 107 days. During the monitoring of both bridges, samples were taken at a rate of one sample every 50 s. This meant 1728 samples in one day per measuring point. In the course of a single day, there were deviations in the strain curve owing to temperature changes and different construction stage loads.

In an effort to present clear results, the diagram for each measuring point during the monitoring period was created by using a single reference sample of the point in a day, taken at the same time every day. Original strain samples were converted into approximate stress using Hooke's law. Since the superstructure concrete in both bridges is C40/50, an elastic modulus of 35,220 MPa (according to EN1992-1-1:2004) was multiplied with strain data to attain stress values. Prestressing steel Y1860 was used with an elastic modulus of 195,000 MPa. Unfortunately, the prestressing steel sensors were damaged during cable grouting and no useful conclusions can be extracted from the data at this time owing to small sample sizes. Strain and stress results obtained from the numerical models with and without creep and shrinkage are shown along with measured data. Measuring points on the upper (B1 and B2) and lower (B3 and B4) slab are grouped since they have similar values and behaviour.

The strain results comparing measured strain with numerical results with and without creep and shrinkage are shown below (*Figs. 4–7*). Furthermore, graphs showing the compressive stress through points B1 to B4 on both bridges relative to characteristic concrete strength $f_{ck}$ are shown (*Figs. 8 and 9*).

In addition to strain and stress, vertical deflections during bridge construction were monitored and the measured results are compared to numerical precamber calculations (*Fig. 10*).

As expected, bridge monitoring results show that all points of the cross section (B1–B4) are in compression owing to cantilever construction processes and prestressing. Self-weight causes compressive strain in the lower slab and tensile strain in the upper slab initially. The prestressing of balanced cantilever cables used for the construction stages, which are located in the upper part of the superstructure, causes a large increase in the compressive strain of the upper slab, and minor or no increase in compressive strain in the lower slab. With this repeating process, compressive strain is expected over the entire cross section.

On Vranduk 1 (120 m main span) several gaps in measurements occurred, with the largest between days 13 and 27, missing some of the segment construction stages. Measuring point B3 shows unrealistic strain values, likely owing to damage during installation of the strain gauges. Nevertheless, the remaining strain gauges show reliable results. Points B1 and B2 on the upper slab show a stepped increase in compressive strain up to 270.25 μm/m (roughly 9.5 MPa) on day 28 when segment 7 was prestressed. Each stepped increase in strain represents prestressing of a segment with cantilever construction cables located in the upper part of

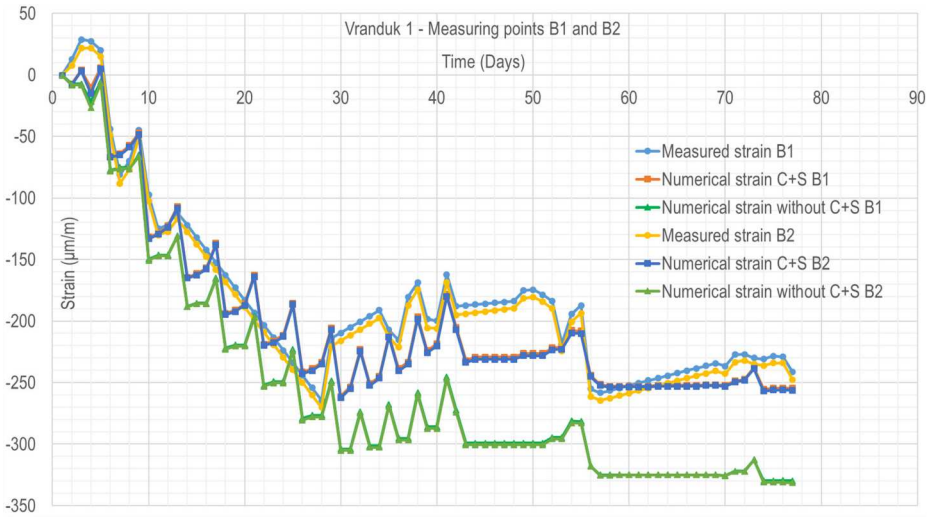


*Fig. 4: Vranduk 1–measured and numerical strain with and without creep and shrinkage (C+S)–points B1 and B2*

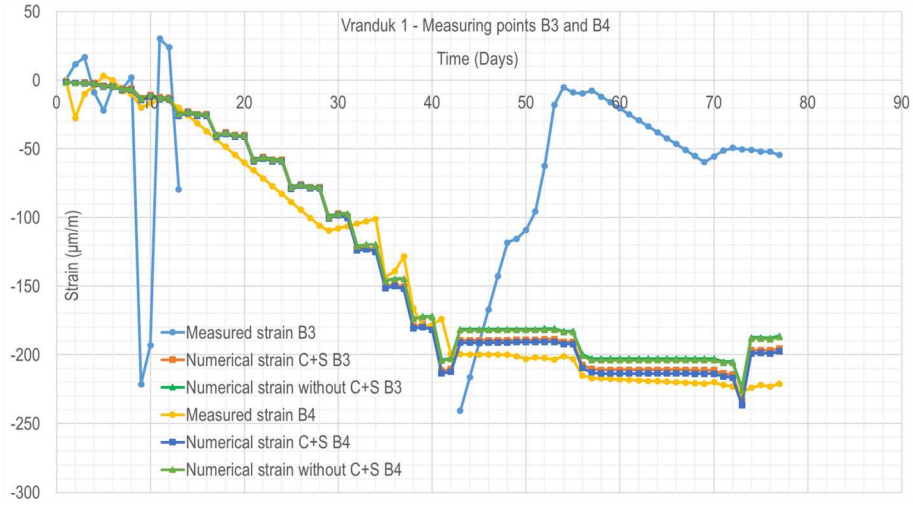


*Fig. 5: Vranduk 1–measured and numerical strain with and without creep and shrinkage (C+S)–points B3 and B4*

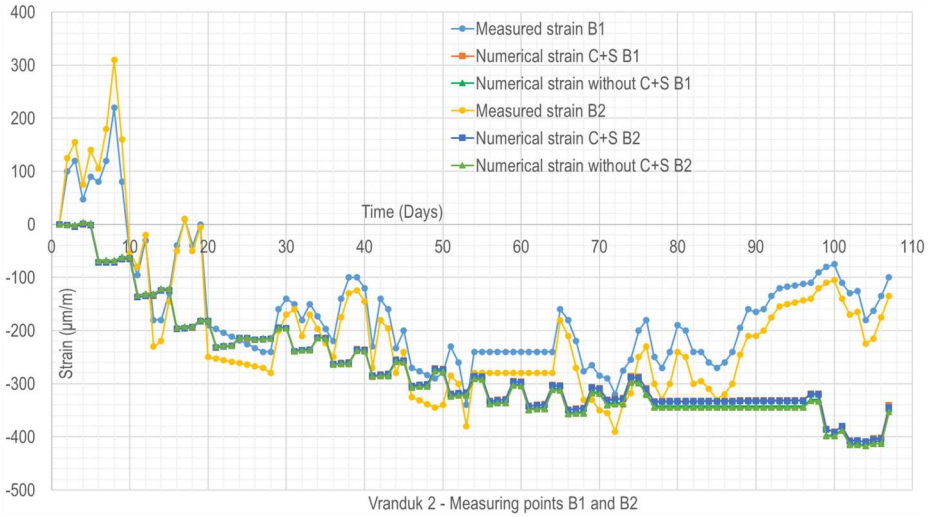


*Fig. 6: Vranduk 2–measured and numerical strain with and without creep and shrinkage (C+S)–points B1 and B2*

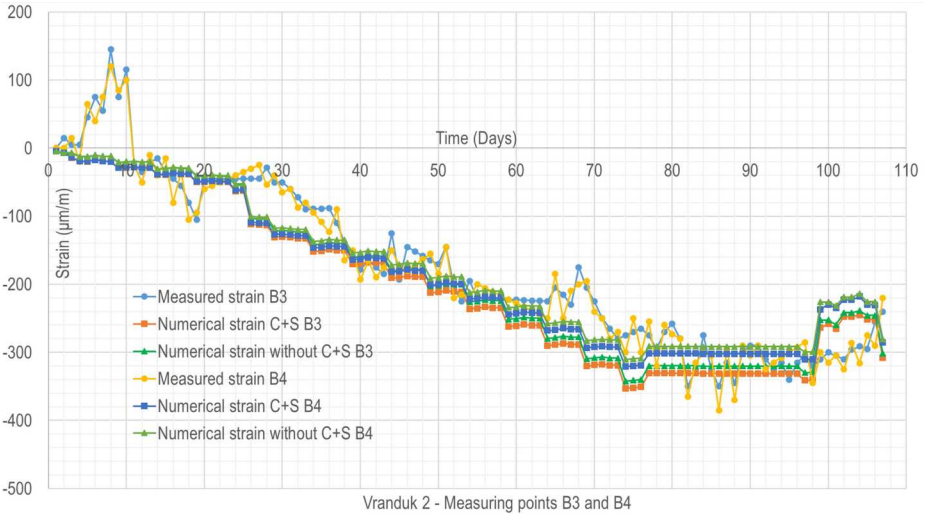


*Fig. 7: Vranduk 2–measured and numerical strain with and without creep and shrinkage (C+S)–points B3 and B4*

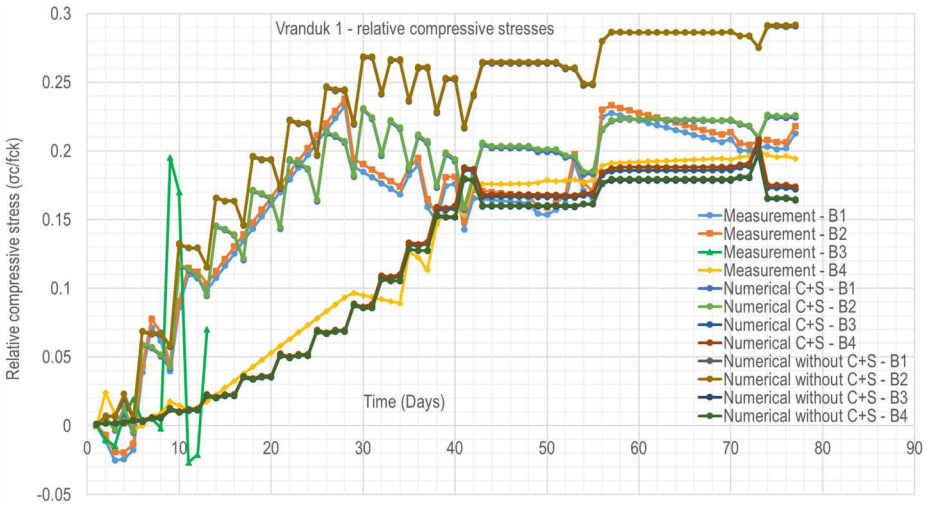


*Fig. 8: Vranduk 1–relative compressive stress ($\sigma_c/f_{ck}$)–points B1 through B4*

the superstructure. Since all segments after segment 3 have four cables per segment, after segment 7 the weight of the cantilever becomes greater than the prestressing force moment and the compressive strain in the upper slab starts lowering. On day 42, the last prestressing step is visible with the completion of the 11th segment where points B1 and B2 have a compressive strain of around 199.56 μm/m (roughly 7.0 MPa). On day 56, the lower slab prestressing cables in the span are prestressed, which causes the compressive strain in the top slab to increase to around 261.26 μm/m (about 9.2 MPa) at points B1 and B2. Compressive strain in the top slab continues to decrease slowly to around 247.67 μm/m (roughly 8.5 MPa) on day 77, likely because of the gradual addition of the dead load of the concrete barriers. Point B4 shows a stepped increase in strain, with each step representing the addition of a dead load due to the next segment.

Unlike points B1 and B2, point B4 has a constant increase in compressive strain up to 199.56 μm/m (about 7.03 MPa) on day 42 when the last segment was activated with prestressing. On day 56, point B4 gains some compressive strain (up to 214.88 μm/m, roughly 7.57 MPa) owing to the lower slab cables in the span being prestressed. The compressive strain in the lower slab continues to increase slowly up to 220.88 μm/m (around 7.78 MPa) owing to the already mentioned additional dead load.

Vranduk 2 Bridge (the 150 m main span) shows similar results with a more jagged strain diagram due to lack of temperature compensation. Points B1 and B2 on the upper slab have a stepped increase in strain up to 320 μm/m (roughly 11.3 MPa) and 390 μm/m (about 13.7 MPa) on day 72. The last segment (the 15th) was prestressed on day 78 with 270 μm/m (around 9.5 MPa) and 330 μm/m (roughly 11.6 MPa) compressive strain. On days 102 and 104, the lower slab prestressing was done with B1 and B2 having 180 μm/m (about 6.3 MPa) and 225 μm/m (around 7.9 MPa) of compressive strain. As with the previous bridge, points B3 and B4 showed a stepped increase in compressive strain each time a new segment's dead weight was added (with deviations due to temperature change and construction stage loads), reaching

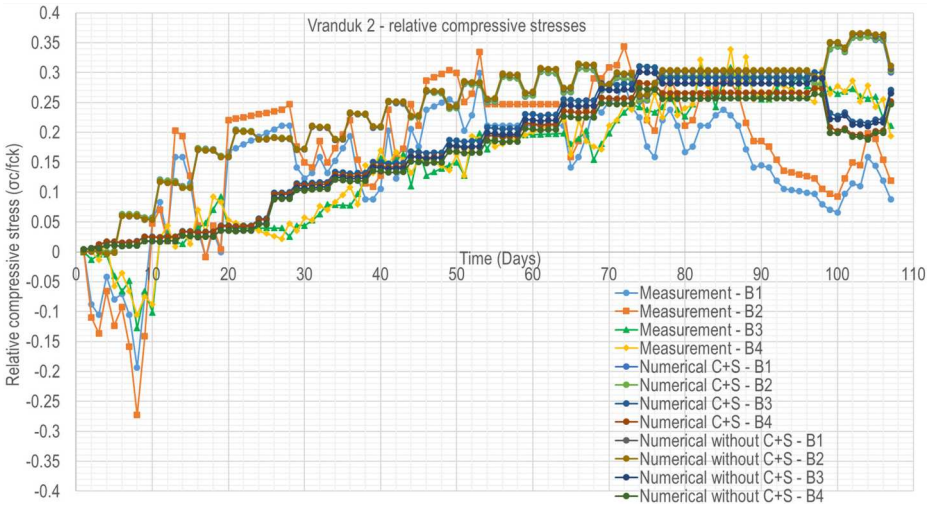


*Fig. 9: Vranduk 2–relative compressive stress ($\sigma_c/f_{ck}$)–points B1 through B4*

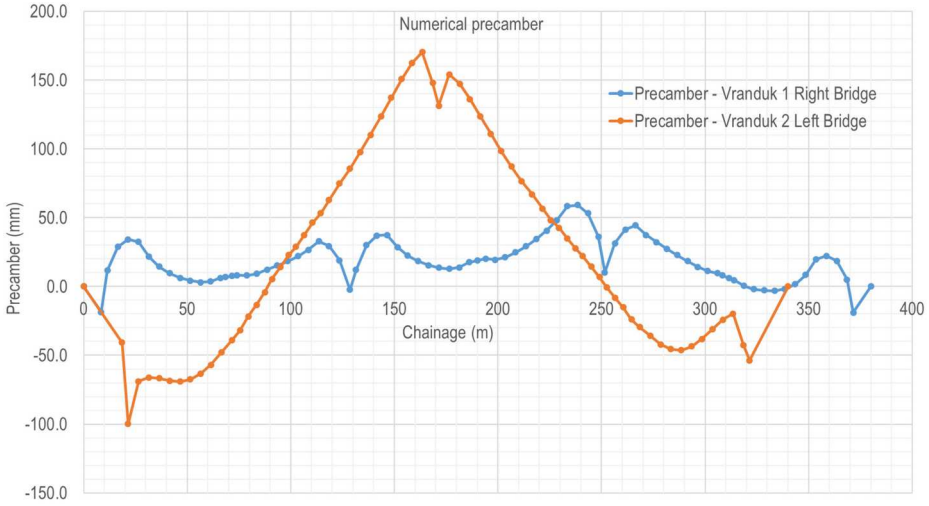


*Fig. 10: Vranduk 1 and Vranduk 2–numerical precamber*

295 μm/m (roughly 10.39 MPa) and 320 μm/m (about 11.27 MPa) on day 78 when the last segment was activated. The maximum measured strain is 350 μm/m (around 12.3 MPa) and 385 μm/m (about 13.6 MPa) on day 86, likely due to uncompensated temperature strain and construction stage loads. When the lower slab cables in the span were prestressed, points B3 and B4 had 290 μm/m (roughly 10.3 MPa) and 315 μm/m (about 11.1 MPa) of compressive strain.

In relation to the characteristic concrete strength $f_{ck}$, the stresses on Vranduk 1 reached up to 0.238 (9.52 MPa) relative compressive stress in the upper slab and up to 0.20 (8 MPa) relative compressive stress in the lower slab. After the bridge was connected, both the upper and lower slabs had roughly 0.20 (8 MPa) relative compressive stress. On Vranduk 2, the relative compressive stress in the upper slab reached up to 0.343 (13.72 MPa), which is a local maximum, while the relative compressive stress in the lower slab reached 0.339 (13.56 MPa).

Numerical models were used to obtain the necessary precamber of the structure so that the bridges would maintain the correct geometry after construction and a 30-year period of use. As expected, Vranduk 1 Bridge shows a much lower necessary precamber with a maximum of 59.50 mm, while Vranduk 2 Bridge shows a greater necessary precamber of 170 mm.

## Discussion

During the monitoring process for both bridges, power outages were common across the entire construction site. Even though the equipment was connected to an uninterrupted power supply to protect from power surges and outages, it was only enough for 20–30 min protection. The outages usually lasted longer than that which would cause the data acquisition system to shut down, saving all data up to that point. As soon as the problem was detected, the system was turned back on as soon as possible. The system also suffered some accidental mechanical damage due to the construction process, severing several extension cables, which were replaced as soon as the damage was noticed. The missing data was interpolated during data processing, losing some construction stage phases, but retaining the general trend that was also confirmed by numerical results.

Strain values on calculated models corresponded well with the measured values on Vranduk 1 and Vranduk 2 Bridges with minor differences. The jagged parts of the measured stress diagrams are due to construction processes and different loads during execution in addition to the form traveller that could not be taken into account in the numerical model such as working personnel, staff and visitors, possibly with hand tools or other small site equipment, the storage of movable items like building and construction materials, precast elements and equipment, or various movable heavy machinery and equipment. The minor differences in calculated and measured stress could be due to a number of reasons. Firstly, the numerical model was a hybrid between line and area elements to keep the system manageable. Better results could be obtained with 3D brick elements; however, due to the large size and specific calculation requirements of balanced cantilever bridges, each construction phase would have to be considered and calculated and that would require large amounts of computing power. Furthermore, the material stress–strain laws are simplified and uniform on the entire structure, while in reality the material (especially concrete) can vary from segment to segment when installed. Accidental deviations during construction were not taken into account in the numerical model. Numerous accidental construction stage loads (workers, equipment and material storage), as well as nonlinear temperature

changes during construction was not taken into account in the numerical model. Specifically, on Vranduk 2 Bridge, temperature strain was not compensated which in turn shows large deviations in measured strain values. Considering the coefficient of linear thermal expansion of concrete is $10^{-5}\,K^{-1}$, the difference could be up to 300 μm/m (10.57 MPa) if a 30 K temperature change is considered. At times, the measurements were interrupted and the results during the interruptions were interpolated. As a result, the numerical values gave a more detailed overview of bridge behaviour during each stage of construction (showing the construction process for each segment, including form traveller positioning, formwork and reinforcement installation, concreting and prestressing), but the general stress trend followed the measured values. As expected, creep and shrinkage reduced compressive stresses in the upper slab, and increased compressive stresses in the lower slab of the cross section.

When comparing measured and numerical values, the diagrams show that the calculated numerical results including creep and shrinkage corresponded very well with the measured values on both bridges. On points B1 and B2, Vranduk 1 showed differences of roughly 50 μm/m (1.76 MPa) on days 42 to 52, with very close results before and after when taking creep and shrinkage into account. The difference was very likely due to an unknown load during the construction stages, since the values match very well after this period. The results excluding creep and shrinkage matched very well in the beginning, but, as expected, there was an almost linear gain in the the strain difference of 70 μm/m (2.65 MPa) at the end of 77 days, showing how creep and shrinkage, as expected, lowered the compressive stress in the upper slab. Point B3 showed unrealistic results as a result of signal loss on day 13, likely due to unintentional measuring cable damage during construction. The numerical results, however, showed that creep and shrinkage increased the compressive strain in the lower slab by up to 10.79 μm/m (0.38 MPa). Point B4 showed good correlation with the numerical results considering creep and shrinkage with measured strains, and, similarly to B3, showed that creep and shrinkage increased compressive strain in the lower slab by up to 10.51 μm/m (0.37 MPa).

On Vranduk 2 Bridge, when looking at points B1 and B2, the diagram represents good correlation with larger local discrepancies of about 141.96 μm/m (5.01 MPa) and 245.47 μm/m (8.64 MPa) at the end. The differences were most likely due to a lack of temperature compensation in the measurements, which showed unrealistic strain that included temperature strain. The numerical results showed that creep and shrinkage decreased compressive strain in the upper slab by roughly 11.35 μm/m (0.40 MPa). The diagram for points B3 and B4 showed an even better correspondence with numerical and measured results, maintaining the larger local differences from lack of temperature compensation, but also maintaining the same strain trend through the construction stages. Average local differences considering creep and shrinkage were about 38.61 μm/m (1.36 MPa), while creep and shrinkage increased the compressive strain in the lower slab by 11.37 μm/m (0.40 MPa).

## Conclusion

In conclusion, balanced cantilever bridges sustain high compressive strains and stresses in concrete during construction and use. The general behaviour of all these structures is similar, but, due to the different spans, the superstructure characteristics (self-weight, cross-section properties, number and position of balanced cantilever prestressing cables) are different, which causes differences. It was clearly shown that, during the construction stage, the maximum compressive strain in the upper slab in the 120 m span bridge Vranduk 1 was 270.25 μm/m (roughly 9.5 MPa), while the 150 m span Vranduk 2 had a maximum compressive strain of 390 μm/m (about 13.7 MPa) which is a difference of 119.75 μm/m (around 4.2 MPa) or roughly 30%. In the lower slab, Vranduk 1 had a maximum compressive strain of 226.86 μm/m (roughly 8.0 MPa), while Vranduk 2 had 385 μm/m (around 13.6 MPa), which is a difference of 158.14 μm/m (about 5.6 MPa) or roughly 40%. Even if the lack of temperature compensation is taken into account on Vranduk 2 Bridge and average values compared, Vranduk 2 still had a higher compressive strain of around 283.93 μm/m (roughly 10.0 MPa). This is to be expected, as longer spans require more robust superstructure, which generally sustains a higher load.

Creep and shrinkage have a considerable effect on balanced cantilever bridges in terms of deflections that have to be taken into account so that the segments get the proper precamber. This is especially important on stitch segments where two cantilevers are joined with the end goal of correct road geometry. This research shows the effect of creep and shrinkage on strains in the construction phases. On Vranduk 1, the maximum difference is 70 μm/m (2.65 MPa) in the upper slab, which is roughly 28% of the maximum compression strain. On Vranduk 2, the maximum local difference is 245.47 μm/m (8.64 MPa), i.e. around 63% of the maximum compression strain. Excluding the maximum values, creep and shrinkage make a difference of around 11 μm/m (0.40 MPa) ,which is 4.2% of the maximum on Vranduk 1 and 2.94% of the maximum on Vranduk 2. The small differences are probably due to stress fluctuations between box-cross-section slabs and webs. The results also show the importance of temperature compensation when monitoring strain and stress for a longer period of time, since the Vranduk 1 Bridge results have a better correlation with numerical results owing to temperature compensation. Most importantly, the strain differences and trends at all measured points are similar when measured and numerical results are compared, which represents a very good match with strain results and confirms the expected bridge behaviour through the entire cantilever construction stage including stitch segment and bridge monolitization.

Relative compressive stresses show that Vranduk 1 Bridge is less stressed than Vranduk 2 when comparing the characteristic concrete strength, with a ratio of 0.238. On the other hand, Vranduk 2 Bridge has a higher stress level, with a ratio of 0.343. Precamber calculations show that the maximum precamber of Vranduk 1 is significantly lower compared to Vranduk 2, being only 35% of its value.

Finally, a recommendation is given for the design and construction of 120 m span bridges if the site conditions allow

it and the piers are not too high. A 120 m span superstructure will generally have lower strain and stress levels, as well as lower self-weight. The real benefit is that the superstructure will have a lower cross section (in this case the difference is 1.60 m on the piers, and 0.80 m in the central part of the span), which is much simpler and safer to build. A smaller structure has lower chances of encountering issues during construction inherent in the construction method (fewer prestressing cables to install, easier cable placement and control, smaller forces for local tendon radial force issues and cracking on the lower slab, blisters or through the web due to large prestressing forces). Smaller stress levels, smaller necessary precamber and a leaner structure imply less uncertainty during the construction period and greater feasibility.

## Disclosure Statement

No potential conflict of interest was reported by the authors.

## Funding

This research is partially supported through project KK.01.1.1.02.0027, co-financed by the Croatian Government and the European Union through the 10.13039/501100008530 European Regional Development Fund under the Competitiveness and Cohesion Operational Programme.

## Data Availability Statement

All data, models, or code that support the findings of this study are available from the corresponding author upon reasonable request.

## References

[1] Mathivat J. The cantilever construction of prestressed concrete bridges; Editions Eyrolles: 61, boulevard Saint-Germain, 75005 Paris, France, 1979

[2] Skrinar M, Strukelj A. Eigen frequency monitoring during bridge erection. *SEI*. 1996;6 (3):191–194.

[3] Casas JR. Reliability-based partial safety factors in cantilever construction of concrete bridges. *J Struct Eng*. 1997;123(3):305–312.

[4] Manjure PJ. Rehabilitation of balanced cantilever bridges. *Indian Concr J*. 2001;75(1):76–82.

[5] McDonald B, Saraf V, Ross B. A spectacular collapse: Koror-Babeldaob (Palau) balanced cantilever prestressed, posttensioned bridge. *Indian Concr J*. 2003;77(3):955–962.

[6] Kwak HG, Son JK. Span ratios in bridges constructed using a balanced cantilever method. *Constr Build Mater*. 2004;18(10):767–779.

[7] Kwak HG, Son JK. Design moment variations in bridges constructed using a balanced cantilever method. *Constr Build Mater*. 2004;18 (10):753–766.

[8] Radić J, Gukov I, Meštrović D. A new approach to deflection analysis of cantilever beam bridges. In: Watanabe E, Frangopol DM, Utsunomiya T, editors. Proceedings of the 2nd International Conference IABMAS – Bridge Maintenance, Safety, Management and Cost; Oct 18–22; Kyoto, Japan. Leiden: A. A. Balkema Publishers; 2004; p. 8.

[9] Pimanmas A. The effect of long-term creep and prestressing on moment redistribution of balanced cantilever cast-in-place segmental bridge. *SJST*. 2007;29(1):205–216.

[10] Jung S, Ghaboussi J, Marulanda C. Field calibration of time-dependent behavior in segmental bridges using self-learning simulation. *Eng Struct*. 2007;29(10):2692–2700.

[11] Hewson N. Balanced cantilever bridges. *Concrete (London)*. 2007;41(10):59–60.

[12] Hedjazi S, Rahai A, Sennah K. Evaluation of creep effects on the time-dependent deflections and stresses in prestressed concrete bridges. *Bridge Struct*. 2007;3(2):119–132.

[13] Marzouk M, Said H, El-Said M. Special-purpose simulation model for balanced cantilever bridges. *J Bridge Eng*. 2008;13 (2):122–131.

[14] Kronenberg J. Continous concrete placing during balanced cantilever construction of a bridge. *Concr Eng Int*. 2008;12(3):38–39.

[15] Kamaitis Z. Field investigation of joints in precast post-tensioned segmental concrete bridges. *Balt J Road Bridge Eng*. 2008;3(4):198–205.

[16] Vonganan B. The second Mekong international bridge, Thailand. *SEI*. 2009;19 (1):67–68.

[17] Pimanmas A, Imsombat S, Neilsen KH. New Phra- Nangklao bridge—A balanced cantilever prestressed concrete bridge in Thailand. *SEI*. 2009;19(1):38–40.

[18] Starossek U. Shin Chon Bridge Korea. *SEI*. 2009;19(1):79–84.

[19] Altuşnişık AC, Bayraktar A, Sevim B, et al. Construction stage analysis of Kömürhan highway bridge using time dependent material properties. *Struct Eng Mech*. 2010;36(2):207–223.

[20] Malm R, Sundquist H. Time-dependent analyses of segmentally constructed balanced cantilever bridges. *Eng Struct*. 2010;32(4):1038–1045.

[21] Stathopoulos S, Seifried G, Kotsanopoulos P, et al. The Metsovo Bridge, Greece. *SEI*. 2010;20(1):49–53.

[22] Ates S. Numerical modelling of continuous concrete box girder bridges considering construction stages. *Appl Math Model*. 2011;35 (8):3809–3820.

[23] Ates S, Atmaca B, Yildirim E, et al. Effects of soil-structure interaction on construction stage analysis of highway bridges. *Comput Concr*. 2013;12(2):169–186.

[24] Pimentel M, Figueiras J. Assessment of an existing fully prestressed box-girder bridge. *Proc Inst Civ*. 2017;170(1):42–53.

[25] Sumerkan S, Bayraktar A, Türker T, et al. A simplified frequency formula for post-tensioned balanced cantilever bridges. *Asian J Civ Eng*. 2019;20:983–997.

[26] Bayraktar A, Kudu FN, Sumerkan S, et al. Near-fault vertical ground motion effects on the response of balanced cantilever bridges. *Proc Inst Civ*. 2020;173:17–33.

[27] Caner, A., Apaydın, N., Cınar, M., Peker, E., Kılıc, M. (2021). Reconstruction of Partially Collapsed Post-tensioned Beğendik Bridge During Balanced Cantilever Construction. In: Gülkan, P., Caner, A., Memisoglu Apaydin, N. (eds) Developments in International Bridge Engineering. Springer Tracts on Transportation and Traffic, vol 17. Springer, Cham. https://doi.org/10.1007/978-3-030-59169-4_17

[28] Bravo J, Benjumea J, Consuegra FA. Parametric Study to Estimate Seismic Displacement Demands of Balanced Cantilever Bridges in Service and Construction Conditions. Conference: fib Symposium 2021 - Concrete Structures: New Trends for Eco-Efficiency and Performance, 2021

[29] Furunes EW. Trysfjord bridge, parametric analysis and modelling for drawingless construction of a concrete balanced cantilever bridge. IABSE Congress: Structural Engineering for Future Societal Needs, Ghent, Belgium, 1999–2004, 2021

[30] Akbar S, Carlie M. *Long-term deformation of balanced cantilever bridges due to non-uniform creep and shrinkage*. KTH Royal Institute of Technology, School of Architecture and the Built Environment, 2021.

[31] Integra Ltd. Mostar. *Preparation of main design and related studies for motorway section in the Corridor Vc, Group F–Structures (Engineering Structures), Book: F 2100–Civil design of the Vranduk 1 bridge, textual part and drawings*, 2018.

[32] Integra Ltd. Mostar. *Preparation of main design and related studies for motorway section in the Corridor Vc, Group F–Structures (Engineering Structures), Book: F 2200–Civil design of the Vranduk 2 bridge, textual part and drawings*, 2018.

[33] EN 1992-1-1:2004+AC:2010. *Eurocode 2: Design of concrete structures–Part 1-1: General rules and rules for buildings*, 2004.

[34] CEB-FIP MODEL CODE 1990. London: Thomas Telford Ltd, 1993.